THE 4.6 $m_{b,Lg}$ NORTHEASTERN KENTUCKY EARTHQUAKE OF SEPTEMBER 7, 1988

R. Street[1], K. Taylor[2], D. Jones[3,a], J. Harris[3,b],
G. Steiner[4], A. Zekulin[3,c], and D. Zhang[5]

[1]Department of Geological Sciences
Kentucky Geological Survey
University of Kentucky
Lexington, KY 40506-0053

[2]Department of Earth and
Atmospheric Sciences
Saint Louis University
Saint Louis, MO 63103

[3]Department of Geological Sciences
University of Kentucky
Lexington, KY 40506-0053

[4]Center for Earthquake
Research and Information
Memphis State University
Memphis, TN 38152

[5]Earthquake Monitoring Department
Seismological Bureau of
Xinjiang Uygur Autonomous Region
WulumuQi, Xinjiang
The People's Republic of China

ABSTRACT

Source parameters for the September 7, 1988 northeastern Kentucky earthquake have been estimated from the analysis of surface-wave amplitude spectra. The source that best fits the observed data had a seismic moment of 2.0×10^{22} dyne-cm, a mechanism with strike = 198° ± 10°, dip = 51° ± 11°, and slip = -178° ± 17°, (T) trend = 160°, plunge = 25°, (P) trend = 55°, plunge = 28°, and source depth of 4 to 7 km.

Thirty-two aftershocks were recorded during 2 weeks of monitoring following the mainshock; 23 of the aftershocks were locatable and fall on a roughly NW-SE linear trend. This trend is subparallel with the NW-SE nodal plane of the mainshock.

Our analysis shows the 1988 event to be different from the July 27, 1980 $m_{b,Lg}$ = 5.3 earthquake located 11 km to the northwest. First, the 1988 event is considerably shallower (4 to 7 km) than the 1980 event (14 to 22 km). Second, data from the 1988 event suggest the motion is on a conjugate fault and is in contrast with the 1980 event, which had right-lateral strike-slip on a southeast-dipping plane.

INTRODUCTION

Historically, northeastern Kentucky and the surrounding areas have experienced few earthquakes during the 200 years the region has been settled. Prior to the 1980's when the first permanent seismographs were installed in northern Kentucky, the only earthquakes known to have occurred in the region are the events indicated in Figure 1 by the open triangles. The largest of these events is the 4.0 $m_{b,Lg}$ event of February 28, 1854, near Lexington, Kentucky (Street, 1984). In this century, the only other earthquakes of any significance known to have occurred in northeastern Kentucky prior to the 1980's are the 3.5 $m_{b,Lg}$ event of May 28, 1933, that was centered near Maysville, Kentucky (Couch, 1986), and the 3.5 $m_{b,Lg}$ event of November 9, 1979, that occurred near Ashland, Kentucky.

On July 27, 1980, an intensity VII MM magnitude 5.3 $m_{b,Lg}$ earthquake occurred at 38.18° N/83.94° W near the community of Sharpsburg, Kentucky causing $4 million worth of property damages in northeastern Kentucky (Street, 1982). Herrmann et al. (1982), using surface waves, P, pP, and sP polarities from the short-period seismic array NORSAR and the aftershock data, concluded

[a]Present address: Larson Software Technology, 11111 Wilcrest Green Drive, Suite 225, Houston, TX 77042
[b]Present address: Kentucky Geological Survey, University of Kentucky, Lexington, KY 40506-0107
[c]Present address: International Business Machine Corporation, 1507 LBJ Freeway, Dallas, TX 75234

that the earthquake was a right-lateral, strike-slip event, striking N30° E and dipping 50° SE. Mauk *et al.* (1982) arrived at a similar conclusion on the basis of first motions of Pn arrivals from the mainshock. The location of the 1980 earthquake and the other instrumentally located events in the area are indicated in Figure 1 by the solid triangles.

On September 27, 1988, at 02:28:09.5 UTC, a 4.6 $m_{b,Lg}$ earthquake occurred in northeastern Kentucky at 38.143° N/83.875° W (see Fig. 2) with a focal depth of 10 km (NEIS). Within the general area of the epicenter, the earthquake caused minor cracking in brick veneer and basement walls, knocked small objects off tables, alarmed some of the residents to the extent that they went outdoors, shook cupboards sufficiently to cause their contents to fall to the floor, and in a few instances caused plaster to fall. On the basis of these reports, the earthquake is assigned a maximum Modified Mercalli (MM) intensity of V-VI in the epicentral region.

This paper reports on the analysis of the mainshock source parameters and the aftershock monitoring conducted during the two weeks following the mainshock.

MAINSHOCK PARAMETERS

Vertical long-period Rayleigh-wave data in the 6 to 35 second period range were obtained from seven WWSSN stations: SCP, OTT, WES, BLA, ALQ, FVM, and FFC. In addition, long-period Love-wave data in the 6 to 35 second period range were collected from six stations: SCH, OTT, WES, BLA, ALQ, and FFC. The data set consisted of 86 Rayleigh-wave and 77 Love-wave spectral amplitude-period data points. The spectra were corrected for anelastic attenuation and geometrical spreading. Surface-wave focal mechanism analysis was performed using the techniques outlined by Herrmann (1979b). A similar analysis was performed by Taylor *et al.* (1989) for the 5.2 $m_{b,Lg}$ 1987 southern Illinois earthquake.

A systematic search for the focal mechanism and seismic moment that best fit the observed spectral amplitude radiation pattern was performed. Identical searches were made over a range of focal depths between 1 and 15 kilometers. For each depth, the theoretical Rayleigh- and
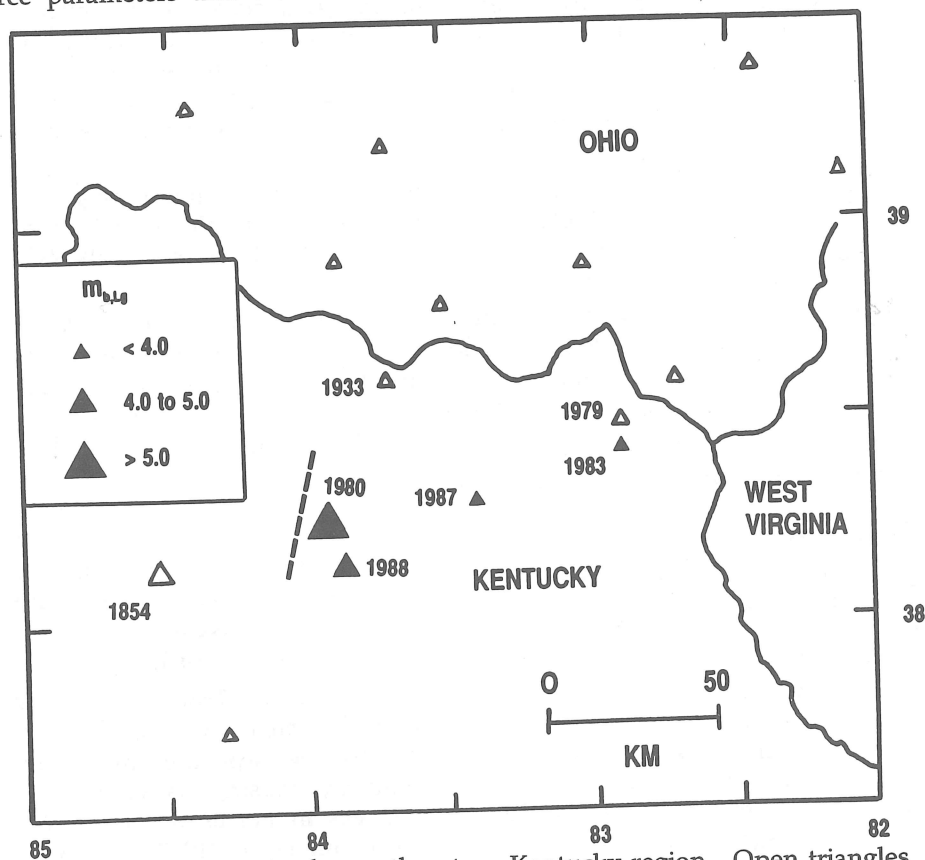

Fig. 1. Seismicity in the northeastern Kentucky region. Open triangles indicate epicentral locations of events that occurred prior to 1980 when the first high-gain seismographs were installed in the region; solid triangles indicate instrumentally located events since January 1980. The dashed line indicates the approximate location of the lateral velocity discontinuity discussed in the Appendix.

Love-wave radiation patterns calculated for a mechanism were defined by a set of strike, dip, and slip angles. The theoretical patterns were calculated using the Central U.S. earth model, which is presented by Herrmann (1986). A 2.5 degree increment in the slip, dip, and strike angles was used in the final search.

For each mechanism, the theoretical Raleigh- and Love-wave radiation patterns were compared to the observed spectral-amplitude data and correlation coefficients (RR [for Rayleigh] and RL [for Love]); two independent estimates of seismic moment (MR[using only Rayleigh] and ML [using only Love]) were obtained. The product of RR, RL, and the ratio ML/MR (or MR/ML if ML G.E. MR) was used as a weighing function to obtain a weighted average solution for each depth (e.g., Taylor *et al.*, 1989). In the analysis of the September 7 mainshock, the weighing function was largest for source depths of 4 to 7 km, and the same focal mechanism was found at each depth.

In calculating a double-couple focal mechanism from surface-wave amplitude spectra, there is a 180° ambiguity in the mechanism orientation. Because amplitude spectra are used, the P and T axes can be interchanged without affecting the predicted spectra. Thus, four equally consistent mechanisms will fit the amplitude spectra. These four preliminary mechanisms for the September 7, 1988 event are shown in Figure 3. All have the same seismic moment of $2.0 x 10^{22}$ dyne-cm, and source depth of 5 km. For these mechanisms, the correlation coefficients RR and RL are 0.821 and 0.641, respectively. Using clear, impulsive P-wave first motions from local and regional stations, the correct surface-wave mechanism may be selected.
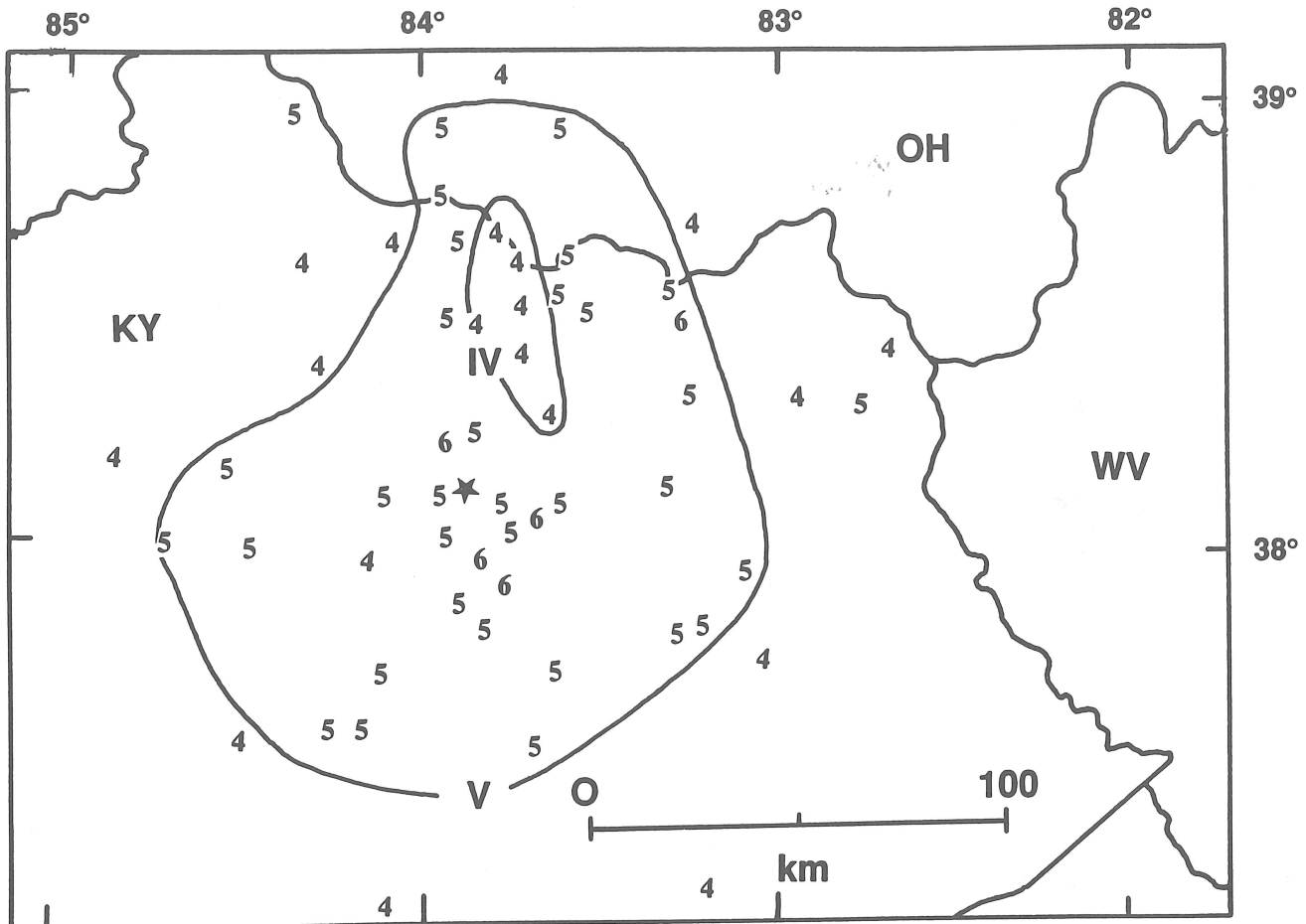

Fig. 2. Isoseismal map for the September 7, 1988 northeastern Kentucky earthquake. Individual MM intensity values are given in Arabic numerals, and isoseismal contours are labeled with Roman numerals. At the northern edge of the intensity V contour are the Ohio river valley communities that are typically underlain by a few tens of meters of alluvium. The area within the intensity IV contour in the northeastern part of the figure is underlain by a few meters of stiff clay overlying limestone. We believe that the higher intensities in the river communities are due to site effects.

P-wave first motions for the mainshock were read at 29 stations and are listed in Table 1. Incident angles were calculated by a modified version of the computer program FASTHYPO (Herrmann, 1979a), using the SLU network UPLANDS earth model. Unambiguous impulsive arrivals were seen only at seven stations: ELC(d), CIRL(d), IN3(c), TKL(c), BRTN(c), CRTN(c), and ONTN(c). Based only on these seven arrivals, two of the four preliminary mechanisms (those that predicted northeast or southwest tension) were eliminated (Mech "B" and "D" in Figure 3). Both of the other mechanisms showed northeast-southwest compression, but mechanism "A" was still inconsistent with the polarities of the first-motions observed at four of the seven stations. Only mechanism "C" was consistent with all seven of the observed impulsive arrivals. This mechanism was therefore chosen as the final solution, and has strike = 198° ± 10°, dip = 51° ± 11°, and slip = -178° ± 17°, with tension and pressure axes of (T) trend = 160°, plunge = 25° and (P) trend = 55°, plunge = 28°. The mechanism is plotted in Figure 4 with all 29 of the first motions observed. The mainshock focal parameters are listed in Table 2.

AFTERSHOCK STUDY

Aftershocks of the September 7, 1988, earthquake were monitored with nine Sprengnether

MECH "A"

MECH "B"

STRIKE=18°, DIP=51°, SLIP=-178°
(T) TR=340°, PL=25°; (P) TR=235°, PL=28°

STRIKE=18°, DIP=51°, SLIP=2°
(T) TR=235°, PL=28°; (P) TR=340°, PL=25°

MECH "C"

MECH "D"

STRIKE=198°, DIP=51°, SLIP=-178°
(T) TR=160°, PL=25°; (P) TR=55°, PL=28°

STRIKE=198°, DIP=51°, SLIP=2°
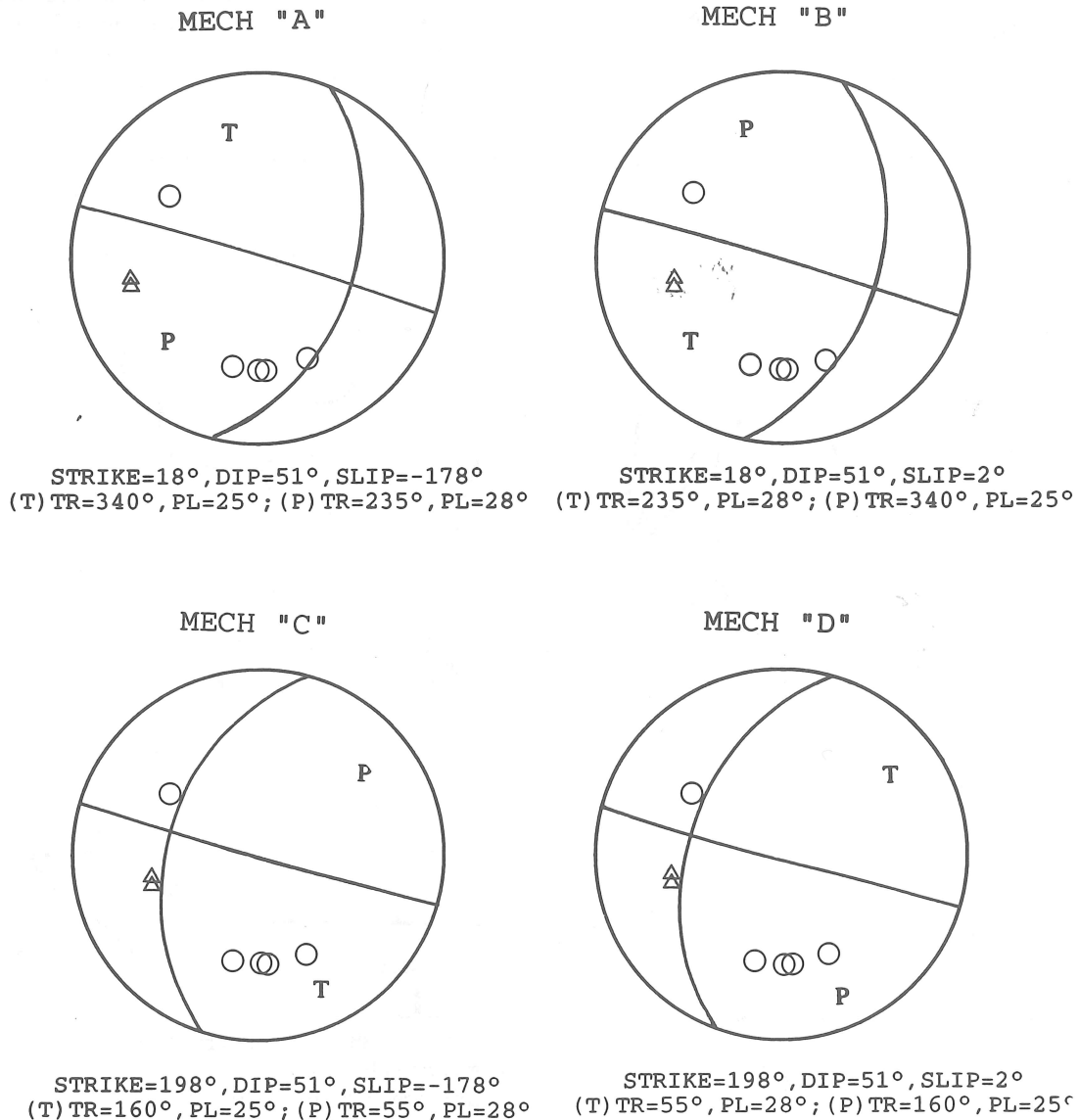(T) TR=55°, PL=28°; (P) TR=160°, PL=25°

Fig. 3. The four preliminary surface-wave mechanisms for the September 4, 1988 mainshock. These plots are lower hemisphere equal-area projections with the unambiguous dilatational and compressional P wave first motions being indicated by the triangles and circles, respectively. The pressure and tension axes are indicated by P and T.

Table 1
P-Wave First Motions for Mainshock

Station Name	Azimuth (°)	TOA (°)	Polarity
CLE	27	48	-
MEN	27	48	-
TBR	74	48	+
VWV	102	48	-
BLAZ	107	48	+
SLTN	140	48	+
BRTN	156	48	c
TKL	178	48	c
CRTN	180	48	c
ORT	189	48	c
TQTN	195	48	+
ONTN	196	48	+
WMTN	198	48	-
ANTN	210	48	+
ABTN	219	48	-
SHTN	225	48	+
HAKY	245	48	-
MOTN	246	48	+
ELC	259	48	d
CIRL	260	48	d
BLO	297	48	-
IN3	307	48	c
IN2	308	48	-
AN3	342	48	+
AN10	348	48	-
AN9	348	48	-
AN12	354	48	-
AN4	358	48	-
AN7	359	48	-

TOA = "take-off" angle
c = compression
d = dilatation
+ = compression of lesser quality
- = dilatation of lesser quality

MEQ-800B portable seismographs from the University of Kentucky and Memphis State University, and one Kinemetrics SSA-1 digital strong-motion accelerometer provided by Lamont-Doherty. Figure 5 illustrates the distribution of the temporary stations occupied during the aftershock study. Table 3 gives the station coordinates and dates when the stations were opened and closed. Stations SBKY, BETH, JUDY, and SNR are sites that were occupied during the aftershock study of the 1980 Sharpsburg, Kentucky, earthquake (Herrmann *et al.*, 1982). Recording parameters for the portable recorders used in the 1988 study included; a rotational speed of 120 mm/s, low and high filter settings of 5 and 10 Hz, tic marks at every second, smoked paper records, and gain settings of 96 to 108 db. Given the rotational speed and thickness of the stylus trace on the smoked paper records, arrival times were read to the nearest 1/40th of a second with the aid of a 7x comparator.

Transducers at the temporary stations, with the exception of the installations at SBKY and

SNR, consisted of a Mark Products L-28 (4.5 Hz) geophone, buried half a meter below the surface in an open field. The L-28 at SBKY was installed in a 5 m cased borehole that had been drilled and used for the permanent seismic station operated at the site from 1981 through 1983 by the University of Kentucky. At SNR, both a MEQ-800B with a Geosource HS-10 and a SSA-1 accelerograph were

Table 2
Surface-Wave Source Parameters of September 7, 1988 Mainshock

Nodal Plane (1)			Nodal Plane (2)		
Strike	Dip	Slip	Strike	Dip	Slip
198°	51°	-178°	107°	88°	-39°

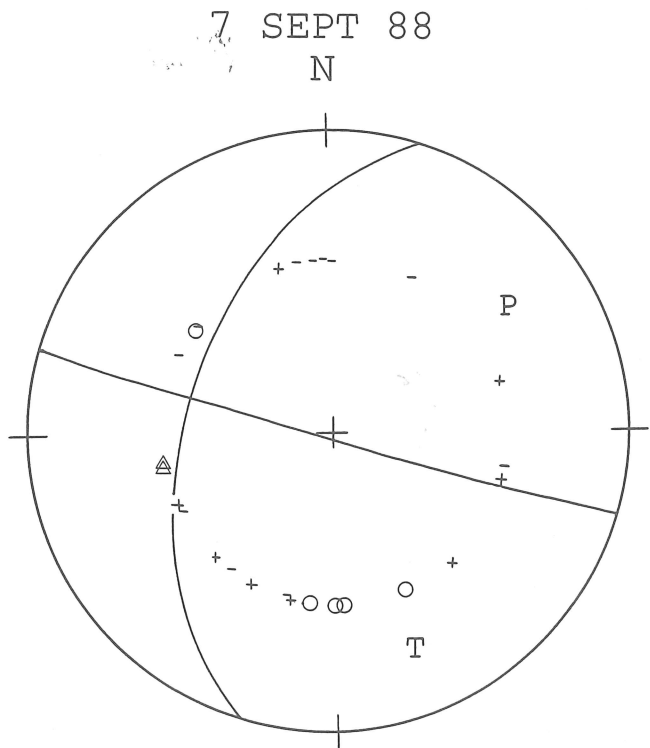| Tension Axis		Pressure Axis		Depth (km)	M_o (dyne-cm)
Trend	Plunge	Trend	Plunge		
160°	25°	55°	28°	4-7	2.0×10^{22}

Fig. 4. Focal mechanism calculated for the September 7, 1988 mainshock from surface-wave amplitude spectral analysis. Observed P-wave first motions are also plotted. The pressure and tension axes are marked with a P and T. The plot is a lower hemisphere equal-area projection with the unambiguous dilatational P wave first motions as triangles and compressional ones as circles. The "+" and "-" symbols indicate lesser quality compressions and dilatations for P wave first motions, respectively.

placed in the root cellar that had been used during the aftershock study of the 1980 earthquake. The SSA-1 was bolted to the concrete floor of the cellar, but unfortunately it was not "triggered" by any of the aftershocks.

The principal advantage of using the L-28's and burying them and their cables, as compared to using surface installations, was the improved signal-to-noise ratio achieved during the windy

and rainy days of the second week of the study. Polarities of the L-28's and HS-10 were established by comparing their responses to the response of a geophone of known polarity resulting from a seismic hammer striking the ground approximately 50 m away from where the geophones were set up. Responses of the geophones were recorded simultaneously on a 24-channel engineering seismograph at a recording speed of 25.4 mm/12.5 ms. While slight differences were noted in the amplitude and phase responses between the various geophones, the principal result of the experiment was that the polarity and phase response of the geophone used first at BETH and later at STKY was substantially different from that of the other geophones in the study. Consequently, the records from these two stations were not used in the first-motion studies discussed below.

Time corrections for the portable recorders were determined daily by use of a Sprengnether TS-400 portable chronometer, and a VLF digital comparator. The TS-400 was synchronized daily with the chronometer used in the Seismic Lab at the University of Kentucky. Typically, the chronometers in the portable recorders had to be retarded by 40 to 60 ms/day.

Table 3
Station Coordinates

| Station	Lat (° N)	Long (° W)	Elevation (m)	Opened (m/d/y)	Closed (m/d/y)
BETH	38.2463	83.8540	277	9/08/88	9/14/88
EJUD	38.1310	83.8816	296	9/13/88	9/25/88
HDKY	38.0980	83.9190	283	9/17/88	9/21/88
JUDY	38.1373	83.9495	290	9/07/88	9/25/88
NSBK	38.2265	83.9057	299	9/07/88	9/08/88
REYN	38.2032	83.8618	265	9/09/88	9/16/88
ROCK	38.1898	83.8618	274	9/07/88	9/14/88
SBKY	38.2249	83.9257	296	9/07/88	9/14/88
SRN	38.1790	83.9580	290	9/10/88	9/14/88
STKY	38.1661	83.9109	308	9/15/88	9/25/88
TUKY	38.1609	83.8412	277	9/20/88	9/25/88
UNIO	38.2444	83.9704	293	9/10/88	9/12/88
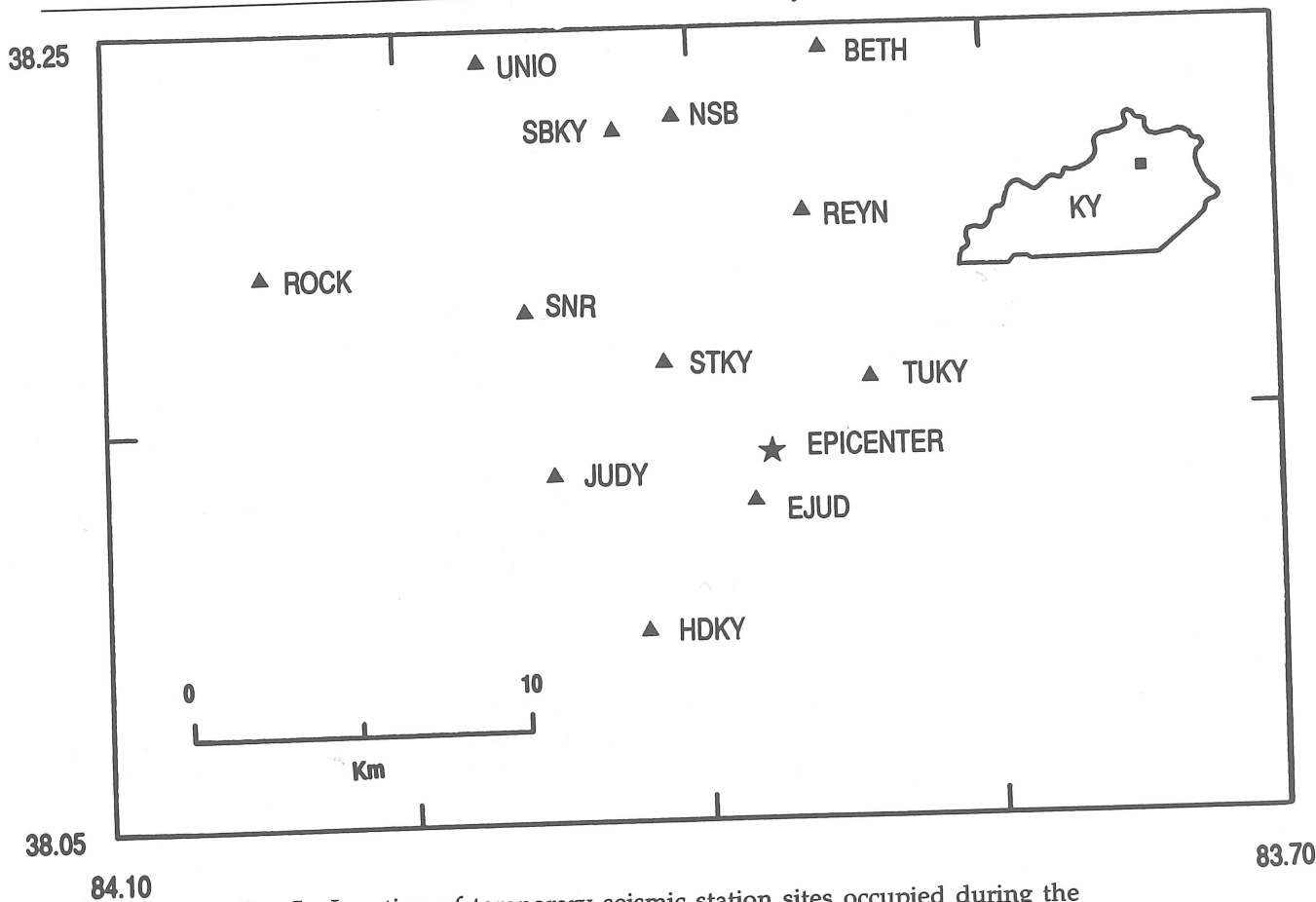
Fig. 5. Location of temporary seismic station sites occupied during the aftershock study of the September 7, 1988 northeastern Kentucky earthquake.

Table 4
Aftershock Locations

No.	Date	Time (UT)	Mag	Lat (°N)	Lon (°W)	Depth (km)	Error Hor (km)	Error Ver (km)	Nearest Station	Algorithm Used
1.	09/07	093101.5	3.1	38.143	83.875					PDE
2	09/08	095619.325	0.7	38.150	83.803	5/46			JUDY/ND	BHYPO
3	09/08	145639.050	1.6	ND						
4	09/09	095938.525	2.7	38.150	83.877	5.35	1.3	1.9	JUDY/6.5	HYPO71
5	09/09	101427.075	1.5	38.150	83.835	7.49	2.4	4.5	JUDY/10.2	HYPO71
6	09/09	115538.450	1.5	38.167	83.875	10.00	9.6	7.9	SBKY/7.7	HYPO71
7	09/09	215835.750	1.7	38.126	83.854	6.03			SBKY/ND	BHYPO
8	09/11	022740.510	1.5	38.150	83.900	7.69	2.6	2.6	JUDY/4.6	HYPO71
9	09/11	031651.050	0.9	38.133	83.856	3.53	0.5	1.4	REYN/7.9	HYPO71
10	09/11	040104.950	0.9	38.133	83.857	1.70	1.3	11.4	REYN/7.9	HYPO71
11	09/11	051245.525	0.6	ND					JUDY/ND	BHYPO
12	09/11	054035.135	2.2	38.136	83.864	6.69			REYN/7.8	HYPO71
13	09/11	065828.675	1.1	38.134	83.856	3.90	0.7	1.6		
14	09/11	074739.625	0.4	ND						
15	09/11	101300.350	1.1	38.135	83.855	3.92	0.6	1.5	JUDY/8.3	HYPO71
16	09/11	190427.500	0.9	38.150	83.900	7.44	3.3	3.6	REYN/6.8	HYPO71
17	09/11	203956.325	0.7	ND						
18	09/11	211035.100	0.8	38.138	83.913	10.00	1.2	0.9	JUDY/3.2	HYPO71
19	09/13	070914.575	0.9	ND						
20	09/13	092947.275	0.9	38.138	83.867	6.32	0.4	0.6	JUDY/7.2	HYPO71
21	09/15	050058.350	0.8	38.132	83.857	4.57	0.5	0.5	EJUD/2.1	HYPO71
22	09/15	185715.000	0.6	38.150	83.882	5.46	0.9	1.1	EJUD/2.1	HYPO71
23	09/16	032607.525	1.3	38.139	83.864	5.95	0.3	0.2	EJUD/1.8	HYPO71
24	09/16	070410.225	0.8	ND						
25	09/17	111320.700	0.7	ND						
26	09/17	175030.250	1.2	38.141	83.859	4.48	0.7	1.1	STKY/5.3	HYPO71
27	09/18	043545.150	1.1	ND						
28	09/19	082559.775	1.5	38.150	83.900	7.20	1.5	0.8	STKY/2.0	HYPO71
29	09/19	082812.225	2.1	38.140	83.882	6.09	0.4	0.5	EJUD/1.0	HYPO71
30	09/19	171823.700	2.4	38.141	83.880	5.46	0.8	0.6	EJUD/1.0	HYPO71
31	09/22	013213.900	0.3	ND						
32	09/22	031737.375	0.8	38.138	83.865	4.87	0.4	0.4	EJUD/1.7	HYPO71
33	09/22	092128.075	0.5	38.139	83.873	4.47	0.9	0.6	EJUD/1.1	HYPO71

Events 1, 4, 29 and 30 were felt.

ND = Location not determined due to insufficient data

PDE = Preliminary Determination of Epicenters (No. 36-88)

Temporary seismic stations SBKY and NHKY were established within 5 hours after the occurrence of the main event. Between then and September 25, when the aftershock study was discontinued because of the lack of seismic activity, 29 microearthquakes and four felt events were recorded. Table 4 is a list of the events, their origin times, epicentral locations, focal depths, and distances to the nearest seismic station. Magnitudes given for the aftershocks in Table 4 are based on a duration scale specifically derived for this study with the use of the seismograms from stations JUDY and ROCK.

Epicentral locations, focal depths, and origin times of the aftershocks are based on the velocity model given in Table 5. The 5.55 km/s sedimentary layer over a crustal layer of 6.85 km/s P- wave velocity and corresponding S-wave velocities are assumed on the basis of the studies cited in the Appendix, and for compatibility with the velocity model used by Herrmann et al. (1982) in their study of the July 27, 1980, Sharpsburg earthquake. Variations in the velocity model, including P-wave velocities of 6.8 and 6.9 km/s for the basement rock, and Vp/Vs ratios of 1.70, 1.75, and 1.80, were tried as a matter of interest. The principal effect of these variations was to modify the focal depths of the events. While some of these variations are thought be to less likely than others, all are within one standard deviation of observed P- and S-wave velocities (see the Appendix).

Three computer programs for locating the aftershocks were used during the study. BASIC-HYPO (Mendoza and Morgan, 1985) was used during the first phase of the study to help in delineating the source zone of the aftershocks, while FASTHYPO (Herrmann, 1979a) and HYPO71 (Lee and Lahr, 1975) were used in the second phase of the study for determining more precisely the epicentral locations, focal depths, and origin times of the events. In general, epicentral locations calculated by FASTHYPO and HYPO71 were consistent
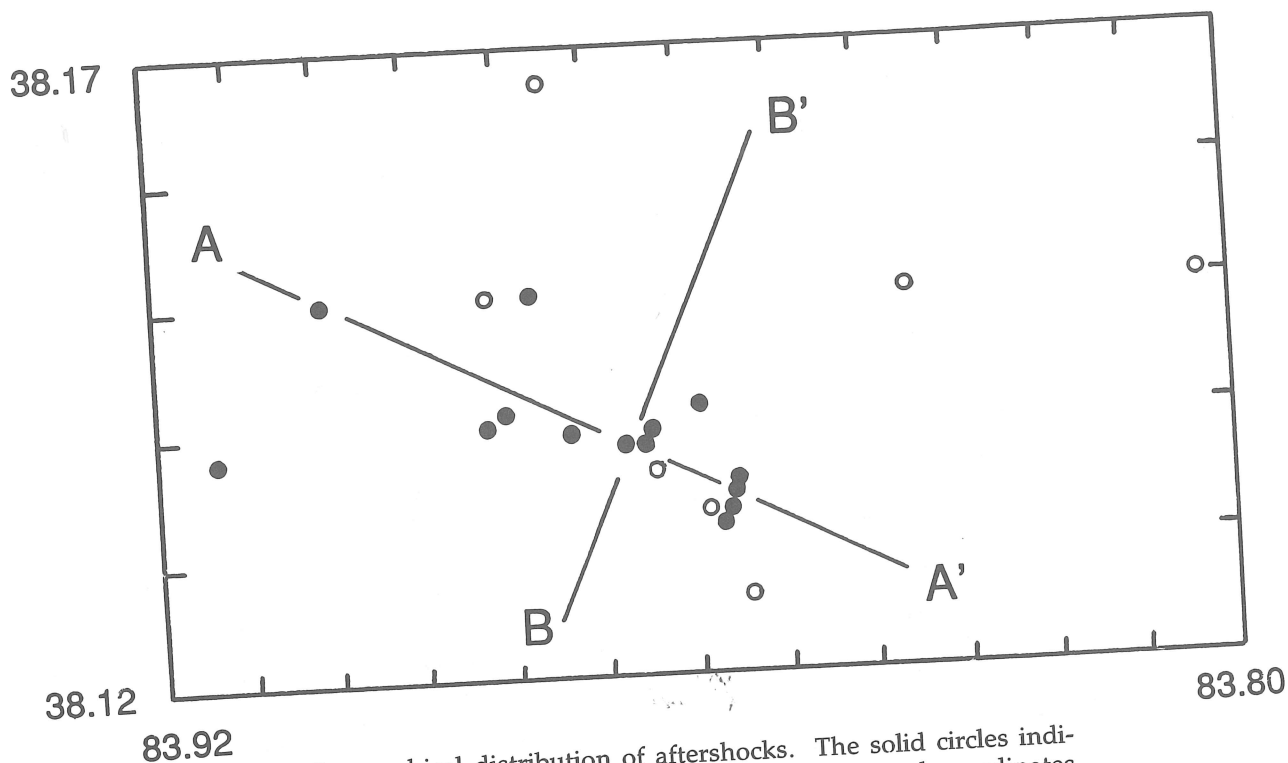
Fig. 6. Geographical distribution of aftershocks. The solid circles indicate the locations of events whose errors in epicentral coordinates and focal depth are less than 2 kilometers, whereas the open circles indicate the locations of events whose epicentral coordinates and/or focal depths have errors in excess of 2 kilometers.

with one another. Focal depths calculated by the two programs however, differed due to the use of P-wave arrival times in FASTHYPO versus the use of both P- and S-wave arrival times in HYPO71. Since errors associated with the focal depths calculated by HYPO71 were less than those calculated by FASTHYPO, the former were preferred. Weights assigned to the arrival times were the same for all computer runs, with most of the P-wave arrivals being assigned a weight of 0 (the highest weight), and most of the S-wave arrivals being assigned a weight of 2 because of the usual difficulties in picking secondary arrival times.

A composite focal mechanism plot of the first-motion P-wave data was constructed, but the results were inconclusive because of the lack of first-motion data from stations to the east and southeast of the source zone.

The geographical distribution of the aftershocks listed in Table 4 are indicated in Figure 6.

Table 5
Crustal Model Used in Aftershock Study

Layer Thickness (km)	Depth to Top (km)	V_P (km/s)	V_S (km/s)
0.92	0.00	5.52	3.15
39.0	0.92	6.85	3.91

Epicenters of those events whose error in location or focal depth exceed 2 km are indicated in the figure by an open circle. The epicenters of the better located events in Figure 6 (i.e., the solid circles) are distinctly oriented along the southeast-northwest trending line A-A'. Figure 7 is a vertical profile oriented along line A-A' in Figure 6. The distribution of the better located hypocenters shown in Figure 6 suggests an elliptical rupture plane with its major axis dipping about 40° to the northwest. Vertical profiles striking +20° to line A-A' yield about the same results. A vertical plane through B-B' in Figure 6 is shown in Figure 8.

Using the same assumptions used by Herrmann et al. (1982), i.e. (1) the aftershock zone corresponds to the fault surface of the mainshock and (2)

$$\mu = 4 \times 10^{11} dyne/cm^2,$$ the stress drop ($\Delta\sigma$) for an instantaneous dislocation on a circular fault plane can be calculated by the Brune (1970) model:

$$\Delta\sigma = (7/16)M_0 r^{-3}$$

where M_0 is the seismic moment and r is the radius. The area outlined by the dashed line in Figure 7 is approximately 14 km², which is equivalent to a circular area having a radius of 2 km. With these assumptions and a seismic moment of 2.0×10^{22} dyne-cm, we find $\Delta\sigma = 0$ bars, which is somewhat lower than the 2.8 to

194

bar stress drop estimated by Herrmann *et al.* (1982) for the July 27, 1980 Sharpsburg, Kentucky, earthquake.

DISCUSSION

The results from the aftershock monitoring and analysis of the mainshock of the September 7, 1988, earthquake show two fundamental differences with the results reported by Herrmann *et al.* (1982) for the July 27, 1980, magnitude 5.3 $m_{b,Lg}$ earthquake located 11 km to the northwest. First, the 1988 mainshock is considerably shallower (4 to 7 km) than the 1980 mainshock (14 to 22 km). This conclusion is also supported by the hypocentral

depths calculated from the two aftershock sequences. Both sequences are plotted together in map view in Figure 9, with the two mainshocks plotted as larger symbols in the figure.

The second difference is that the mechanisms calculated for the two events are not the same. The 1980 mechanism reported by Herrmann *et al.* (1982) had almost pure right-lateral strike-slip on a southeast-dipping plane. The aftershocks located in 1980 also supported this choice because the epicenter distribution was elongated slightly to the northeast and the hypocenters increased in depth to the southeast.
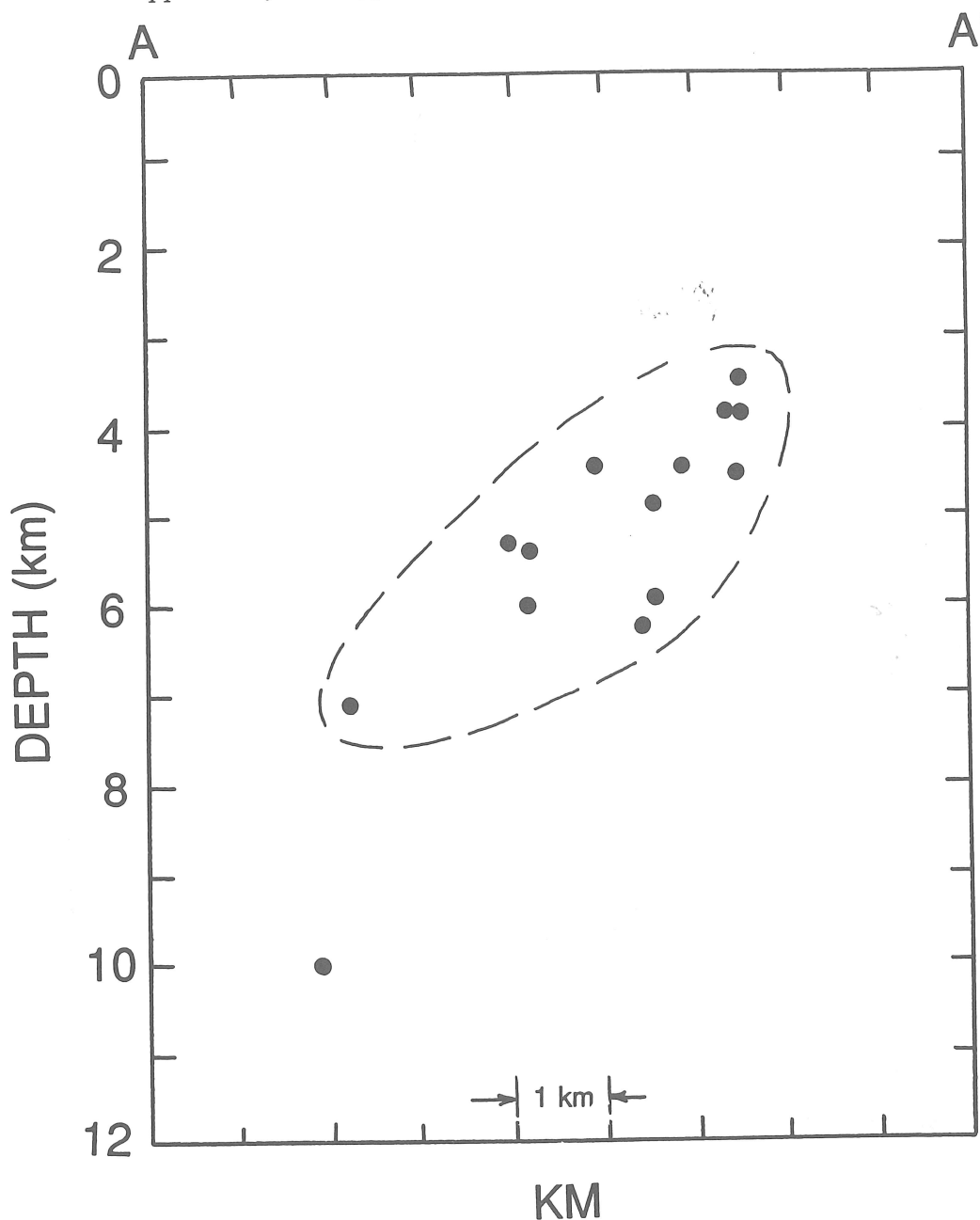
Fig. 7. Hypocenters projected onto a vertical plane along line A- A' in Figure 5.

The 1988 aftershocks, however, fall roughly on a NW-SE linear trend, with the hypocenters increasing in depth from east to west. The mechanism calculated for the 1988 mainshock (Figure 4) has one nodal plane striking NE-SW and dipping to the northwest. The other plane is nearly vertical and strikes subparallel to the aftershock distribution. This suggests the motion was left-lateral strike- slip on the vertical plane. Such motion would mean the 1988 sequence occurred on a conjugate fault to the 1980 rupture.

An alternative hypothesis is that the rupture occurred on the other nodal plane, and the motion is right-lateral strike-slip on the northwest-dipping plane. This hypothesis suggests the motion could represent strike-slip faulting on the west (1980 sequence) and east (1988 sequence) sides of a northeast-trending graben-like structure. This structure would be similar to one reported by Wetmiller et al. (1984) for the Miramichi earthquake sequence.

Either of these hypotheses is supported by the regional structure. Within 15 kilometers of the epicentral region of the two events are the east-west-trending Kentucky River Fault Zone, the NE-SW-trending Lexington Fault Zone, and a series of
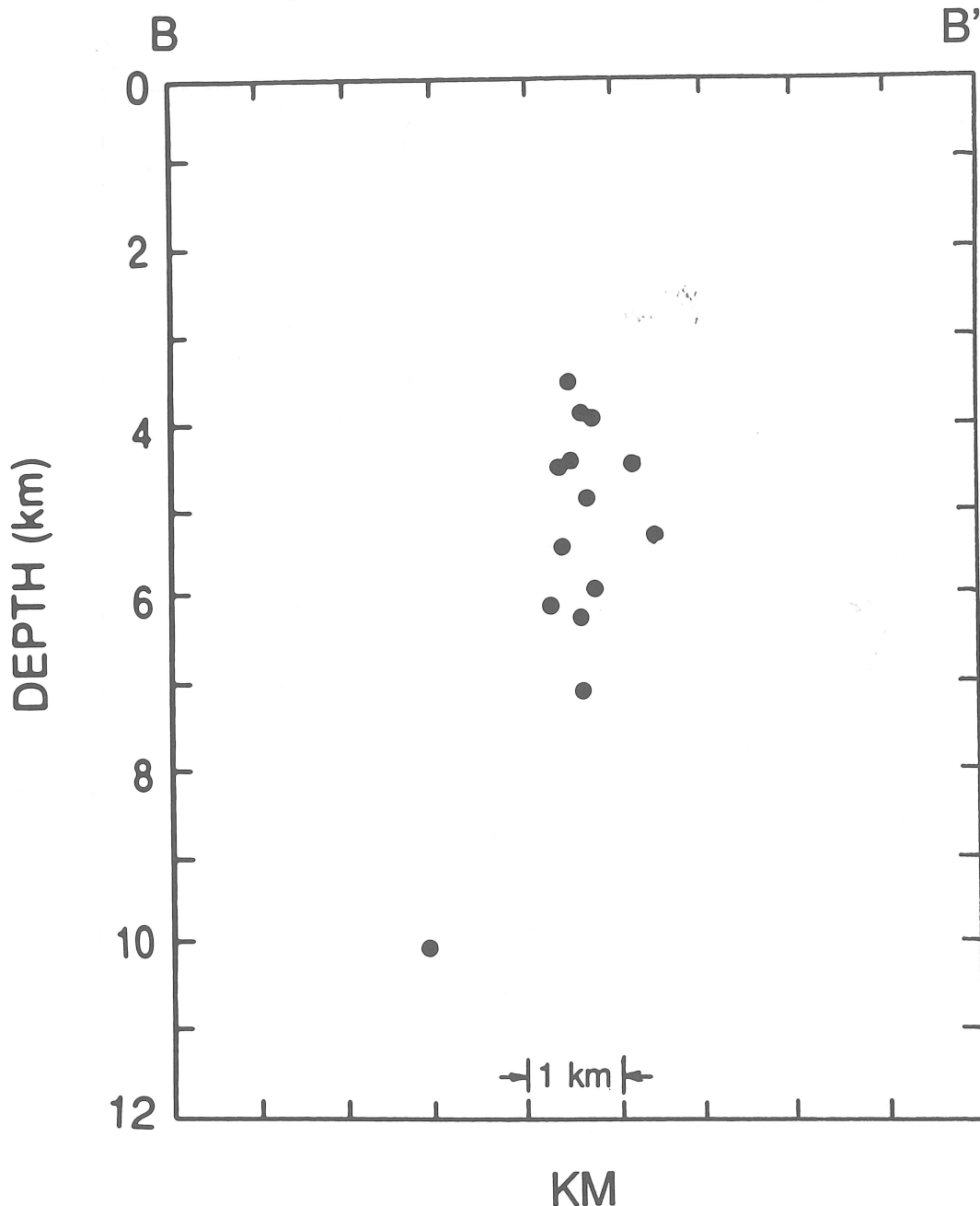

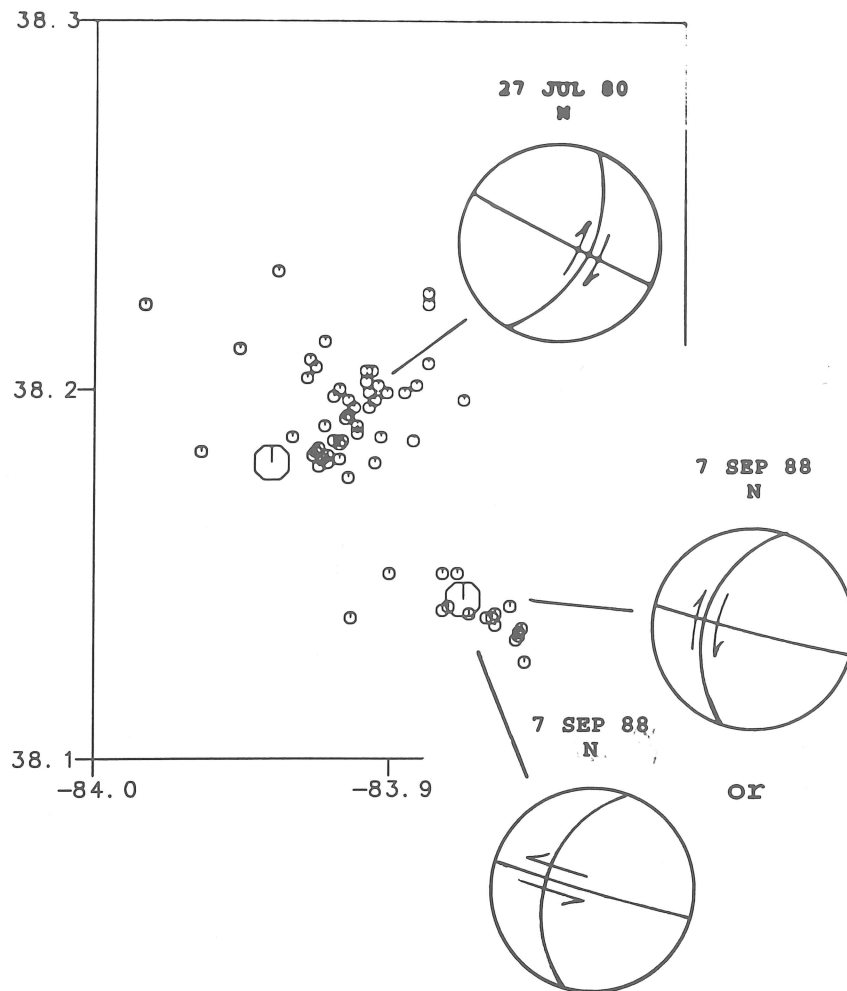Fig. 8. Hypocenters projected onto a vertical plane along line B- B' in Figure 5.

Fig. 9. Focal mechanisms for the September 7, 1988 mainshock (from this study) and the July 27, 1980 mainshock (from Herrmann *et al.*, 1982), with the better located (i.e., error in epicentral location is less than 2 km) aftershocks recorded from the two studies. The mainshocks are plotted as larger symbols.

NW-SE-trending tear faults. These and other basement anomalies have been previously discussed, most recently by Black (1986). In addition, as shown by Street *et al.* (1985), there is a NE-SW-trending lateral velocity discontinuity at the top of the Precambrian basement in the vicinity of the 1980 earthquake.

CONCLUSIONS

The September 7, 1988 earthquake is related to the earlier and somewhat larger earthquake of July 27, 1980, by occurring on a conjugate fault to the 1980 rupture; or the 1988 and 1980 earthquakes were the result of strike-slip faulting on the east and west sides, respectively, of a northeast-trending graben-like structure. These conclusions are supported by the sense of motions along the respective rupture planes and the east-northeast orientation of the stress axes of the two faults. Both interpretations relate the only two significant earthquakes to have occurred in the area in the last 200 years.

197

REFERENCES

Black, D.F.B. (1986). Basement faulting in Kentucky, *Proceedings of the 6th International Conference on Basement Tectonics*, 125-139.

Brune, J.N. (1970). Tectonic stress and the spectra of seismic shear waves from earthquakes, *J. Geophys. Res.* **75**, 4997-5009.

Couch, D.L. (1986). Seismicity and crustal structure of the East Continental Gravity High, *M.S. Thesis*, University of Kentucky, Lexington, Kentucky, 158 p.

Herrmann, R.B. (1979a). FASTHYPO - A hypocenter location program, *Earthquake Notes* **50** (2), 25-38.

Herrmann, R.B. (1979b). Surface wave focal mechanisms for eastern North American earthquakes with tectonic implications, *J. Geophys. Res.* **84**, 3543-3552.

Herrmann, R.B., C.A. Langston, and J.E. Zollweg (1982). The Sharpsburg, Kentucky, earthquake of 27 July 1980, *Bull. Seism. Soc. Am.* **72**, 1219-1239.

Herrmann, R.B. (1986). Surface-wave studies of some South Carolina earthquakes, *Bull. Seism. Soc. Am.* **76**, 111-122.

Lee, W.H.K., and J.C. Lahr (1975). HYPO71 (revised): A computer program for determining hypocenter, magnitude, and first-motion pattern of local earthquakes, *U.S. Geol. Survey Open-File Rpt. 75-311*, 113 p.

Mauk, F.J., D. Christensen, and S. Henry (1982). The Sharpsburg, Kentucky, earthquake of 27 July 1980: Main shock parameters and isoseismal maps, *Bull. Seism. Soc. Am.* **72**, 221-236.

Mendoza, J., and D. Morgan (1985). BASIC-HYPO: A basic language hypocenter location program user's guide, *Stanford University Publications, Geological Sciences*, XIX(1), Stanford, California, 33 p.

Street, R. (1982). Ground motion values obtained for the 27 July 1980 Sharpsburg, Kentucky, earthquake, *Bull. Seism. Soc. Am.* **72**, 1295-1307.

Street, R. (1984). The historical seismicity of the central United States: 1811-1927, *U.S. Geol. Survey Open-File Rpt. 14-08-0001-21251*, 556 p.

Street, R., A. Zekulin, M. Allsop, and D. Couch (1985). The spatial correlation between a lateral seismic velocity discontinuity in the Precambrian basement rock and the Sharpsburg, Kentucky, earthquake of July 27, 1980, *Earthquake Notes* **56** (2), 47-54.

Taylor, K.B., R.B. Herrmann, M.W. Hamburger, G.L. Pavlis, A. Johnston, C. Langer, and C. Lam (1989). The southern Illinois earthquake of 10 June 1987, *Seism. Res. Letters* **60**, 101-110.

Thurber, C.H., and M.M. Bell (1984). Joint inversion for P and S seismic velocity ratio: Application to the Sharpsburg, Kentucky, aftershock sequence, *Earthquake Notes* **55** (3), 13-15.

Wetmiller, R.J., J. Adams, F.M. Anglin, H.S. Hasegawa, and A.E. Stevens (1984). Aftershock sequences of the 1982 Miramichi, New Brunswick, earthquakes, *Bull. Seism. Soc. Am.* **74**, 621-653.

Willis, M.E., and M.N. Toksoz (1983). Automatic P and S velocity determination from full waveform digital acoustic logs, *Geophysics* **48**, 1631-1644.

APPENDIX
Velocity Measurements
in the Aftershock Study Area

Five to seven kilometers to the east of the 1980 and 1988 earthquakes is the upper crustal velocity discontinuity first mentioned by Herrmann *et al.* (1982) in their study of the P- and S- wave travel times recorded during the aftershock study of the 1980 earthquake. Further studies by Street *et al.* (1985) have confirmed the existence of the discontinuity and its approximate location (dotted line in Fig. 1). Of immediate importance to this study is the lack of knowledge about the extent of the velocity discontinuity and the velocity structure of the lower crust and upper mantle, which makes locating earthquakes in northeastern Kentucky, with reasonable accuracy, difficult. This is particularly true for the September 7 event, since the closest operational seismic stations to the epicenter at the time of the event were the Memphis State University seismic stations in northeastern Tennessee at epicentral distances in excess of 260 km.

Table A-1 lists velocities, V_P/V_S ratios, and the Poisson's ratios (ν) that have been suggested for the sedimentary and basement rocks shown on either side of the velocity discontinuity. Standard deviations in the Poisson's ratios listed in Table A-1 are based on the following assumptions: the standard deviations in the P-wave velocities (σ_P) for the basement rocks is ±0.05 km/s, and the standard deviation in the corresponding S-wave velocities (σ_S) is twice that of the P-wave velocities. These estimates are based on published (Street *et al.*, 1985) and unpublished refraction profiles in the area, and the fact that S-wave arrival times are very susceptible to errors when picked from short-period, vertical- component geophones. Knowing σ_P and σ_S, the standard deviation in ν (σ_ν) is given by

$$\sigma_\nu^2 = \frac{(V_P/V_S)^2/V_S^2}{\left[1-(V_P/V_S)^2\right]^2}\left[\sigma_P^2 + \sigma_S^2(V_P/V_S)^2\right] \text{ (A-1)}$$
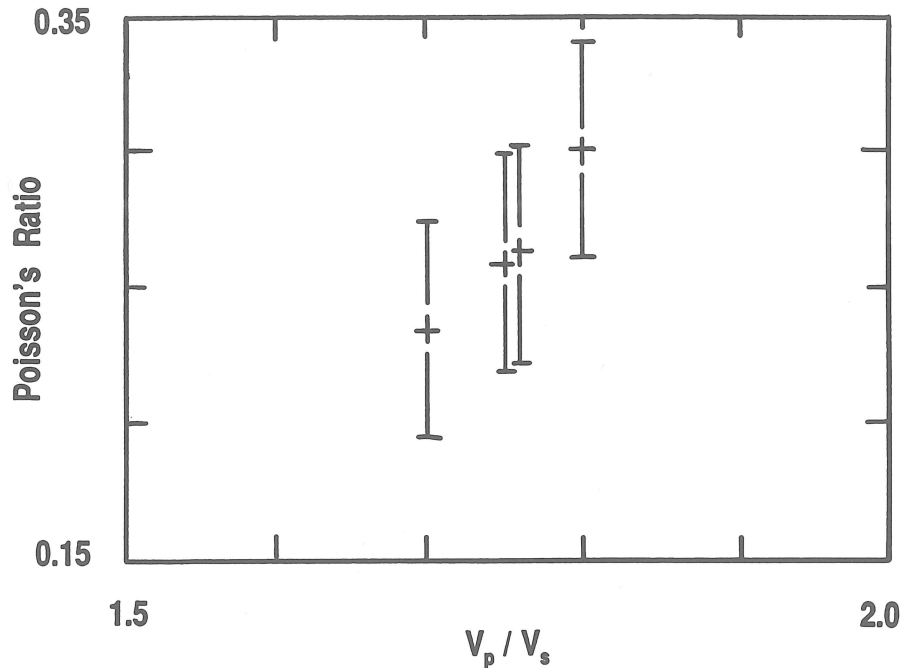
Fig. A-1. Graph of Poisson's ratios and their standard deviations based on equation A-1.

(Willis and Toksoz, 1983). Figure A-1 illustrates the Poisson's ratios and estimated standard deviations calculated using Equation A-1 and our estimates of σ_P and σ_S.

Thurber and Bell (1984) determined a V_P/V_S ratio of 1.7 $\pm$0.01 for the Precambrian basement east of velocity discontinuity using aftershock data obtained from the 1980 earthquake. Recordings of timed quarry blasts obtained during the aftershock study of the 1988 earthquake, however, suggest a V_P/V_S ratio more on the order of 1.80 to 1.85, from which we assume a value of 1.8.

Differences in the V_P/V_S ratios obtained in the two studies can be, in part, attributed to the difference in significant numbers associated with the arrival times used. Thurber and Bell (1984) used arrival times compiled on a computer to the third decimal place. As indicated in the text, the maximum resolution on smoked-paper records claimed for the 1988 earthquake is 1/40th of a second; i.e., $\pm$0.03 seconds. This value is based on a drum rotation speed of 2 mm/s, a trace thickness of 0.07 mm, and second marks on all records. The resolution on the records for the aftershock study of the 1980 earthquake was less. Many of the 1980 records are from lower resolution (thicker traces) pen-and-ink records, some are records that were recorded at a rotation speed of 1 mm/s, and some of the records lack second marks. Consequently, the overall resolution in arrival times for the aftershocks of the 1980 earthquakes is somewhat less than the $\pm$0.03 second achieved for the 1988 aftershock study, and certainly less than the three decimal places used in the Thurber and Bell (1984) study.

Table A-1
Regional Velocities

Unit	V_P (km/s)	V_S (km/s)	V_P/V_S	Poisson's Ratio (ν)	Reference
Sedimentary	5.55				B
Precambrain basement west of the velocity discontinuity	6.15	3.51	1.75	0.26±.04	B
Precambrain basement east of the velocity discontinuity	6.85	3.91	1.75	0.26±.04	A
	6.9			B	
	6.85	4.03	1.70	0.24±.04	C
	6.8	3.7	1.8	0.28±.04	D

A. Herrmann et al. (1982)
B. Street et al. (1985)
C. Thurber and Bell (1984)
D. This study

AUSTRALIA'S DEEPEST KNOWN EARTHQUAKE

Kevin McCue and Marion Michael-Leiba

Australian Geological Survey Organisation
GPO Box 378, Canberra ACT 2601, Australia

ABSTRACT

Depth phases, pP and sP, of an intraplate earthquake offshore from Arnhem Land, Northern Territory, Australia on 30 September 1992 were recorded on seismographic stations throughout southern Australia and on two stations telemetered to Australia from Antarctica. The computed focal depth is 38.8 (±2.5) km, which is near the crust-mantle boundary, deeper than any other known earthquake in Australia. The near-horizontal principal stress direction, 094°, is similar to that of shallow earthquakes in southwest Australia, but the mechanism has a small dip-slip component in contrast to the predominant thrust mechanism of all past shallow earthquakes that were large enough for mechanisms to have been computed.

INTRODUCTION

Chen and Molnar (1983) and Chen (1988) have discussed intracontinental earthquakes and their possible correlation with heat flow and tectonic age. Evaluation of Australian earthquake focal depths is important not only for constraining physical models of the crust and upper mantle in the region, and for providing insight into causative models of intraplate seismicity but also for establishing appropriate attenuation constants in earthquake hazard estimates.

Few Australian earthquakes have accurately determined focal depths. Body-wave inversion (Fredrich *et al.*, 1988; Choy and Bowman, 1990) and the observation of extensive surface faulting has established that 10 large earthquakes in the Proterozoic and Archaean crust of Central and Western Australia over the last 25 years had focal depths in the range 0 to 13 km, all in the upper crust. Two moderate earthquakes, one off the northwest and the other off the southeast coast had depths of 26 ± 3 and 21 ± 1 km. Dense network monitoring of aftershocks of the 1988 Tennant Creek NT and 1989 Newcastle NSW earthquakes revealed that focal depths at Tennant Creek ranged from the near-surface to 9 km (Bowman *et al.*, 1990; Jones *et al.*, 1991), whereas the single Newcastle aftershock of 29 December 1989 was at 13.8 ± 2 km (Gibson *et al.*, 1990). The focus of the Newcastle earthquakes is near the edge of the continent under a Permian basin in Palaeozoic crust which is about 25 km thick (Collins, 1988).

Depth phases have been observed for few Australian earthquakes, a notable exception being those for the Newcastle mainshock which were particularly well recorded on the British Geological Survey's array in Scotland (McCue *et al.*, 1990). The two PKP branch arrivals were accompanied by the corresponding surface reflections 4 s later which established a focal depth of 11.5 ± 0.5 km, similar to that of the aftershock.

THE OFFSHORE ARNHEM LAND EARTHQUAKE

A magnitude M_L 5.1 earthquake (PDE (NEIS): m_b 5.4, M_S 4.9) occurred at 11 18 07 UTC on 30 September 1992 in the Arafura Sea north of Arnhem Land NT, 425 km ENE of Darwin, the Territory's largest city (Figure 1). The epicenter determined by the authors at 11.35°S, 134.57°E, was based on arrivals from 40 seismographs in Australia, Papua New Guinea and Indonesia. The nearest seismograph was 410 km away and the greatest azimuthal gap was 95° resulting in uncertainties of ±13 km east-west and ±10 km north-south. The magnitude was averaged from amplitudes measured at 10 Australian stations and Port Moresby, Papua New Guinea.

The epicenter of the Arnhem Land earthquake is about equidistant from the southeastern end of the Goulburn graben (Figure 1) and the northwestern end of the Walker Fault Zone. The Goulburn graben contains over 10 km of Palaeozoic sediments that are tilted and folded, and underlain by the Middle Proterozoic strata of the McArthur basin (Moore and Bradshaw, 1991). Late reactivation of faults in the Arafura basin has produced reverse throws in the Jurassic-Cretaceous sedimentary sequence (Moore and Bradshaw, 1991).

From questionnaires and telephone and newspaper reports, an isoseismal map (Figure 1) was compiled. The earthquake was felt most strongly at Nhulunbuy, Milingimbi and Maningrida. At Nhulunbuy assessed intensities varied between III and VI on the modified Mercalli scale; one reliable

DATE: 30 SEPTEMBER 1992   EPICENTRE: 11.35°S 134.57°E   ▲ Epicentre
TIME: 11:18:07 UTC   DEPTH: 38.8 ± 2.5 KM   II Zone of intensity designation
MAGNITUDE: 5.1 ML   2 Earthquake felt (MM)
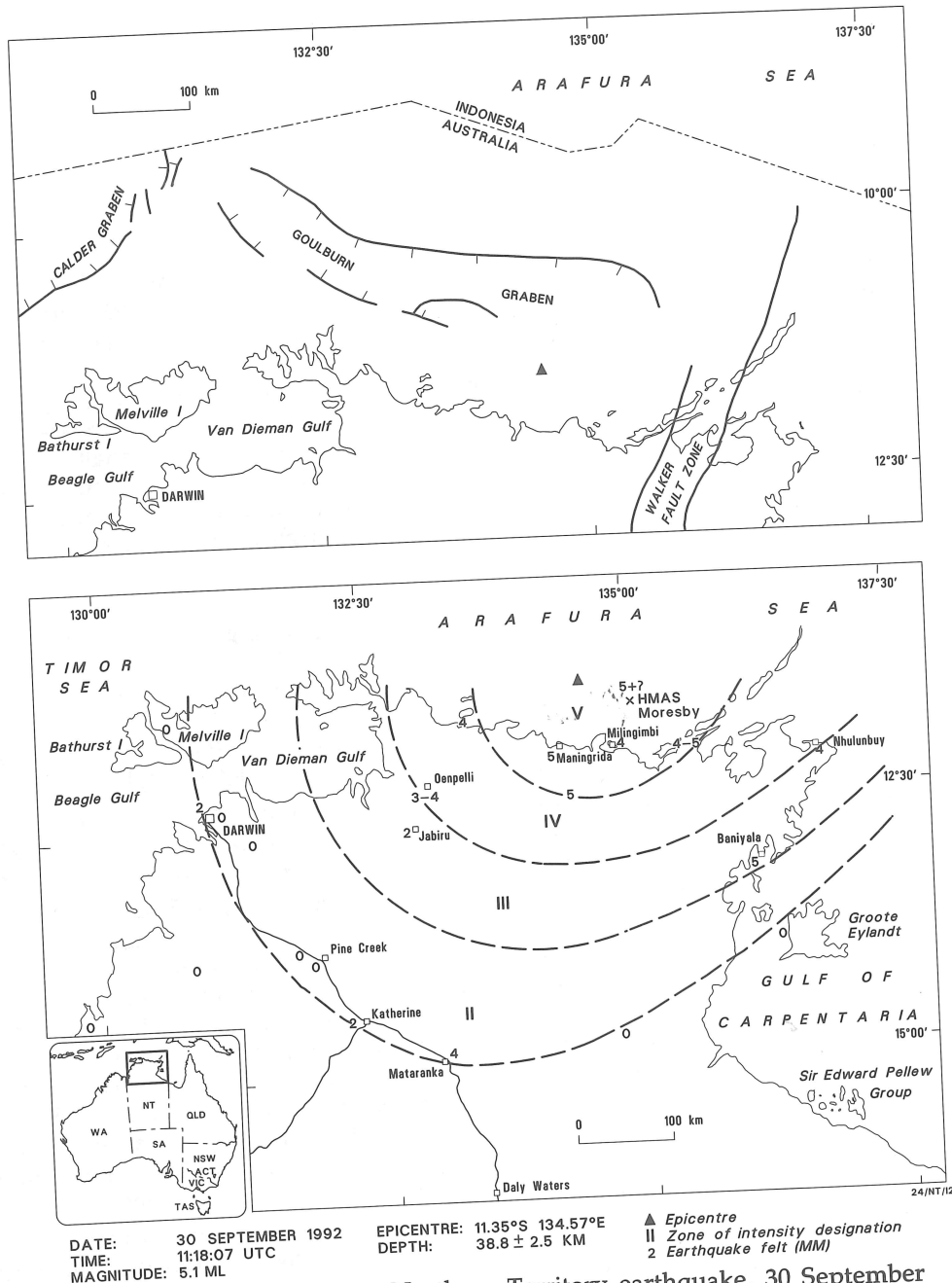
Fig. 1.   The Arafura Sea, Northern Territory earthquake, 30 September 1992.   (a) Epicentral location with gross geological structure and political boundaries   (b) Isoseismal map, modified Mercalli intensity, with approximate position of the ship, HMAS Moresby, and nearest city Darwin.

observer reported seeing waves ripple a concrete pavement and there was a single report of plaster cracks. At Milingimbi and Maningrida, household objects rattled and some people were frightened, but not because the sensation was new as large earthquakes in the Banda Sea arc are felt throughout this part of Australia about once per year on average. The HMAS Moresby, an Australian naval vessel, was anchored off Maningrida in calm water at the time of the earthquake. One

of the ship's officers reported that the ship shook violently and that the shaking was apparently transmitted up the anchor chain. Very few people felt or heard the earthquake in Darwin.

How the seismicity in the region is distributed within the crust and upper mantle is not known. Two small earlier earthquakes nearby, on 8 February 1984 magnitude M_L 4.1, and 3 June 1985 M_L 3.8, were at too great an epicentral distance

from local seismographic stations to constrain their focal depth and not recorded at sufficient distance to see depth phases.

DEPTH PHASES

The depth phases pP and less frequently sP were observed on seismograms across Australia at distances between 19° and 29° (Figure 2), and one of the clearest recordings was on a short-period vertical seismograph at Cairncurran (CRN) in Victoria at an epicentral distance of 26.9°. Both pP and sP phases are clearly seen, 10.5 s and 15 s after the P, and 50 s later still a PP. The short-period record from Adelaide (ADE) South Australia is similar although the pP is not as large and impulsive as that at CRN. But for the pP recorded so clearly at Mawson (MAW) and Casey (CSY) in the Antarctic, these regional depth phases could have been incorrectly identified as reflections from the upper mantle discontinuities, which are visible as a discrete phase group on the closer seismograms recorded on the arrays at Warramunga (WB2) and Alice Springs (ASPA) and the SRO station at Charters Towers (CTA) (Figure 3). Using the IASPEI travel-time tables (Kennett, 1991) for the clearest eleven pP - P and five sP - P times (Table 1), an average focal depth of 38.8 (±2.5) km was obtained.

Published velocity profiles (Jacobson *et al.*, 1979; Rynn and Reid, 1983) indicate that the mantle depth thins from 40 km in the shield to just 34 km in the western Arafura Sea, so this earthquake occurred near the crust/mantle boundary.

FOCAL MECHANISM

Impulsive P-wave first motions on Australian National Seismographic Network stations throughout Australia and Antarctica, supple-

Table 1
Focal depth from depth phases at Australian seismograph stations

Station State*	Distance Δ°	pP-P (sec)	Depth (km)	sP-P (sec)	Depth (km)
Rockhampton Qld (UCQ3)	19.5	9.0	35		
PNA SA	20.8	10.5	43	15.0	39
Wivenhoe Dam Qld (WTG)	23.0	10.8	42		
Wivenhoe Dam Qld (WBA)	23.1	10.7	42		
Sedan SA (SDN)	23.5	10.2	36		
ADE SA	23.8	10.6	38	16.5	42
BWA NSW	26.0	11.1	41		
Cairncurran Vic (CRN)	26.9	10.5	38	15.0	37
CSY Ant	57.3	11.0	37	17.9	44
MAW Ant	72.5	11.8	39		

*Registered Station Code and Australian State, or Antarctica, or Station name, State and (local code)

mented with early bulletins from Indonesian and Thai stations, were sufficient to constrain the mechanism (Figure 4). A predominantly strike-slip solution was obtained with P and T axes plunging at shallow angles in east-west and north-south directions respectively (Table 2). No Harvard centroid, moment tensor was computed.
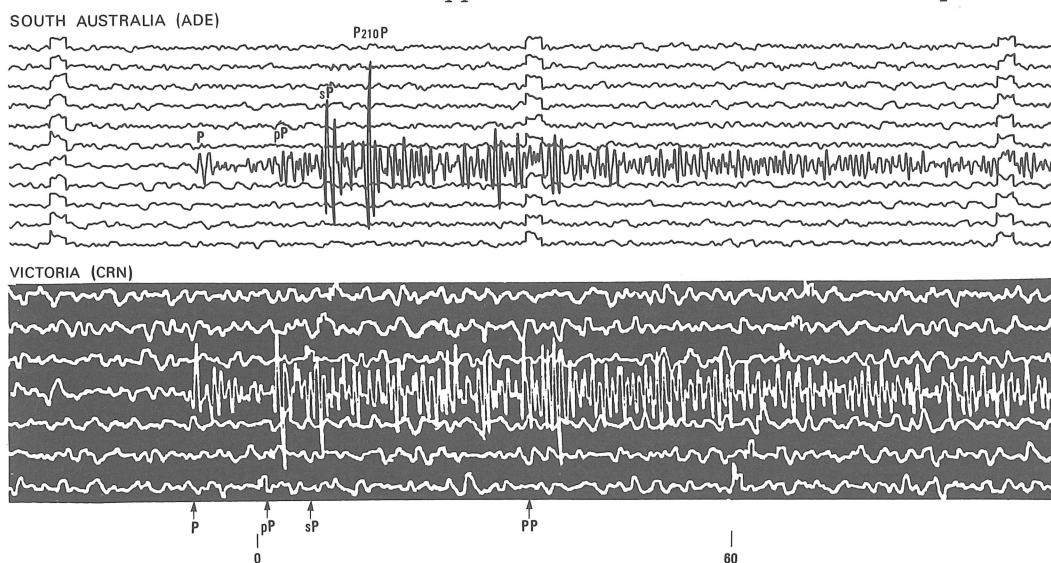

Fig. 2. Short period seismograms at 23.8° (ADE) and 26.9° (CRN) showing clear pP and sP phases as well as a surface reflection and upper mantle discontinuity reflections.
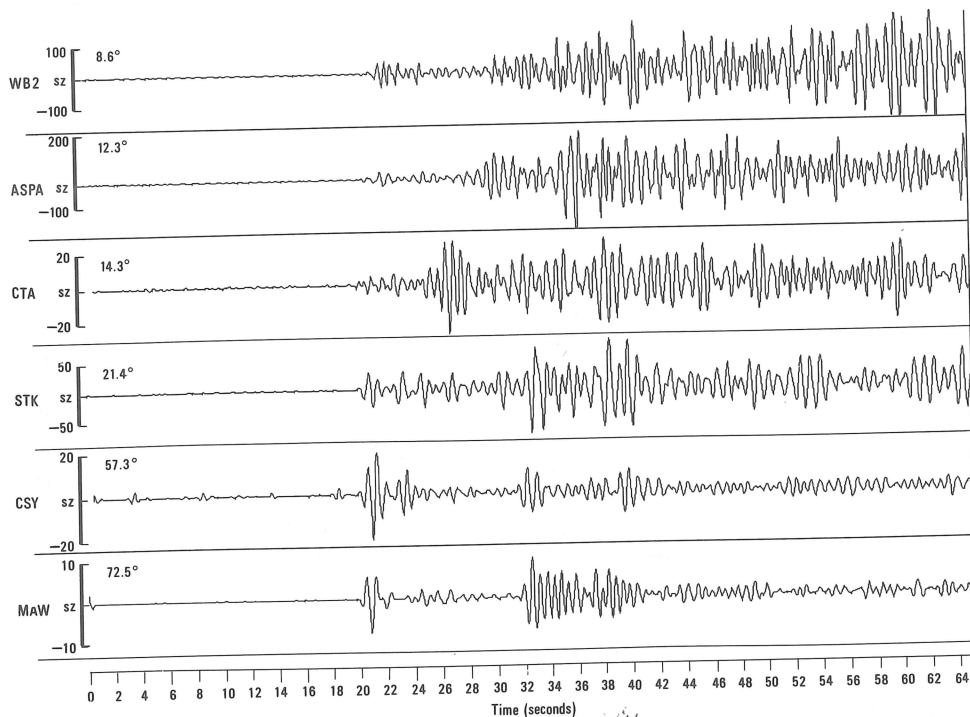
Fig. 3. Sample seismograms on the arrays, ASPA and WRA (WB2) and filtered broad band stations, showing the clear pP on distant seismograms and upper-mantle discontinuity phases on closer seismograms.

Table 2
Focal mechanism solution, Arnhem Land earthquake

	Azimuth/strike	Dip
Stress axis		
P	094	19
T	000	17
B	233	65
Nodal planes		
1	049	88
2	138	64

The nodal planes both dip steeply so the earthquake was not caused by slip on the crust - upper mantle interface. The northwest trending nodal plane parallels the strike of the Goulburn graben but it dips to the southwest, opposite that of the closest graben boundary fault.

The nearest measurements of crustal stress, 600 km to the west in the Timor Sea (Hillis and Williams, 1992) and a comparable distance to the south near Tennant Creek (Jones et al., 1991), are quite similar, and each indicate that the greatest compressive principal stress axis in the upper crust has a northeast-southwest strike. The Timor Sea results were derived from the orientation of wellbore break-outs whilst the Tennant Creek data are from the study of the focal mechanisms of three large earthquakes in 1988 and nearby over-coring tests in a mine. These widely spaced stress measurements made in different ways indicate that the stress orientation in the upper crust is uniform over a large area of northwest Australia. The east-west orientation of P in the lower crust or upper mantle reported here appears to be rotated 45° clockwise from that in the upper crust but this single observation may not be significant.
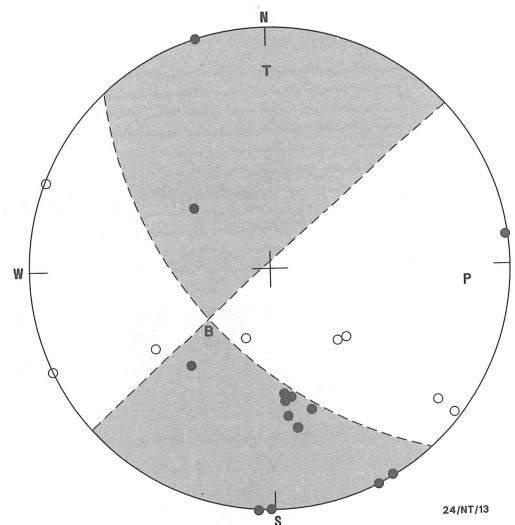

Fig. 4. Fault plane solution, lower hemisphere projection; P,T and B are the principal stress axes, closed and open circles represent compressions and dilatations respectively on short period seismograms.

204

What is different is the interchange of the B and T axes, converting the thrust mechanisms in the upper crust to a strike-slip mechanism in the lower crust or upper mantle which indicates that some bending of the crust is occurring, perhaps in response to subduction at the closest plate boundary.

DISCUSSION

Stress in the upper crust of Australia seems to be everywhere compressive (Denham and Windsor, 1991), but the direction of the P-axis, whilst constant over large crustal areas or domains, varies from one domain to another. The east-west P-axis orientation of the Arnhem Land earthquake is the same as that in the Archaean shield of Western Australia. P is oriented southeast-northwest in the Palaezoic crust of south-eastern Australia, and north-northeast in the Proterozoic crust of central Australia. Whether the stress pattern in the Australian crust influences the location of earthquakes, their frequency and style of faulting is not yet clear; available stress measurements are too sparse.

Heat flow measurements in Ausralia (Cull, 1982) show that surface heat flow is higher in eastern Australia than in the west. Furthermore, seismic travel time residuals are negative in the west and zero or positive in the east. Together these are indicative of a low velocity layer in the upper mantle under eastern Australia which is supported by surface wave studies (Muirhead and Drummond, 1991). The Eastern Australian lower crust is consequently hotter and more ductile than that under Western Australia (Drummond *et al.*, 1989). To date no earthquakes are known to have occurred at comparable depths in Eastern Australia.

Whether this Arnhem Land earthquake occurred in the lower crust or upper mantle is not known.

The epicenter is between the 60 and 80 mW/m^2 heat flow contour of Cull (1982), the second 'deep' earthquake near a low to moderate heat flow. With the shallow Tennant Creek sequence from 1987 to the present near a heat flow high, and those near Newcastle at mid-crustal depth with low heat flow, there is not much evidence of a correlation between maximum focal depth and heat flow in Australia, as Chen (1988) acknowledges.

ACKNOWLEDGMENTS

REFERENCES

Bowman, J.R., G. Gibson, and T. Jones (1990). Aftershocks of the 22 January 1988 Tennant Creek, Australia intraplate earthquake: evidence for a complex fault geometry, *Geophys. J. Int.* **100**, 87-97.

Chen, W.-P. (1988). A brief update on the focal depths of intracontinental earthquakes and their correlations with heat flow and tectonic age, *Seism. Res Lett.* **59**, 263-272.

Chen, W.-P. and P. Molnar (1983). Focal depths of intracontinental and intraplate earthquakes and their implications for the thermal and mechanical properties of the lithosphere, *J. Geophys. Res.* **88**, 4183-4214.

Choy, G.L., and R.L. Bowman (1990). Rupture process of a multiple main shock sequence: analysis of teleseismic, local, and field observations of the Tennant Creek, Australia, earthquakes of January 22, 1988, *J. Geophys. Res.* **95**, 6867-6882.

Collins, C.D.N. (1988). Seismic velocities in the crust and upper mantle of Australia, *BMR Geol. Geophys. Aust. Report 277*.

Cull, J. P. (1982). An appraisal of Australian heat flow data, *BMR J. Aust. Geol. Geophys.* **7**, 11-21.

Denham, D., and C. R. Windsor (1991). The crustal stress pattern in the Australian continent, *Expl. Geophys.* **22**, 101-106.

Drummond, B. J., K. J. Muirhead, C. Wright, and P. Wellman. (1989). A teleseismic travel time residual map of the Australian continent, *BMR J. Aust. Geol. Geophys.* **11**, 101-105.

Fredrich, J., R. McCaffrey, and D. Denham (1988). Source parameters of seven large Australian earthquakes determined by body wave inversion, *Geophys. J.* **95**, 1-13.

Gibson, G., V. Wesson, and K. McCue (1990). The Newcastle earthquake aftershock and its implications, in *Conference on the Newcastle Earthquake, 15-17 February 1990.*, R.E. Melchers ed., Institution of Engineers, Australia, 90/15, 14-18.

Hillis, R.R., and A.F. Williams (1992). Borehole breakouts and stress analysis in the Timor Sea, in *Geological Applications of Wireline Logs II*, Hurst, A., C.M. Griffiths, and P.F. Worthington eds., Australian Geological Society Special Publication 65, 157-168.

Jacobson, R.S., G.G. Shor, R.M. Kieckhefer, and G.M. Purdy (1979). Seismic reflection and

refraction studies in the Timor trough system and Australian continental shelf, *Amer. Assoc. Petrol. Geolog. Memoir* **29**, 209-222.

Jones, T.D., K.F. McCue, D. Denham, P. Gregson, R. Bowman, and G. Gibson (1991). Three large intraplate earthquakes near Tennant Creek, Northern Territory on 22 January 1988, *BMR J. Aust. Geol. Geophys.* **12**, 339-344.

Kennett, B.L.N., (ed.), (1991). *IASPEI 1991 Seismological Tables*, Research School of Earth Sciences, Australian National University, 167 pp.

McCue, K.F., V. Wesson, and G. Gibson, (1990). The Newcastle, New South Wales, earthquake of 28 December 1989, *BMR J. Aust. Geol. Geophys.* **11**, 559-568.

Moore, A., and J. Bradshaw (1991). Arafura Sea - seismic reconnaissance with geochemistry, *Yearbook of BMR Geol. Geophys. Aust.* **BMR91**, 40-41.

Muirhead, K.J., and B.J. Drummond (1991). The base of the lithosphere under Australia, *Geol. Soc. Aust. Spec. Publ.* **17**, 23-40.

Rynn, J.M.W., and I.D. Reid (1979). Crustal structure of the western Arafura Sea from ocean bottom seismograph data, *J. Geol. Soc. Aust.* **30**, 59-74.

DID (OR WILL) FLUID INJECTION CAUSE EARTHQUAKES? - CRITERIA FOR A RATIONAL ASSESSMENT

Scott D. Davis* and Cliff Frohlich

*Institute for Geophysics
University of Texas at Austin
8701 North Mopac Blvd.
Austin, Texas 78759*

ABSTRACT

Occasionally, the injection of fluids into deep wells causes or triggers earthquake activity. We propose two lists of yes-or-no questions to assess 1) whether an ongoing injection project has induced an earthquake that has already occurred; or 2) whether a proposed injection project is likely to induce a nearby earthquake. The answers to these questions form a descriptive profile of the injection project that facilitates comparison with other projects. To illustrate the application of these questions, we describe the answers in detail for the first set of questions at two sites: 1) the Rocky Mountain Arsenal near Denver, Colorado, where three significant earthquakes occurred in 1967; and 2) an injection site near Painesville, Ohio, near the epicenter of an earthquake that occurred 31 January, 1986. We also present a table of answers to these questions for several additional sites, and review other factors that may affect the potential for induced seismic activity. The profiles of injection sites presented herein provide a convenient tool for deciding whether an injection site more closely resembles other sites where injection does, or does not induce earthquakes.

INTRODUCTION

Since 1966, when Evans (1966) established that injection of waste fluids in a deep well near Denver induced earthquakes, scientists have generally agreed that injection may induce earthquakes in tectonically favorable situations. In the interim, there have been numerous other case studies where the injection of fluids into the crust apparently caused earthquakes. The primary objective of this paper is to suggest criteria that we as professional seismologists can apply to assess seismic hazard from fluid injection. Also, as a resource for assessing cases of possible induced activity, we provide relevant information for 20 case studies in which investigators have suggested a connection between injection and earthquakes.

Although felt earthquakes are rare in many areas, they do occur occasionally nearly everywhere; indeed, the historical record contains earthquake reports from all 50 states. The practice of fluid injection for waste disposal or petroleum recovery is also common; in some states there are thousands of injection wells. Thus when an earthquake does occur near a site of fluid injection, it is reasonable to ask whether the injection caused or triggered it. In addition, when an injection project is proposed there may be public concern that damaging earthquakes may result.

In particular, as earthquake seismologists we should be prepared to address the following questions:

Situation 1) If injection is ongoing and an earthquake has occurred: *Did this injection project induce the earthquake activity?*

Situation 2) If injection is proposed and earthquake hazard is uncertain: *Is this injection project likely to induce damaging seismic activity?*

In each case, there are compelling social and economic incentives for finding the best possible answers to these questions. We have assisted in the evaluation of several injection projects, both in the presence and absence of possible related seismic activity. The present paper summarizes our approach to providing reasonable answers to the questions posed above (Davis, 1985; 1989; Davis and Frohlich, 1987; 1988; Davis and Pennington, 1989).

We first present seven questions (Table 1) for assessing whether an ongoing fluid injection project may have induced an earthquake (Situation 1 above). These questions address four factors: 1) the historical seismicity of the region, 2) the presence or absence of correlation between injection

---

*Presently at U. S. Geologcial Survey, Memphis State University/CERI, Memphis, TN 38152

and seismic activity, 3) the geographical and geological relationship between the sites of injection and seismic activity, and 4) the expected effect of fluid injection on the stress regime at the injection sites. We have phrased these questions so that a "yes" answer supports injection as the cause of the earthquake, while a "no" answer suggests that injection is not the cause.

We then answer these seven questions for 20 earthquake sequences (Tables 2 and 3), including a fictional account of seismicity induced by injection down a deep well near Boston, Massachusetts (Franzen, 1992). Many of these earthquake sequences are clearly induced by injection, while for other sequences the causal relationship between injection and earthquakes is less clear. To illustrate the use of these questions we give detailed justifications for our yes-or-no answers at two injection sites: Denver, Colorado, and Painesville, Ohio. Although the individual yes-or-no questions may be somewhat subjective, we would argue that the cumulative effect of the entire series provides a basis for an informed judgement about the relation of the earthquakes to the injection. While there is no specific number of "yes" answers which constitutes proof that injection caused an earthquake sequence, generally more "yes" answers make it more likely that injection is

responsible. Our practical result is that in every case we studied where five or more of the questions had "yes" answers, most professional seismologists would conclude that injection induced the earthquake sequence (Table 2).

Finally, we present a second list of ten questions (Table 4) that evaluate whether a proposed injection project is likely to induce an earthquake (Situation 2 above). From the profile developed above, we conclude that prior to injection, Denver would have received four "yes" answers to these questions. To further illustrate the method, we give answers for two other sites: Tracy, Quebec, and Texas City, Texas.

At present it is impossible to predict the effects of injection with absolute certainty. This uncertainty arises both because the underlying physical mechanisms of earthquakes are poorly understood, and because in nearly every specific situation there is inadequate or incomplete information about regional stresses, fluid migration, historical seismicity, etc. Clearly, a series of seven or ten yes-or-no questions oversimplifies many of these issues. Thus, these profiles should not be used as an absolute predictor of whether fluid injection at a particular site will induce earthquakes. Rather, they provide a means for comparing specific injection projects with others that have

Table 1
Seven Questions Forming a Profile of a Seismic Sequence

Question	Earthquakes Clearly NOt Induced	Earthquakes Clearly Induced	I Denver, Colorado	II Painesville Ohio
Background Seismicity				
1 Are these events the first known earthquakes of this character in the region?	NO	YES	YES	NO
Temporal Correlation				
2 Is there a clear correlation between injection and seismicity	NO	YES	YES	NO
Spatial Correlation				
3a Are epicenters near wells (within 5 km)?	NO	YES	YES	YES?
3b Do some earthquakes occur at or near injection depths?	NO	YES	YES	YES?
3c If not, are there known geologic structures that may channel flow to sites of earthquakes?	NO	YES	NO?	NO?
Injection Practices				
4a Are changes in fluid pressure at well bottoms sufficient to encourage seismicity?	NO	YES	YES	YES
4b Are changes in fluid pressure at hypocentral locations sufficient to encourage seismicity?	NO	YES	YES?	NO?
TOTAL "YES" ANSWERS	0	7	6	3

Table 2
Locations of Possible Injection-Induced Earthquakes Examined

SITE	Maximum Magnitude	Date[1]	Injection Depth (km)	Focal[2] Mech	Surface[3] Pres. (bars)	YES[4] Answers
WASTE DISPOSAL						
Denver RMA, Colorado	5.3-5.5	08 / 67	3.7	N / SS?	?	6
El Dorado, Arkansas	3.0	12 / 83	2.2	?	20 - 60	7
Painesville, Ohio	5.0	01 / 86	1.8	SS	110	3
Peabody, Massachusetts[5]	6.1	06 / 92	7.6 ?	TH	?	(3)
SECONDARY RECOVERY / PRESSURE MAINTENANCE						
Ashtabula County, Ohio	3.6	07 / 87	1.8	SS	100	5
Cogdell Oil Field, Texas	4.6	06 / 78	2.1	N	184	5
The Geysers, California	4.0 ?	09 / 92	1.7 - 2.5	N / SS	0	6
Gobles Oil Field, Ontario	3+	08 / 81	0.9	N / TH	?	(2)
Los Angeles Basin, California	3.2	05 / 71	0.9 - 1.5	N?	?	(2)
Rangely, Colorado	3.4	08 / 64	1.7	SS	72	6
Sleepy Hollow, Nebraska	2.9	07 / 79	1.1 - 1.2	?	50	(3)
SOLUTION MINING / ACID TREATMENT						
Beowawe, New Mexico	-1	08 / 83	1.3	?	~ 100	(4)
Dale, New York	0.8	11 / 73	0.4	TH	129	7
EXPERIMENTAL / INJECTION TESTS / HYDRAULIC STIMULATION						
Baca, New Mexico	-2	05 / 82	1.7	?	?	6
Fenton Hill, New Mexico	-2	12 / 83[6]	2.7 - 3.5	N / LP	45 - 50	6
Matsushiro, Japan	2.8	01 / 70	1.8	SS	50	(3)
Orcutt Oil Field, California	3.5	01 / 91	0.1 - 0.3	TH	80	7
Puhagan field, Philippines	2.4	05 / 83	~ 1	N	< 10	6
Soultz-Sous-Forets, France	?	12 / 88	2.0	?	82	6
Wairakei, New Zealand	3.0	06 / 84	1.3	SS?	20 - 30	(4)

[1]Date of the largest event or injection experiment.

[2]Focal Mech is the focal mechanism: LP = Long Period Tensile Events, N = Normal, SS=Strike-Slip, TH = Thrust, ? = Unknown or not available.

[3]Surface Pres is a typical surface injection pressure (bars) for that site.

[4]YES Answers denotes number of criteria questions answered "Yes" in Table 3; parentheses indicate 3 or more questions were unanswered, or 5 or more questions were uncertain or unanswered.

[5] fictional account

[6] one of several injection periods

or have not induced earthquakes.

However, we make no apologies for our approach. In our experience these yes-or-no profiles do provide a convenient way of applying current scientific knowledge to these problems and communicating this information to the public. Moreover, our description of how we arrived at the profiles for sites in Colorado, Quebec, Ohio, and Texas provides examples of many of the difficulties one may encounter when assessing injection sites.

In some cases, it may be useful to make a distinction between earthquakes as either "triggered" or "induced", depending on what fraction of energy released in the earthquake was created artificially. Using the terminology of McGarr (1991), "triggered" earthquakes would include cases where most of the energy accumulated naturally by geologic forces, whereas "induced" earthquakes would only include those in which most of the energy release could be directly related to man-made sources. However, the magnitudes of in situ principal stresses are often poorly known (Zoback and Zoback, 1980); thus in practice this distinction is not always clear. Consequently, in this report we use the term "induced" to include both "triggered" and "induced" earthquakes.

Several recent studies also describe earthquakes caused by the withdrawal of fluids (Pennington et al., 1986; Segall, 1989; Grasso and Wittlinger, 1990; Doser et al., 1991). However, in this paper we will not discuss the effects of production or withdrawal on seismic activity, as our focus is the evaluation of seismic hazard from fluid injection.

SITUATION 1: DID INJECTION INDUCE EARTHQUAKES?

Seven Questions

In this section we discuss seven questions (Table 1) that address the four factors mentioned above concerning the relationship between an earthquake and ongoing injection activity. We have phrased these questions so that the answers will be "yes" for earthquakes clearly induced by injection, and "no" for an earthquake apparently unrelated to fluid injection. In many instances, the case for a particular "yes" or "no" answer is uncertain because of incomplete or conflicting information, and we denote these less certain answers with question marks -- "yes?" or "no?".

To illustrate the application of these questions, we discuss how we arrived at the answers for the earthquake sequence that occurred at the Rocky Mountain Arsenal near Denver, Colorado (Healy et al., 1968; Hsieh and Bredehoeft, 1981). In 1961, the Army Corps of Engineers drilled a well to a depth of 3671 m into crystalline Precambrian basement; injection for waste disposal began in 1962. Beginning in 1962, a series of earthquakes occurred near the well, with the three largest earthquakes having estimated magnitudes of 5 and above (Healy et al., 1968).

For contrast, we also discuss our answers for a sequence of earthquakes that occurred in 1986 near Painesville, Ohio. This sequence included an mb=5.0 event within 17 km of a nuclear power plant. While some (Ahmad and Smith, 1988) have suggested that injection at three waste disposal wells may have triggered the earthquakes, other studies have favored a natural, tectonic origin for the seismicity (Nicholson et al., 1988; Talwani and Acree, 1986; Wesson and Nicholson, 1986).

Question 1 (Background Seismicity): Are these events the first known earthquakes of this character in the region?

Clearly, if earthquakes occur regularly in the target region, the occurrence of an earthquake sequence near an injection well is not strong evidence for a causal relationship unless the character of the earthquake is unusual. In Denver, there may have been occasional very small earthquakes, and a possible larger earthquake occurring in 1882 (Coffman et al., 1982); however, the sequence beginning in 1962 was clearly anomalous in that the events were so numerous, and so widely felt.

Table 3

Yes-and-no profiles (as described in Table 1) for the 20 sites of possible injection induced seismicity listed in Table 2.

Site	1 Historical Earthquakes	2 Temporal Correlation	3a Earthquake Epicenters	3b Earthquake Depths	3c Geologic Structures	4a Pressures (Well)	4b Pressures (Hypocenters)
WASTE DISPOSAL							
Denver RMA, Colorado	YES	YES	YES	YES	NO?	YES	YES?
El Dorado, Arkansas	YES	YES	YES	YES	YES	YES?	YES?
Painesville, Ohio	YES	YES?	YES?	YES?	NO?	YES	NO?
Peabody, Massachusetts	NO	NO	YES?	YES?	YES?	?	?
SECONDARY RECOVERY / PRESSURE MAINTENANCE							
Ashtabula County, Ohio	YES	NO?	YES	YES	NO?	YES	YES
Cogdell Oil Field, Texas	YES	NO	YES	YES	-	YES	YES
The Geysers, California	NO	YES	YES	YES	YES	YES?	YES?
Gobles Oil Field, Ontario	?	NO	YES	YES	NO	?	?
Los Angeles, California	NO	NO?	YES	NO	YES?	?	?
Rangely, Colorado	?	YES	YES	YES	YES	YES	YES
Sleepy Hollow, Nebraska	?	NO?	YES	YES	YES?	?	?
SOLUTION MINING / ACID TREATMENT							
Beowawe, New Mexico	?	YES?	YES	YES	YES	?	?
Dale, New York	YES	YES	YES	YES	YES	YES	YES
EXPERIMENTAL / INJECTION TESTS / HYDRAULIC STIMULATION							
Baca, New Mexico	?	YES	YES	YES	YES	YES?	YES?
Fenton Hill, New Mexico	?	YES	YES	YES	YES?	YES	YES
Matsushiro, Japan	NO	NO?	YES	YES	YES	NO?	NO?
Orcutt Oil Field, California	YES	YES?	YES	YES	YES	YES?	YES?
Puhagan field, Philippines	YES?	YES?	YES	YES	YES	YES?	NO?
Soultz-Sous-Forets, France	?	YES	YES	YES	YES	YES?	YES?
Wairakei, New Zealand	NO?	YES?	YES	?	YES	YES?	?

Table 4
Criteria to Determine if Injection May Cause Seismicity

Question	NO APPARENT RISK	CLEAR RISK	Texas City, Texas	Tracy Quebec	Denver RMA, Colorado
Background Seismicity					
1a Are large earthquakes (M ≥ 5.5) known in the region (within several hundred km)?	NO	YES	NO	YES	YES
1b Are earthquakes known near the injection site (within 20 km)	NO	YES	NO	YES	NO?
1c is rate of activity near the injection site (within 20 km) high?	NO	YES	NO	NO	NO
Local Geology					
2a Are faults mapped within 20 km of the site?	NO	YES	YES	YES	NO?
2b If so, are these faults known to be active?	NO	YES	NO	NO	NO
2c Is the site near (within several hundred km of) tectonically active features?	NO	YES	NO?	YES	YES
State of Stress					
3 Do stress measurements in the region suggest rock is close to failure?	NO	YES	NO	NO?	YES[1]
Injection Practices					
4a Are (proposed) injection practices sufficient for failure?	NO	YES	NO?	YES	YES[1]
4b If injection has been ongoing at the site, is injection correlated with the occurrence of earthquakes?	NO	YES	NO	N.A.	N.A.
4c Are nearby injection wells associated with earthquakes?	NO	YES	NO	N.A.	N.A.
TOTAL "YES" ANSWERS	0	10	1	5	4

[1]Assumes stress measurements completed prior to survey

This was clearly the first documented sequence of this character for the region. [Answer: DENVER = YES]

In Ohio, the historical record shows that earthquakes having Mercalli Intensity IV or V were felt in northwestern Ohio in 1906, 1928, 1943, and 1958 (Coffman et al., 1982). The 1943 event, with intensity V, has been relocated near the epicenter of the 1986 event (Dewey and Gordon, 1984), and had a comparable magnitude. These data suggest that similarly felt earthquakes occur approximately every twenty years in this region, and thus the occurrence of an intensity VI event in 1986 is not in and of itself unusual. [Answer: OHIO = NO]

Question 2 (Temporal Correlation): Is there a clear correlation between the time of injection and the times of seismic acitivity?

Even if we lacked a clear scientific understanding of the processes causing earthquakes, most people would be convinced of a causal relationship if the seismicity "turned on" when injection began and "turned off" when injection stopped. In Denver, scientists were able to establish a clear relationship between the volume of injection and the number of seismic events, with a time lag of about ten days (Healy et al., 1968). More recently,

Hsieh and Bredehoeft (1981) were able to explain the spatial and temporal extent of seismic activity in Denver in terms of the flow of fluids along a permeable semi-infinite rectangular region which approximately contained the activity. Earthquakes occurred when fluid pressures in the model had increased approximately 32 bars or more above hydrostatic. [Answer: DENVER = YES]

In Ohio, injection had been ongoing for about 15 years before the recent sequence of earthquakes began. As felt earthquakes have occurred approximately every 20 years in this area, we cannot easily attribute the 1986 event to the onset of injection. [Answer: OHIO = NO]

Question 3a (Spatial Correlation): Are epicenters near the wells?

It is more plausible that deep well injection triggers earthquakes if we can establish that the injection would cause fluid pressure increases at hypocentral distances. In Denver, most of the epicenters were within 8 km of the well, and several were within 2 km. The average distance was about 4 km. There was also an apparent migration of activity away from the well as time passed. [Answer: DENVER = YES].

In Ohio, two small earthquakes in 1983 (magnitudes 2.5 and 2.7) had reported epicenters within 5 km of one of the injection wells; however, these locations are uncertain (Nicholson et al., 1988). The mainshock on 31 January 1986 and all but one of its immediate aftershocks occurred at distances of about 10 to 15 km from the well. The single exception was an aftershock with magnitude -0.2 which occurred on 12 March 1986 about 3 km from the well. Between April 1986 and April 1987, several small (magnitude 1.0 or less) earthquakes were located near one of the injection wells (see addendum in Nicholson et al., 1988). Apart from these events, which may not have been detected if the network had not been installed due to the 31 January 1986 event, the aftershocks seem too distant to have been affected by fluid injection if the fluids behave as expected for radial fluid flow models. Nevertheless, we assign a tentative "yes?" answer as some earthquakes do occur near the injection site, although it is not clear if these earthquakes are related to the magnitude 5.0 earthquake. [Answer: OHIO = YES?]

Question 3b (Spatial Correlation): Do some earthquakes occur at depths comparable to the depth of injection?

Induced earthquakes would be most likely to occur close to the injection well or nearby at similar depths if the injectate flows along approximately horizontal strata. In Denver, earthquakes did occur near the injection depth, although some occurred at shallower depths and some occurred up to about 3.3 km deeper than the well. [Answer: DENVER = YES]

In Ohio, the majority of aftershocks occurred in the vicinity of the hypocenter of the 31 January 1986 earthquake, with depths about 3 km deeper than the injection point. However, several small earthquakes were also subsequently located near the injection well, and at depths of 2 km or less. Although it is not clear if there is a connection between the two sets of earthquakes, we assign a tentative "yes?" on the basis of these shallow events. [Answer: OHIO = YES?]

Question 3c (Local Geology): If some earthquakes occur away from wells, are there known geologic structures that may channel fluid flow to the sites of the earthquakes?

Fluid pressure might affect activity at considerably greater distances if there are geological structures that channel pressure increases toward the hypocentral region, making a radial flow model inappropriate. At Denver no such structure has been mapped, although some investigators have postulated the existence of a fault or fracture system on the basis of earthquake focal mechanisms, hypocentral locations, and fractures observed in well cores and in neighboring rocks (Hsieh and Bredehoeft, 1981). A seismic reflection survey reported several minor faults with displacement less than 30 meters in the epicentral region (Healy et al., 1968), although the nearest well-mapped faults are over 30 km to the northwest (Hsieh and Bredehoeft, 1981). [Answer: DENVER = NO?]

In Ohio, there are no known structures that should channel fluid flow in either the Precambrian basement or in the overlying Paleozoic strata. Ahmad and Smith (1988) propose the existence of a fault zone on a weak linear trend in the aftershock locations, an observed magnetic anomaly, the isoseismal pattern of the 31 January earthquake, and slight variations in basement topography. However, Roeloffs et al. (1989) find no evidence for anisotropic permeability in their hydrologic modelling. As the contact between the Precambrian and the Paleozoic strata is very nearly horizontal and there are no mapped faults in this region, we assign a tentative "no?". [Answer: OHIO = NO?]

Question 4a (Injection Practices): Are changes in fluid pressure sufficient to encourage seismic or aseismic failure at the bottom of the well?

Clearly, for any reasonable hydrological model, the largest pressure increases will occur in close proximity to the well bottom. If well bottom pressures are insufficient to induce failure, it is unlikely that the lower fluid pressures found at hypocentral distances will induce earthquakes. The Mohr-Coulomb model is the most common method for evaluating shear failure induced by increases in pore fluid pressure (e.g. Davis and Pennington, 1989; Nicholson and Wesson, 1990). According to the Mohr-Coulomb failure criterion, the critical shear stress t_{crit} needed to cause slip on a fault is related to the normal stress σ_n across the fault, the fluid pressure p, the coefficient of friction μ_f, and the inherent shear strength τ_0 of the rock by the equation:

$$\tau_{crit} = \tau_0 + \mu_f (\sigma_n - p)$$

This criterion appears as a straight line on a Mohr circle diagram (Figure 1), and the crustal state of stress can be described as a circle that intersects the normal stress axis at $(\sigma_1 - p)$ and $(\sigma_3 - p)$, where σ_1 and σ_3 are the maximum and minimum principal stresses, respectively (Hubbert and Rubey, 1959). Thus, an increase in fluid pressure has the effect of shifting the Mohr circle to the left, or closer to failure.

In both Denver (Healy et al., 1968) and Ohio (Nicholson et al., 1988), calculations that utilize the available estimates of tectonic deviatoric stresses, the known or probably injection pressures, and the Mohr-Coulomb failure law, suggest that it is plausible that failure would occur near the bottom of the injection well. [Answer: DENVER = YES, OHIO = YES]

with displacem...
entral region (He...
earest well-mapp...
orthwest (Hsieh a...
ENVER = NO?]

own structures t...
either the Preca...
ing Paleozoic stra...
ose the existence...
r trend in the ...
magnetic anoma...
31 January ear...
ns in basem...
fs et al. (1989) fi...
ermeability in th...
contact between ...
strata is very nea...
apped faults in t...
e "no?". [Answ...

Are changes in fl...
seismic or aseis...

nable hydrologi...
reases will occu...
om. If well bott...
nduce failure, it...
pressures found...
nduce earthquak...
the most comm...
failure induced ...
re (e.g. Davis a...
nd Wesson, 199...
nb failure criteri...
ded to cause slip...
stress σ_n across t...
e coefficient of f...
r strength τ_0 of t...

$-p)$

ight line on a M...
the crustal state ...
rcle that interse...
and (σ_3-p), wh...
d minimum prin...
bbert and Rub...
id pressure has ...
rcle to the left, ...

al., 1968) and O...
tions that utilize t...
deviatoric stress...
pressures, and t...
gest that it is pl...
near the bottom ...
DENVER = YE...

Question 4b (Injection Practices): Are changes in fluid pressure sufficient to encourage seismic or aseismic failure at the hypocentral locations?

In order to determine if fluid pressures at the locations and depths where earthquakes occur are sufficient for failure, it is usually necessary to perform some kind of hydrologic modelling. Because the geologic settings at different injection sites are so varied, no single hydrologic model will be appropriate for every case study. Nicholson et al. (1988) present a detailed account of fluid pressure calculations for the Painesville, Ohio site, and compare results for two models: one for an infinite, isotropic reservoir; and one for a reservoir of infinite length but finite rectangular cross section.

In both Denver and Ohio, hydrologic calculations suggest that if the fluid flows in a radial pattern the change in pressures would be too small to induce seismic activity. However, in both cases it was possible to achieve a sufficient increase in pressure at the hypocenter if fluid flow was confined to a favorably oriented zone of rectangular cross sectional area, in approximate coincidence with the zone of earthquake activity. For Denver, a reservoir of 3.35 km width, based on earthquake locations and on long term declines in fluid levels, was sufficient to explain the observed seismicity (Hsieh and Bredehoeft, 1981). For Ohio, the calculations only achieved large pressure increases if flow was confined to a narrow strip approximately km wide; however, the observed well response was more consistent with radial flow (Nicholson et al., 1988). [Answer: DENVER = YES?, OHIO = NO?]

Profile of Induced Seismic Activity

We now apply the above seven questions to 20 seismic sequences which are possibly related to well injection (Tables 2 and 3). Our purpose is to obtain a profile of induced seismic activity as measured by these questions. To answer these questions we thoroughly evaluated the available published literature concerning these sequences (see Appendix).

Of the 20 sequences considered, profiles for twelve sites (Ashtabula, Baca, Cogdell, Dale, Denver, El Dorado, Fenton Hill, The Geysers, Orcutt, Puhagan, Rangely, and Soultz-Sous-Forets) have five or more "yes" answers. We conclude that there is strong evidence that these sequences are related to the injection process. At two other sites (Beowawe and Wairakei), there were four "yes" answers, suggesting a link between injection and seismicity, although incomplete or conflicting evidence makes the relation somewhat more ambiguous.

For the remaining seven sequences, we found three or fewer "yes" answers. In many of these cases the only strong evidence favoring an

---

injection-induced cause is that earthquakes occurred near injection wells. Thus the presently available data do not encourage us to conclude that these sequences are induced by injection.

Several of the answers listed in Table 3 are open to some interpretation. For example, at Matsushiro, Ohtake (1974) reports a correlation between the timing of activity and injection as well as an apparent migration of activity away from the well following injection. However, we have carefully read Ohtake's paper, and we feel the correlation between injection and seismic activity is not nearly so clear as he reported (see Appendix). Thus, with only three "yes" answers, we conclude that it is questionable whether the Matsushiro events are induced by injection.

In several cases, incomplete information prevents us from answering one or more of the questions, and thus the relationship between injection and seismicity remains inconclusive. For example, we assigned only three "yes" answers for the fictional account by Franzen (1992). However, no injection data (volume or pressures) were available in that account, although it seems probable from the novel that injection volumes were substantial. If a study of the injection showed it to be sufficient to cause failure, the additional "yes" answers for questions 4a and 4b would produce a profile suggesting the earthquakes were induced.

Finally, we note that any profile is open to revision if new information or evidence becomes available. For example, a profile of the Painesville site made shortly after the 31 January 1986 earthquake (Frohlich and Davis, 1987) contained 6 "no" answers and only one "yes" answer, with the sole "yes" answer given because well-bottom pressures were high enough to cause failure (question 4a). During the following year, however, several small (magnitude 1.0 or less) earthquakes were located in the vicinity of the injection well, making a stronger (but still inconclusive) case for relating the earthquakes to injection.

SITUATION 2:
WILL INJECTION INDUCE EARTHQUAKES?

Ten Questions

In this section we present ten questions (Table 4) which concern whether a proposed injection project may induce damaging earthquake activity. The questions in Table 4 are similar to those in Table 1 in that they again evaluate four factors related to possible earthquake hazard: historical background seismicity, local geology, the regional state of stress, and the nature of the proposed injection. However, the focus of these questions is somewhat different. In the first case (Table 1), an earthquake has already occurred, and the question to be evaluated is whether or not the earthquake

213

was caused by injection. In the second case (Table 4), the problem is trying to evaluate the potential for future, damaging earthquakes at a specific injection site.

To illustrate the application of these questions, we discuss results for two proposed or ongoing injection sites we have previously evaluated (Frohlich and Davis, 1988, 1990): a proposed injection project near Tracy, Quebec, and an injection well near Texas City on the Texas Gulf Coast. As before, "yes" answers support the hypothesis that injection may induce seismic activity while "no" answers oppose this hypothesis.

As a further illustration, we also present the profile for the Denver Rocky Mountain Arsenal project as if injection had not yet taken place there. This allows us to "test" the criteria at a site where seismologists generally agree that injection has induced earthquakes. We chose the Denver site as it is the most well-known case study of injection induced earthquakes.

Using our ten-question profile (Table 4), we find only one "yes" answer for the Texas City site: there are known faults within 20 km of the injection site. However, the faults appear to be currently inactive, and in view of the lack of local and regional seismicity, the low deviatoric stresses in the Gulf Coast, and the lack of seismicity associated with nearby injection projects, we would find the Texas City site an unlikely candidate for large induced earthquakes.

In contrast, we find four "yes" answers at the Denver site. We could not answer two of the questions with the available data, and we assigned "no" answers to the other four questions. However, the presence of large regional earthquakes, nearby active tectonic features, and an in situ stress state near failure suggest that Denver might be a reasonable candidate for injection induced earthquakes. In this hypothetical evaluation, note that several of the questions receive "no" answers because we are presuming that our assessment takes place prior to injection. In actuality, if one were to propose injection at a site near Denver today, the existence of the earthquake activity between 1962 and 1972 would alter the profile, and there would be six or more "yes" answers.

At the Tracy, Quebec site we find five "yes" answers. This site lies within several hundred km of the Charlevoix seismic zone, the site of several large (M ≥ 6) historical earthquakes. Moderate seismicity occurs near Tracy itself (Wahlstrom, 1987). This area overlies a failed rift arm; such structures represent planes of weakness in the crust and are often associated with large, damaging earthquakes (Sykes, 1978; Keller at al., 1983; Johnston and Shedlock, 1992). While calculations of the in situ stress from hydrofracture do not sug-

gest that rocks at the proposed depth of injection are naturally close to failure, bottom hole pressures following injection would place the rock at or near failure (Frohlich and Davis, 1988). We would thus conclude that the situation is more similar to Denver than the Texas Gulf Coast.

OTHER CONSIDERATIONS

The yes-and-no profiles described above, in conjunction with the Mohr-Coulomb failure model (Figure 1), provide a useful way to evaluate the possible seismic hazard at injection sites. In particular, it allows one to make comparisons to other sites, and to communicate these comparisons to non-seismologists. However, to effectively evaluate a site one must consider the possibility that rock failure will occur aseismically, and determine the faulting characteristics expected for possible "worst-case" earthquakes that might be induced.

Rock Failure Without Earthquakes

When stress analyses suggest that rock failure is likely, this does not necessarily indicate that earthquakes will occur. There is considerable evidence that rocks can, and do, fail aseismically, as by stable sliding. For example, Byerlee and Brace (1972) and Lockner et al. (1982) found in the laboratory that there was a transition from stick-slip (earthquake-like) behavior to stable sliding behavior as pore pressures increased. Indeed, in some oil and gas fields near San Antonio, Texas, Pennington et al. (1986) concluded that small (M ≤ 3.9) earthquakes began to occur only when ambient pore pressures decreased due to fluid withdrawal. They suggested that a transition from aseismic to seismic behavior, caused by decreased fluid pressures from oil and gas production, may have played a role in the timing and location of the earthquakes. In California, networks of "creepmeters" document that aseismic motion occurs along sections of the San Andreas Fault (Louie et al., 1985; Schulz et al., 1982). These creep events last hours to days, accommodating fault slip a few mm at a time, and can occur in the complete absence of earthquakes.

Elsewhere there are thousands of injection wells in regions where no earthquakes are known to occur, but where an analysis of injection pressures and probable principal stresses suggests that rock failure occurs. Davis (1989) and Davis and Pennington (1989) analyzed Railroad Commission data summarizing injection activity from 2420 injection projects in Texas. For these projects, the Mohr-Coulomb model predicted rock failure at well bottoms for somewhere between 5% and 36% of the sites that inject under pressure, depending on the failure criteria used (Figure 2). However, earthquakes were only clearly identified with one project, the Cogdell Oil field near Snyder, Texas. No earthquakes are known at numerous other sites
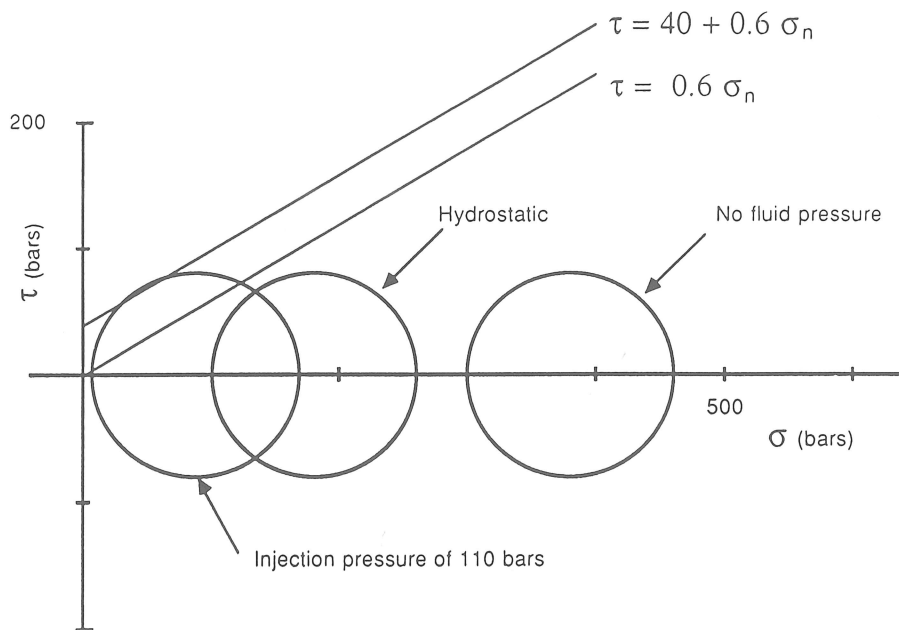
Fig. 1. Mohr circle diagram showing inferred state of stress at the bottom of the injection wells (1.8 km depth) for the Painesville, Ohio site, from Nicholson et al. (1988). Each point on the perimeter of a Mohr circle represents the stress field for a fault plane of a particular orientation; σ is the normal stress across the plane, while τ is the shear stress along the plane. The two lines indicate failure criteria for Mohr-Coulomb failure (see text); failure occurs if the Mohr's circle intersects (or lies to the left of) the failure line. The circle at the right indicates in-situ stresses (typically estimated from the inferred overburden pressure, hydrofracture measurements, and other stress indicators such as earthquake focal mechanisms) in the absence of fluid pressure. In the center Mohr's circle, the principal stresses have been shifted to the left by the hydrostatic fluid pressure in accordance with the effective stress law. The leftmost circle indicates stresses at the well bottom during injection (fluid pressure = hydrostatic + surface injection pressure). The fact that the circle intersects both lines indicates that pressures at the well bottom are not only sufficient for failure if pre-existing faults with zero strength exist (failure line at right), but are sufficient to cause failure even in intact rock with a shear strength of 40 bars (failure line at left).

in Texas, even where injection pressures exceed the Mohr-Coulomb failure criterion.

Earthquake Magnitudes and Fault Characteristics

Even at sites where earthquakes are known to occur, the earthquakes may be of such small magnitude as to make the possibility of damage unlikely. For example, profiles for the Baca and Fenton Hills sites (Tables 2 and 3) strongly indicate the earthquakes are related to injection. However, all of the earthquakes observed have been small (approximate magnitude -2 or less) and would be unlikely to produce damage. Although one cannot rule out the possibility of larger earthquakes occurring at these sites, the presently available evidence suggests that the induced seismicity is limited to small, non-damaging earthquakes.

Two useful parameters for describing the physical nature of earthquakes are the fault area A of the rupture and the slip S that takes place over this area as the earthquake occurs. Suppose an injection project induces an earthquake with magnitude M. Does the associated fault area and slip pose a hazard? The generally accepted method for evaluating the slip and fault area involves analysis of seismic moment, M_0, of an earthquake:

$$M_0 = \mu A S$$

where μ is the rigidity of crustal rocks (approximately 3×10^{11} dyne/cm^2). The most commonly used relationship (Hanks and Kanamori, 1979) between moment magnitude M and seismic moment M_0 is:

$$\log_{10} M_0 = 1.5M + 16.05$$

Empirical studies (Abe, 1978; Kanamori and Anderson, 1975) of the relationship between fault dimension R and fault slip S find that $S \sim 10^{-4} R$. If R is the radius of a circular fault, then combining the above equations we obtain the relationship between fault dimension R (in meters), fault slip S (in mm) and moment magnitude M as:

$$\log_{10} R \ (meters) = 0.5M + 0.7$$
$$\log_{10} S \ (mm) = 0.5M - 0.3$$

Thus for earthquakes with magnitudes M between 0 and 2, we would expect fault dimensions of 5 to 50 meters, and slips of 0.5 to 5 mm. However, for an earthquake with magnitude of 5.0, similar to the largest of those earthquakes in the Denver sequence, R and S would be 1.6 km and 16 cm, respectively.

Whether the faulting associated with an earthquake poses a hazard depends on the situation. For example, an earthquake with magnitude 2 would be unlikely to pose a risk to any man-made structure, while even aseismic failure in an area with considerable preexisting faulting might allow chemical wastes to enter a nearby aquifer. However, seismologists are usually asked only to evaluate the characteristics of past or possible future seismic activity, and other experts must decide whether these conditions represent a significant risk.
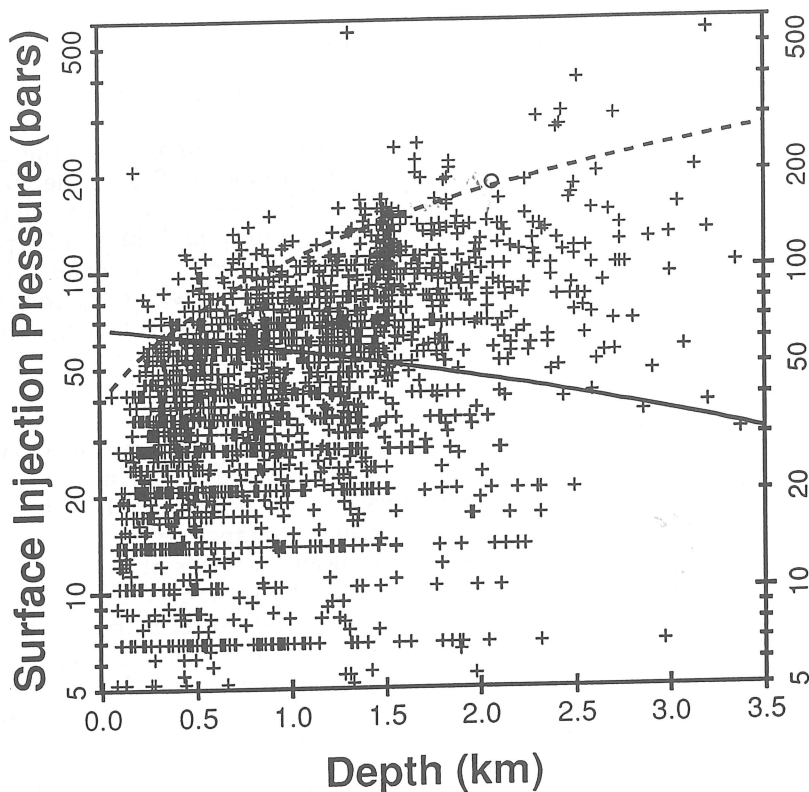
Fig. 2. Injection pressure versus depth for 2420 projects in the state of Texas which inject water under pressure at depths of 0 to 3.5 km. The two lines represent failure curves with different assumptions about deviatoric stresses, friction, and rock shear strength (see Davis and Pennington, 1989 for details). In each case, failure is estimated for conditions at the well bottoms; we correct these to surface injection pressures as recorded by the state of Texas (Railroad Commission of Texas, 1983). Projects which plot above the lines should be in failure at well bottom conditions. The solid line is a typical failure curve, whereas the dashed line is an extremely conservative failure curve (high friction and low deviatoric stresses). 877 projects lie above the typical failure line, and 112 projects should be in failure even by the conservative failure law. Nevertheless, induced earthquakes are only unambiguously associated with the Cogdell Oil Field (open circle).

DISCUSSION

Liability and Public Concern

While there are thousands of injection projects, there is surprisingly little available information about the effects of these projects on seismic activity. In places such as Ohio and Quebec, the fact that fluid injection might affect seismic activity has only recently become a factor in obtaining permits for injection projects. While this has created an inducement for companies to study seismicity prior to a proposed injection project, after injection begins the recording of any earthquake, no matter how small or how distant, can only add expense or delay to the project. Often, individuals and groups in the community may oppose the injection, because of either real or misguided environmental concerns, or simply because the development is not in their interest. Thus after injection begins there is little inducement for a company to operate a seismic network or publicize recorded activity.

However, these companies may be held liable for any resulting damage or interference from induced earthquakes under the legal concepts of strict liability, negligence, and/or nuisance (Cypser and Davis, 1993). Evaluation of the potential for injection-induced earthquakes (e.g. Frohlich and Davis, 1988; 1990; Nicholson and Wesson, 1990) can help companies avoid the possibility of costly lawsuits and the adverse publicity which would accompany induced seismic activity. In addition, it is economically more efficient to determine the potential for induced seismicity in the early stages of a project rather than dealing with the consequences of induced earthquakes, including the possibility of abandoning the site, after injection begins.

As previously mentioned, there may be cases where one can make a distinction between "induced" and "triggered" earthquakes, in which the energy release from "triggered" earthquakes primarily resulted from stresses built up over time by natural tectonic processes (McGarr, 1991). One might be tempted to argue that "triggered" earthquakes would not be a cause for legal concern, as the triggering mechanism (e.g., injection) has only hastened the release of tectonic energy, and the earthquakes would have happened anyway. However, a study on liability for induced earthquakes (Cypser and Davis, in preparation) shows that this argument does not hold. Rather, it is possible that human intervention could release energy that might have remained stored in the crust for centuries (Allen, 1982). Further, one could argue that such perturbations might influence the character of seismicity, perhaps creating earthquakes of larger magnitude than would have occurred naturally

(Pennington et al., 1986). There are reasons to find legal causation even in the case where the triggering process merely hastened the release of stored energy, and the inducer would still be held liable for any resulting damage (Cypser and Davis, 1993).

While the potential for a damaging earthquake is often real, in some situations the threat of damage may be as costly to society as any damage from the earthquake itself. For example, these societal costs may be in the form of lawsuits, or they may arise from public concern over seismic hazard in situations where the possibility of damage from induced earthquakes is remote. The application of the criteria presented in this paper may help provide a framework for determining when such concern is warranted.

Other Characteristics of Induced Earthquakes

It is possible that there exist other characteristics that are diagnostic of induced seismic activity in addition to the characteristics addressed in Tables 1 and 4. In Table 2 we have compiled additional information about each of the 20 sequences studied. These data show that the induced earthquakes have either strike-slip, thrust, or normal focal mechanisms, and can occur over a large range of depths. However, future research may determine other factors that might be of use in determining if seismic activity is natural or induced.

There is some indication that the rate of seismic activity is higher in sequences clearly attributed to injection than not (Talwani and Acree, 1986; Frohlich and Davis, 1987). This is not too surprising, as swarm-like behavior is often observed where fluid movement or fluid pressure changes are thought to cause earthquake activity. These include earthquakes induced by the filling of reservoirs (Gupta, 1992) and those associated with volcanic activity and magma intrusions (e. g., Stuart and Johnston, 1975; Malone et al., 1983).

Finally, we note that the literature on injection-induced earthquakes is surprisingly large. In addition to those listed in Tables 2 and 3 and in the Appendix, other cases have been made for injection-induced earthquakes in a variety of settings. Earthquakes possibly related to injection at oil and gas fields have been found in East Texas (Carlson, 1984), the Texas Panhandle (Davis et al., 1989), and in Alberta (Milne, 1970; Milne and Berry, 1976). Earthquakes associated with injection at geothermal sites are common; these include the Salton Sea field, California (Hutchings et al., 1988), the Texas Gulf Coast (Knutson, 1981; Mauk, 1985), the Tongonan field, Philippines (Sarmiento, 1986), the Cambourne Hot Dry Rock site in the United Kingdom (Pine and Batchelor, 1984; Crampin and Booth, 1989; Parker, 1989), and the Larderello-

Travale geothermal area in Italy (Batani et al., 1985). Solution mines where earthquakes have been related to injection include those in southeastern Utah (Wong et al., 1985) and Iraq (Terashima, 1981). Other locations where earthquakes have been related to injection for experimental or other purposes include central France (Cornet et al., 1992), the Buffelsfontein Gold Mine in South Africa (Board et al., 1992), the Lucky Friday Mine in Idaho (Whyatt et al., 1992), and a small-scale experiment at the Canadian Underground Research Laboratory (Majer and Doe, 1986). Finally, injection at the Inglewood Oil Field, California, has been related to surface faulting which led to the destruction of the Baldwin Hills Reservoir (Hamilton and Meehan, 1971). Note that this is not intended to be a complete list, as there exist other locations where a connection between deep well injection and earthquakes has been suggested (e.g., see Nicholson, 1992).

CONCLUSIONS

The question "Is it possible that injection may induce (or may have induced) seismic activity?" is often a difficult one for the professional seismologist to answer, as it is impossible to rule out a connection between earthquakes and injection with complete certainty, even in the absence of evidence linking the two. Rather, the profiles described answer the question, "How similar is this injection situation to other situations where injection did cause seismic activity?" We emphasize that this analysis does not, by itself, determine whether or not injection should take place. However, by using criteria such as those presented in this paper, seismologists can provide information to assist industry and government in making responsible decisions concerning the initiation of injection, continued injection, or, after an earthquake, about whether it is plausible that injection was a contributing factor.

We note that differences in the quality of data sets for injection histories, historical seismicity, and geology and hydrology between different sites precludes the use of a consistent, quantitative set of criteria for evaluating these questions. Thus, most of the questions in Tables 1 and 4 are inherently subjective. However, their usefulness is that they do provide a framework for comparing different injection projects to one another, utilizing whatever information is available at a particular site.

In evaluating the seismic hazard from fluid injection projects, we encourage people to assess the magnitudes of potential earthquakes. Many injection situations are similar to those where small earthquakes may be induced, but the likely fault areas and fault slips would pose little or no hazard for most engineering applications. However, where there are concerns about the possible damage from induced seismic activity, it would be prudent to take appropriate precautions (Nicholson and Wesson, 1990; Cypser and Davis, 1993). These precautions might include evaluating the site for the potential of induced seismic hazard, and monitoring the injection site for seismic activity.

REFERENCES

Abe, K. (1978). Dislocations, source dimensions and stresses associated with earthquakes in the Izu Peninsula, Japan, *J. Phys. Earth* **26**, 253-274.

Ahmad, M. U. and J. A. Smith (1988). Earthquakes, injection wells, and the Perry nuclear power plant, Cleveland, Ohio, *Geology* **16**, 739-742.

Ahmad, M. U. and J. A. Smith (1989). Reply to Comment on "Earthquakes, injection wells, and the Perry nuclear power plant, Cleveland, Ohio", *Geology* **17**, 383-384.

Allen, C. R. (1982). Reservoir-induced earthquakes and engineering policy, *California Geology* **35**, 248-250.

Allis, R. G. (1982). Mechanism of induced seismicity at The Geysers geothermal reservoir, *Geophys. Res. Lett.* **9**, 629-632.

Bardwell, G. E. (1966). Some statistical features of the relationship between Rocky Mountain Arsenal waste disposal and frequency of earthquakes, *Mountain Geologist* **3**, 37-42.

Bane, D. and M. Fehler (1986). Observations of long period earthquakes accompanying hydraulic fracturing, *Geophys. Res. Lett.* **13**, 149-152.

Batani, F., Console, R. and G. Luongo (1985). Seismological study of Larderello-Travale geothermal area, *Geothermics* **14**, 255-272.

Batra, R., J. N. Albright and C. Bradley (1984). Downhole seismic monitoring of an acid treatment in the Beowawe geothermal field, *Trans Geothermal Research Council* **8**, 479-483.

Beauce, A., H. Fabriol, D. Le Masne, C. Cavoit, P Mechler and X. K. Chen (1991). Seismic studies at the HDR site of Soultz-Sous-Forets (Alsace France), *Geotherm. Sci. Tech.* **3**, 239-266.

Board, M., T. Rorke, G. Williams and N. Gay (1992). Fluid injection for rockburst control in deep mining, *Proceedings of the 33rd U. S. Symposium on Rock Mechanics*, 111-120.

Bromley, C. J., C. F. Pearson, D. M. Rigor Jr. and PNOC-EDC (1987). Microearthquakes at the Puhagan geothermal field, Philippines - a case of induced seismicity, *J. Volcan. Geotherm. Res.* **31**, 293-311.

Byerlee, J. D. and W. F. Brace (1972). Fault stability and pore pressure, *Bull. Seism. Soc. Am.* **62**, 657-660.

Carlson, S. (1984). Investigations of recent and historical seismicity in East Texas, *M.S. Thesis*, University of Texas at Austin, 197 pp.

Coffman, J. L., C. A. von Hake and C. W. Stover (1982). Earthquake history of the United States, *U. S. Geological Survey Publication 41-1*, 264 pp.

Cornet, F. H., Y. Jianmin, and L. Martel (1992). Stress heterogeneities and flow paths in a granitic rock mass, Pre-Workshop Volume for the Workshop on Induced Seismicity, *33rd U, S. Symposium on Rock Mechanics*, 184-185.

Cornet, F., and P. Julien (1989). Stress determination from hydraulic test data and focal mechanisms of induced seismicity, *Int. J. Rock Mech. Min. Sci, & Geomech. Abtr.* **26**, 235-248.

Cox, R. T., (1991). Possible triggering of earthquakes by underground waste disposal in the El Dorado, Arkansas area, *Seism. Res. Lett.* **62**, 113-122.

Crampin, S. and D. C. Booth (1989). Shear-wave splitting showing hydraulic dilation of pre-existing joints in granite, *Scientific Drilling* **1**, 21-26.

Cypser, D. A. and S. D. Davis (1993). Liability for induced earthquakes, *Columbia Law Review*, (submitted).

Davis, S. D. (1985). Investigations of natural and induced seismicity in the Texas Panhandle, *M.S. Thesis*, University of Texas at Austin, 230 pp.

Davis, S. D. (1989). Investigations concerning the nature of aftershocks and earthquakes induced by fluid injection, *Ph.D. Thesis*, University of Texas at Austin, 157 pp.

Davis, S. D. and C. Frohlich (1987). New objective criteria to determine if fluid injection has induced earthquakes (abs), *EOS,. Trans. Am. Geophys. Union* **68**, 1369.

Davis, S. D. and C. Frohlich (1988). Potential for earthquakes induced by fluid injection (abs), *EOS,. Trans. Am. Geophys. Union* **69**, 1315.

Davis, S. D. and W. D. Pennington (1989). Induced seismic deformation in the Cogdell oil field of west Texas, *Bull. Seism. Soc. Am.* **79**, 1477-1494.

Davis, S. D., W. D. Pennington and S. M. Carlson (1989). A compendium of earthquake activity in Texas, *Univ. of Texas Bureau of Econ. Geol. Circ.* **89-3**, 27 pp. (printed), 219 pp. (microfiche).

Dewey, J. W. and D. W. Gordon (1984). Map showing recomputed hypocenters of earthquakes in the eastern and central United States and adjacent Canada, 1925-1980, *U. S. Geological Survey Map MF-1699*.

Doser, D. I., M. R. Baker and B. B. Mason (1991). Seismicity in the War-Wink gas field, west Texas, and its relationship to petroleum production, *Bull. Seism. Soc. Am.* **81**, 971-986.

Eberhart-Phillips, D. and D. H. Oppenheimer (1984). Induced seismicity in The Geysers geothermal area, California, *J. Geophys. Res.* **89**, 1191-1207.

Evans, D. M. (1966). The Denver earthquakes and the Rocky Mountain Arsenal disposal well, *The Mountain Geologist* **3**, 23-36.

Evans, D. G. and D. W. Steeples (1987). Microearthquakes near the Sleepy Hollow oil field, southwestern Nebraska, *Bull. Seism. Soc. Am.* **77**, 132-140.

Evans, K. F. (1987). Assessing regional potential for induced seismicity from crustal stress measurements: an' example from northern Ohio, in *Proc. Symp. Seismic Hazards, Ground Control Motions, Soil-Liquefaction and Engineering Practice in North America, NCEER Tech. Rept. 87-0025*, 99-126.

Fehler, M. C. (1989). Stress control of seismicity patterns observed during hydraulic fracturing experiments at the Fenton Hill Hot Dry Rock Geothermal Energy site, New Mexico, *Int. J. Rock Mech. Min. Sci. & Geochem. Abstr.* **26**, 211-219.

Fehler, M., L. House and H. Kaieda (1987). Determining planes along which earthquakes occur: method and application to earthquakes accompanying hydraulic fracture, *J. Geophys. Res.* **92**, 9407-9414.

Fehler, M. and W. S. Phillips, (1991). Simultaneous inversion for Q and source parameters of microearthquakes accompanying hydraulic fracturing in granitic rock, *Bull. Seism. Soc. Am.* **81**, 553-575.

Ferrazini, V., B. Chouet, M. Fehler and K. Aki (1990). Quantitative analysis of long-period events recorded during hydrofracture experiments at Fenton Hill, New Mexico, *J. Geophys. Res.* **95**, 21871-21884.

Fletcher, J. B. and L. R. Sykes (1977). Earthquake related to hydraulic mining and natural seismic activity in western New York State, *J. Geophys. Res.* **82**, 3767-3780.

Franzen, Jonathan (1992). *Strong Motion*, Farrar Straus Giroux Publishing, New York, 508 pp.

Frohlich, C. and S. D. Davis (1987). New objective criteria to determine if fluid injection has

induced earthquakes, with special attention to the 31 January 1986 earthquake in Painesville, Ohio, Proprietary in-house report for Ken. E. Davis Associates, Houston, Texas, 24 pp.

Frohlich, C. and S. D. Davis (1988). Earthquake activity and the potential effects of fluid injection near Tracy, Quebec, Ohio, Proprietary in-house report for Research and Engineering Consultants, Inc., Butte, Montana, 22 pp.

Frohlich, C. and S. D. Davis (1990). The potential for earthquake activity or fault slip due to fluid injection near Texas City, Texas, Proprietary in-house report for International Technology Corporation, Austin, Texas, 21 pp.

Gibbs, J. F., J. H. Healy, B. Raleigh and J. Coakley (1973). Seismicity in the Rangely, Colorado, area: 1962-1970, *Bull. Seism. Soc. Am.* **63**, 1557-1570.

Grasso, J. R. and G. Wittlinger (1990). Ten years of seismic monitoring over a gas field, *Bull. Seism. Soc. Am.* **80**, 450-473.

Gupta, H. K. (1992). Reservoir-Induced Earthquakes, *Developments in Geotechnical Engineering* **64**, Elsevier Science Publishers, The Netherlands, 364 pp.

Haimson., B. C. (1972). Earthquake stresses at Rangely, Colorado, in New Horizons in Rock Mechanics; Earthquakes and Other Dynamic Phenomena, ed. F. R. Hardy and R. Stefanko, eds., *Symp. Rock Mech. Proc.* **14**, 689-708.

Hamilton, D. H. and R. L. Meehan (1971). Ground rupture in the Baldwin Hills, *Science* **172**, 333-344.

Hanks, T. C. and H. Kanamori (1979). A moment-magnitude scale. *J. Geophys. Res.* **84**, 2348-2350.

Harding, S. T., (1981). Induced seismicity in the Cogdell Canyon Reef oil field, *USGS Open-File Report 81-167*, p. 452-455.

Healy, J. W., W. W. Rubey, D. T. Griggs, and C. B. Raleigh (1968). The Denver earthquakes, *Science* **161**, 1301-1310.

Herrmann, R. B., S. Park and C. Y. Wang (1981). The Denver earthquakes of 1967-1968, *Bull. Seism. Soc. Am.* **71**, 731-745.

House, L. S. (1987). Locating microearthquakes induced by hydraulic fracturing in crystalline rock, *Geophys. Res. Lett.* **14**, 919-921.

House, L. S., M. C. Fehler and W. S. Phillips (1992). Studies of seismicity induced by hydraulic fracturing in a geothermal reservoir, Pre-Workshop Volume for the Workshop on Induced Seismicity, *33rd U, S. Symposium on Rock Mechanics*, 186-189.

Hsieh, P. A. and J. D. Bredehoeft (1981). A reservoir analysis of the Denver earthquakes: a case of induced seismicity, *J. Geophys. Res.* **86**, 903-920.

Hubbert, M. K. and W. W. Rubey (1959). Role of fluid pressure in overthrust faulting, *Geol. Soc. Am. Bull.* **70**, 115-206.

Hunt, T. M. and J. H. Latter (1982). A survey of seismic activity near Wairakei Geothermal Field, New Zealand, *J. Volcan. Geotherm. Res.* **14**, 319-334.

Hutchings, L. J., S. Jarpe, P. Kasameyer and T. Hauk (1988). Microseismicity of the Salton Sea geothermal field (abs), *EOS, Trans. Am. Geophys. Union* **69**, 1312.

Johnston, A. C. and K. M. Shedlock (1992). Overview of research in the New Madrid seismic zone, *Seism. Res. Lett.* **63**, 193-208.

Kanamori, H. and D. L. Anderson (1975). Theoretical basis of some empirical relations in seismology, *Bull. Seism. Soc. Am.* **65**, 1073-1095.

Kanamori, H. and E. Hauksson (1992). A slow earthquake in the Santa Maria Basin, California, *Bull. Seism. Soc. Am.* **82**, 2087-2096.

Keller, G. R., E. G. Lidiak, W. J. Hinze and L. W. Braile (1983). The role of rifting in the tectonic development of the midcontinent, U. S. A., *Tectonophysics* **94**, 391-412.

Knutson, C. F., (1981). Some Pleasant Bayou, Brazoria County, Texas, brine injection experience, in: Geopressured-Geothermal Energy, *Proc. Fifth U. S. Gulf Coast Geopressured-Geothermal Energy Conf.*, D. G. Bebout and A. L. Bachman, eds., 101-103.

Lockner, D. A., P. G. Okubo and J. H. Dieterich (1982). Containment of stick-slip failures on a simulated fault by pore fluid injection, *Geophys. Res. Lett.* **8**, 801-804.

Louie, J. N., C. R. Allen, D. C. Johnson, P. C. Haase and S. N. Cohn (1985). Fault slip in southern California, *Bull. Seism. Soc. Am.* **75**, 811-833.

Majer, E. L. and T. W. Doe (1986). Studying hydrofractures by high frequency seismic monitoring, *Int. J. Rock Mech. Min. Sci, & Geomech Abtr.* **23**, 185-199.

Malone, S. D., C. Boyko and C. S. Weaver (1983) Seismic precursors to the Mount St. Helen Eruptions in 1981 and 1982, *Science* **221**, 1376-1378.

Mauk, F. J. (1985). Results of the seismic monitoring programs at the Pleasant Bayou and Bayou Parcperdue, geopressured-geothermal design wells, in: Geopressured-Geothermal Energy *Proc. Sixth U. S. Gulf Coast Geopressured Geothermal Energy Conf.*, M. H. Dorfman and A. Morton, eds., 309-318.

McGarr, A. (1991). On a possible connection between three major earthquakes in California and oil production, *Bull. Seism. Soc. Am.* 948-970.

Mereu, R. F., J. Brunet, K. Morrissey, B. Price and A. Yapp (1986). A study of the microearthquakes of the Gobles oil field area

southwestern Ontario, *Bull. Seism. Soc. Am.* **76**, 1215-1223.

Milne, W. G. (1970). The Snipe Lake, Alberta earthquake of March 8, 1970, *Can. J. Earth Sci.* **7**, 1564-1567.

Milne, W. G. and M. J. Berry (1976). Induced seismicity in Canada, *Eng. Geol.* **10**, 219-226.

Nicholson, C. (1992). Earthquakes associated with deep-well activities - comments and case histories, *Proceedings of the 33rd U. S. Symposium on Rock Mechanics*, 1079-1086.

Nicholson, C., and R. L. Wesson (1990). Earthquake hazard associated with deep well injection - a report to the U. S. Environmental Protection Agency, *U. S. Geological Survey Bull.* **1951**, 74 pp.

Nicholson, C., E. Roeloffs and R. L. Wesson (1988). The northeastern Ohio earthquake of 31 January 1986: was it induced?, *Bull. Seism. Soc. Am.* **78**, 188-217.

O'Connell, D. R. H. and L. R. Johnson (1988). Second-order moment tensors of microearthquakes at The Geysers geothermal field, California, *Bull. Seism. Soc. Am.* **78**, 1674-1692.

Oppenheimer, D. H. (1986). Extensional tectonics at The Geysers geothermal area, California, *J. Geophys. Res.* **91**, 11463-11476.

Ohtake, M. (1974). Seismic activity induced by water injection at Matsushiro, Japan, *J. Phys. Earth* **22**, 163-176.

Parker, R. (1989). The Camborne School of Mines hot dry rock geothermal energy project, *Scientific Drilling* **1**, 34-41.

Pearson, C. (1981). The relationship between microseismicity and high pore pressures during hydraulic stimulation experiments in low permeability granitic rocks, *J. Geophys. Res.* **86**, 7855-7864.

Pearson, C., H. Keppler, J. Albright and R. Potter (1982). Rock failure during massive hydraulic simulation of the Baca location geothermal reservoir, *Trans. Geothermal Resources Council* **6**, 157-160.

Pennington, W. D., S. D. Davis, S. M. Carlson, J. DuPree and T. E. Ewing (1986). The evolution of seismic barriers and asperities caused by the depressuring of fault planes in oil and gas fields of south Texas, *Bull. Seism. Soc. Am.* **78**, 188-217.

Pine, R. J. and A. S. Batchelor (1984). Downward migration of shearing in jointed rock during hydraulic injections, *Int. J. Rock Mech. Min. Sci, & Geomech. Abtr.* **21**, 249-263.

Railroad Commission of Texas (1983). *A Survey of Secondary and Enhanced Oil Recovery Operations in Texas to 1982*, Austin, Texas, 608 pp.

Raleigh, C. B., J. H. Healy and J. H. Bredehoeft (1972). Faulting and crustal stress at Rangely, Colorado, *Am. Geophys. Union Geophys. Monograph* **16**, 275-284.

Raleigh, C. B., J. H. Healy and J. H. Bredehoeft (1976). An experiment in earthquake control at Rangely, Colorado, *Science* **191**, 1230-1237.

Roeloffs, E., C. Nicholson and R. L. Wesson (1989). Comment on "Earthquakes, injection wells, and the Perry nuclear power plant", by M. U. Ahmad and J. A. Smith, *Geology* **17**, 382-383.

Rothe, G. R. and C. Lui (1983). Possibility of induced seismicity in the vicinity of the Sleepy Hollow oil field, southwestern Nebraska, *Bull. Seism. Soc. Am.* **73**, 1357-1367.

Sarmiento, Z. F. (1986). Waste water reinjection at Tongonan Geothermal Field: results and implications, *Geothermics* **15**, 295-308.

Schulz, S. S., G. M. Mavko, R. O. Burford and W. D. Stuart (1982). Long-term fault creep observations in central California, *J. Geophys. Res.* **87**, 6977-6982.

Seeber, L. and J. G. Armbruster (1988). Recent and historical seismicity in northeastern Ohio: Reactivation of Precambrian faults and the role of deep fluid injection, Preliminary report to the U. S. Nuclear Regulatory Commission, 26 pp.

Seeber, L. and J. G. Armbruster (1993). Natural and induced seismicity in the Lake Erie-Lake Ontario region: Reactivation of ancient faults with little neotectonic displacement, *Géographie physique et Quaternaire*, submitted.

Segall, P. (1989). Earthquakes triggered by fluid extraction, *Geology* **17**, 942-946.

Sherburn, S. (1984). Seismic monitoring during a cold water injection experiment, Wairakei geothermal field: Preliminary results, *Proc. 6th NZ Geothermal Workshop*, 129-133.

Sherburn, S., R. Allis and A. Clotworthy (1990). Microseismic activity at Wairakei and Ohaaki geothermal fields, *Proc. 12th NZ Geothermal Workshop*, 51-55.

Stark, M. (1990). Imaging injected water in The Geysers reservoir using microearthquake data, *Trans. Geothermal Resources Council* **14**, 1-8.

Stuart, W. D. and M. J. S. Johnston (1975). Intrusive origin of the Matsushiro earthquake swarm, *Geology* **3**, 63-67.

Sykes, L. (1978). Intraplate seismicity, reactivation of preexisting zones of weakness, alkaline magmatism, and other tectonism postdating continental fragmentation, *Rev. Geophys. Space Phys.* **16**, 621-688.

Talebi, S. and F. Cornet (1987). Analysis of microseismicity induced by a fluid injection in a granitic rock mass, *Geophys. Res. Lett.* **14**, 227-230.

Talwani, P. and S. Acree (1986). Deep well injection at the Calhio wells and the Leroy, Ohio

earthquake of January 31, 1986, In-house report for the Cleveland Electric Illuminating Co., 92 pp.

Teng, T. L., C. R. Real and T. L. Henyey (1973). Microearthquakes and waterflooding in Los Angeles, *Bull. Seism. Soc. Am.* **63**, 859-875.

Terashima, T. (1981). Survey on induced seismicity at Mishraq area in Iraq, *J. Phys. Earth* **29**, 371-375.

Wahlstrom, R. (1987). Focal mechanisms of earthquakes in southern Quebec, southeastern Ontario, and northeastern New York with implications for regional seismotectonics and stress field characteristics, *Bull. Seism. Soc. Am.* **77**, 891-924.

Wesson, R. L. and C. Nicholson (1986). Studies of the January 31, 1986 northeastern Ohio earthquake - a report to the U. S. Nuclear Regulatory Commission, *U. S. Geological Survey Open-File Report* **86-331**, 109 pp.

Whyatt, J. K., T. J. Williams, W. Blake and D. Cuvelier (1992). Fault injection experimentation at the Lucky Friday Mine: a progress report, Pre-Workshop Volume for the Workshop on Induced Seismicity, *33rd U. S. Symposium on Rock Mechanics*, 195.

Wong, I., J. R. Humphrey, W. Silva, D. A. Gahr and J. Huizingh (1985). A case of microseismicity induced by solution mining, southeastern Utah (abs), *Earthquake Notes* **56**, 18.

Zoback, M. L. and M. Zoback (1980). State of stress in the conterminous United States, *J. Geophys. Res.* **85**, 6113-6156.

APPENDIX

Listed below are the sources used in preparing entries for Tables 2 and 3. Explanations for entries are given only if there is some conflicting information that requires justification.

Ashtabula, Ohio (waste disposal): Seeber and Armbruster (1988, 1993), Nicholson and Wesson (1990)

2) Injection at Ashtabula had been ongoing for about a year prior to the magnitude 3.6 earthquake on 13 July 1987. Although there is no clear correlation between injection and seismicity, the fairly short lag between the start of injection and the earth quake is suggestive. The detection threshold prior to the installation of the temporary network to locate the aftershocks to the 13 July earthquake was about 1.5, and it is possible that smaller events may have begun before July 1987. Seismic activity has occurred at least through March 1992. [NO?]

3c) The epicenters delineate a possible fault that extends from the injection formation into the basement, where most of the earthquakes occur. A composite fault plane solution is consistent with strike-slip motion on the inferred fault. However, there are no mapped faults in the region, and a reflection survey failed to resolve the fault plane. [NO?]

Baca Location Geothermal Site, New Mexico (hydraulic stimulation / geothermal): Pearson et al. (1982)

4a,b) We did not calculate pressure changes, but volumes were sufficient for hydraulic stimulation. [YES?, YES?]

Beowawe Geothermal Field, Nevada (acid treatment / geothermal): Batra et al. (1984)

2) A burst of seismicity accompanied an injection phase on August 21, 1983, but a second injection stage the following day occurred without seismicity. [YES?]

Cogdell Oil Field, Texas (secondary recovery / oil field): Davis (1985, 1989), Davis and Pennington (1989), Harding (1981)

3c) Earthquakes occur within the injection zone. [NOT APPLICABLE]

Dale, New York (solution mining): Fletcher and Sykes (1977)

1) Although the Attica area of western New York state has experienced a moderate amount of historic seismicity, historic compilations and more recent instrumental locations indicate a low level of background activity near the brine field. A permanent station in Attica recorded an average rate of less than one event per month prior to injection, which increased to up to 80 events per day during injection. Many of these later events were felt or heard by residents in the immediate area. [YES]

Denver RMA, Colorado (waste disposal): Bardwell (1966), Evans (1966), Frohlich and Davis (1987), Healy et al. (1968), Herrmann et al. (1981), Hsieh and Bredehoeft (1981)

see text for comments

El Dorado, Arkansas (waste disposal): Cox (1991)

2) The two principal periods of seismic activity were preceded by increased disposal rates. [YES]

4a,b) Cox (1991) reports that in situ stresses were close to failure. [YES?, YES?]

Fenton Hill Hot Dry Rock Site, New Mexico (hydraulic stimulation / geothermal): Bane and Fehler (1986), Cornet and Julien (1989), Fehler (1989), Fehler and Phillips (1991), Fehler et al. (1987), Ferrazini et al. (1990), House (1987), House et al. (1992), Pearson (1981), Talebi and Cornet (1987)

The Geysers, California (pressure maintenance /

geothermal): Allis (1982), Eberhart-Phillips and Oppenheimer (1984), O'Connell and Johnson (1988), Oppenheimer (1986), Stark (1990)

Maximum Magnitude -- The largest earthquakes in the field have been approximately magnitude 4.0, although it is not clear if the largest earthquakes are associated with injection.

4a,b) The high background rate of seismic activity in the field suggests that in situ stresses are close to failure. [YES?, YES?]

Gobles Oil Field, Ontario (secondary recovery / oil field): Mereu et al. (1986)

Los Angeles Basin, California (secondary recovery / oil fields): Teng et al. (1973), Nicholson and Wesson (1990)

2) Teng et al. (1973) suggest a possible relation between number of earthquakes and net volume of fluid injected at the Inglewood Oil Field for 1971, but the correlation is slight. [NO?]

3c) The Newport-Inglewood Fault may channel fluids to greater depths. [YES?]

Matsushiro, Japan (experimental): Ohtake (1974)

2) Ohtake (1974) purports to see a correlation between the time of injection and seismic activity, with bursts of activity seen 4.8 to 9.3 days following injection periods. However, swarms in the area are not uncommon before and after the injection periods (see figure 3 in Ohtake), and we do not see the proposed correlation. However, the hypocenters do exhibit an apparent migration away from the well following the first injection period (figures 4 and 5 of Ohtake's report). [NO?]

Orcutt Oil Field, California (hydrofracture induced earthquake / oil field): Kanamori and Hauksson (1992)

1) The unusually shallow depth (300 m, based on field evidence) and long duration (2 minutes) of the magnitude 3.5 earthquake was clearly anomalous. [YES]

2) The earthquake occurred a few hours after the hydrofracture. [YES?]

4a,b) We did not calculate pressure changes, but they are presumed to have been sufficient for hydraulic fracturing. [YES?, YES?]

Painesville, Ohio (waste disposal): Ahmad and Smith (1988, 1989), Evans (1987), Frohlich and Davis (1987), Nicholson et al. (1988), Roeloffs et al. (1989), Talwani and Acree (1986), Wesson and Nicholson (1986)

see text for comments

Peabody, Massachsetts (fictional account of waste disposal): Franzen (1992)

1) Historical events are known, although the swarmlike nature of the earthquakes may have been anomalous. [NO?]

2) There was a 16 year lag between the assumed start of injection and the first earthquakes. The second earthquake swarm may have closely followed a second injection period. [NO?]

3a) The closest epicenters are approximately 5 km from the assumed injection site. [YES?]

3b) The injection depths are unknown but are presumed deep. The book mentions an early report suggesting a drilling goal of 25,000 feet [7.6 km]. [YES?]

Puhagan Geothermal Field (injection tests / geothermal): Bromley et al. (1987)

1) Bromley et al. (1987) report a "near-quiescent background" prior to geothermal development. [YES?]

4a,b) Although injection pressures may have been sufficient to induce earthquakes, Bromley et al. (1987) report that most of the seismicity occurs in the production sector of the field, where pressures have decreased. [YES?, NO?]

Rangely Oil Field, Colorado (secondary recovery / oil field): Gibbs et al. (1973), Haimson (1972), Raleigh et al. (1972, 1976)

1) There are possible felt reports of earthquakes prior to injection but no reliable station coverage. [UNKNOWN]

2) An early study (Gibbs et al., 1973) could find no clear relation between injection and monthly numbers of earthquakes, although injection and annual activity were more clearly correlated. However, later studies (e.g. Raleigh et al., 1976) demonstrated a very clear correlation between earthquake activity and fluid pressures in the field. [YES]

Sleepy Hollow Oil Field, Nebraska (secondary recovery / oil field): Evans and Steeples (1987), Frohlich and Davis (1987), Rothe and Lui (1983)

2) No clear correlation exists, although Evans and Steeples (1987) note that the conversion of ten producers to injectors was followed by an increase in activity. However, this may have been an artifact of the catalog (Evans and Steeples, 1987). [NO?]

3c) Contour maps of the Precambrian basement show several vertical faults. However, Evans and Steeples (1987) suggest that the unusually high permeability of the Reagan sandstone (2.9 darcies) would be likely to divert fluid flow horizontally rather than into the basement. [YES?]

Soultz-Sous-Forets Hot Dry Rock Site, France (hydraulic stimulation / geothermal): Beauce et al. (1991)

4a,b) We did not calculate pressure changes, but volumes were sufficient for hydraulic stimulation. [YES?, YES?]

Wairakei Geothermal Field, New Zealand (reinjection test / geothermal): Hunt and Latter (1982), Sherburn (1984), Sherburn et al. (1990)

1) The Wairakei region exhibits low to moderate background seismicity (Hunt and Latter, 1982), although the numbers of earthquakes associated with the 1984 injection test was somewhat anomalous. [NO?]

2) A 1984 injection test at Wairakei was clearly associated with microearthquake activity. However, a later injection test at lower pressures did not appear to significantly increase earthquake activity. [YES?]

3b) Microearthquake depths were not well determined. [UNKNOWN]

SEISMOTECTONICS OF THE 1987-1988 LAKESIDE, UTAH, EARTHQUAKES

James C. Pechmann, Walter J. Arabasz, and Ethan D. Brown[1]

Department of Geology and Geophysics
University of Utah
Salt Lake City, Utah 84112-1183

ABSTRACT

From September 1987 through March 1988, an earthquake sequence which included shocks of M_L 4.8 and 4.7 on September 25 and October 26, respectively, and a total of 8 moderate-sized events of $M_L \geq 3.8$, occurred in NW Utah beneath a desert basin west of the Great Salt Lake (center of activity: 41° 12.0′ N, 113° 10.5′ W). Wood-Anderson seismograms indicate nearly identical magnitudes for the two largest earthquakes but a factor of two to five larger seismic moment for the first. Significant aspects of the 1987-1988 sequence included: foreshock activity, proximity (epicentral distance, Δ, of 7 to 12 km) to a major pumping facility completed in early 1987 to lower the level of the Great Salt Lake, an unambiguous strike-slip focal mechanism for the M_L 4.8 mainshock, and the lack of a clear association with late Quaternary surface faults.

Despite constraints on accessibility to the epicentral area, the stations of the regional seismic network ($\Delta \geq 60$ km) were supplemented with local stations—initially four portable seismographs and later up to four telemetered stations ($2 \leq \Delta \leq 27$ km) that operated continuously from October 7, 1987, through March 1988. Well-located aftershock foci form a 6-by-6-km zone between 6 and 12 km depth which is steeply dipping and trends SSE, parallel to the right-lateral nodal plane of the mainshock focal mechanism. Despite coincidental timing and proximity of the earthquakes to major pumping activity at the surface, the case for induced seismicity related to the pumping is weak.

INTRODUCTION

Between September 1987 and March 1988, an earthquake sequence which included eight shocks of $3.8 \leq M_L$ (local magnitude) ≤ 4.8 occurred beneath the Great Salt Lake desert in NW Utah, 10 km west of the Great Salt Lake and 100 km west of the Wasatch fault (arrow, Figure 1). The two largest earthquakes were felt throughout northern Utah and into southern Idaho and eastern Nevada, with Modified Mercalli intensities of IV to V for the M_L 4.8 mainshock on September 25 and III for an M_L 4.7 aftershock on October 26 (U.S. Geological Survey, 1987). The earthquakes attracted local attention because they were located 7 to 12 km WSW of a new 60-million-dollar pumping facility built to reduce flooding along the shores of the Great Salt Lake. On April 10, 1987, the pumps had begun to transfer water from the lake through a canal to the Great Salt Lake desert to form the large evaporating pond known as West Pond. West Pond filled to its maximum capacity (Figure 1) by early December of 1987, when water began to flow over a spillway in a dike forming part of the eastern edge of the pond and flow back into the Great Salt Lake (Jim Palmer, Utah Division of Water Resources, personal communication, 1993).

This paper presents the results of an aftershock study carried out following the M_L 4.8 earthquake, together with focal mechanisms for the mainshock and some larger aftershocks. Our principal conclusion is that the mainshock was caused by right-lateral strike-slip movement between 6 and 12 km depth on a SSE-striking fault. This finding is important because it emphasizes the role of strike-slip faulting in the contemporary deformation of this region of classic basin-and-range normal faulting.

SEISMOLOGICAL SETTING

The Lakeside earthquakes occurred along the western fringe of Utah's seismically active Wasatch Front area (Arabasz *et al.*, 1992), which forms part of the southern Intermountain Seismic Belt (Smith and Arabasz, 1991) along the eastern boundary of the Basin and Range Province. On the east side of the Great Salt Lake, the 383-km-long Wasatch

---

[1]Present address: Science Applications International Corporation, 10260 Campus Point Drive, San Diego, CA 92121.

normal fault forms a prominent west-facing escarpment which bounds the basin of late Quaternary Lake Bonneville, of which the modern Great Salt Lake is a vestige. It should be noted that the traces of late Quaternary faulting shown in Figure 1 west of the Wasatch fault reflect only the extent of mapped fault scarps in unconsolidated deposits, and not necessarily the entire length of seismogenic range-front faults. Fluctuations of Lake Bonneville (Currey *et al.*, 1984) could have destroyed evidence of late Quaternary surface faulting in many places.

Earthquake activity has occurred episodically since at least 1965 in a broad cluster 10 to 30 km NW of the 1987-1988 earthquakes. (Figure 1; see also Arabasz *et al.*, 1987). This activity included an M_L 4.0 event in February 1967, a swarm of 10 events ($1.1 \leq M_L \leq 3.2$) in March and April of 1979, and another swarm of 9 events ($1.3 \leq M_L \leq 3.1$) in April of 1980. The University of Utah instrumental earthquake catalog, which begins in July 1962, contains only two small seismic events within 10 km of the center of the 1987-1988 activity (41° 12.0′ N, 113° 10.5′ W) prior to
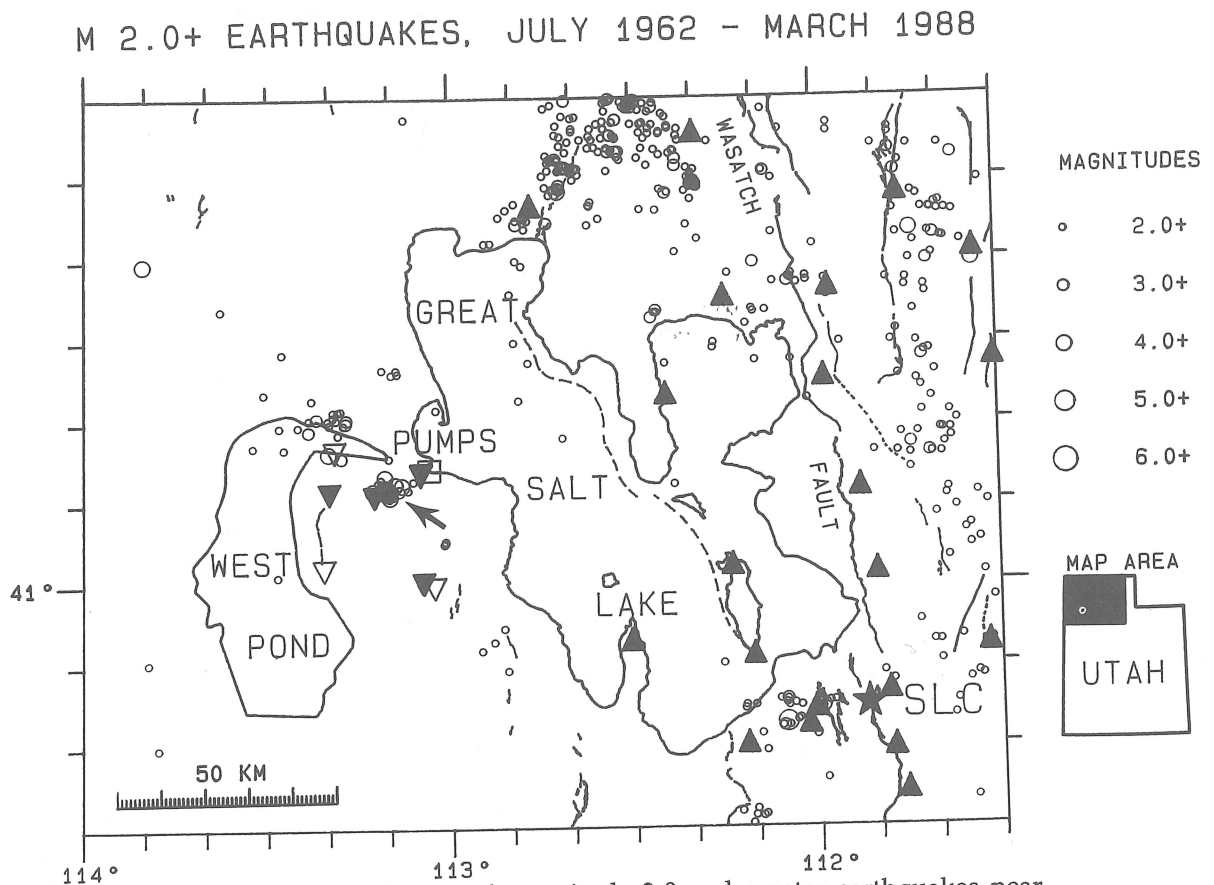
Fig. 1. Epicentral map of magnitude 2.0 and greater earthquakes near the Great Salt Lake located by the University of Utah from July 1962, when the University's regional seismic network began operation, through March 1988. The arrow points to the location of the 1987-1988 Lakeside sequence. Solid upright triangles show permanent stations of the University of Utah network in March 1988. Inverted open and solid triangles show locations of portable seismographs and temporary telemetered stations, respectively, installed to supplement the permanent network during the sequence. The open square labeled "Pumps" marks the location of the West Desert Pumping Station. These pumps pumped water from April 10, 1987, through June 30, 1989, from the Great Salt Lake into the Great Salt Lake Desert, lowering the level of the Great Salt Lake and creating the artificial lake labeled West Pond. The star labelled SLC shows the location of downtown Salt Lake City. Solid and dashed lines show surface traces of late Quaternary faults from the compilation of Arabasz et al. (1992).

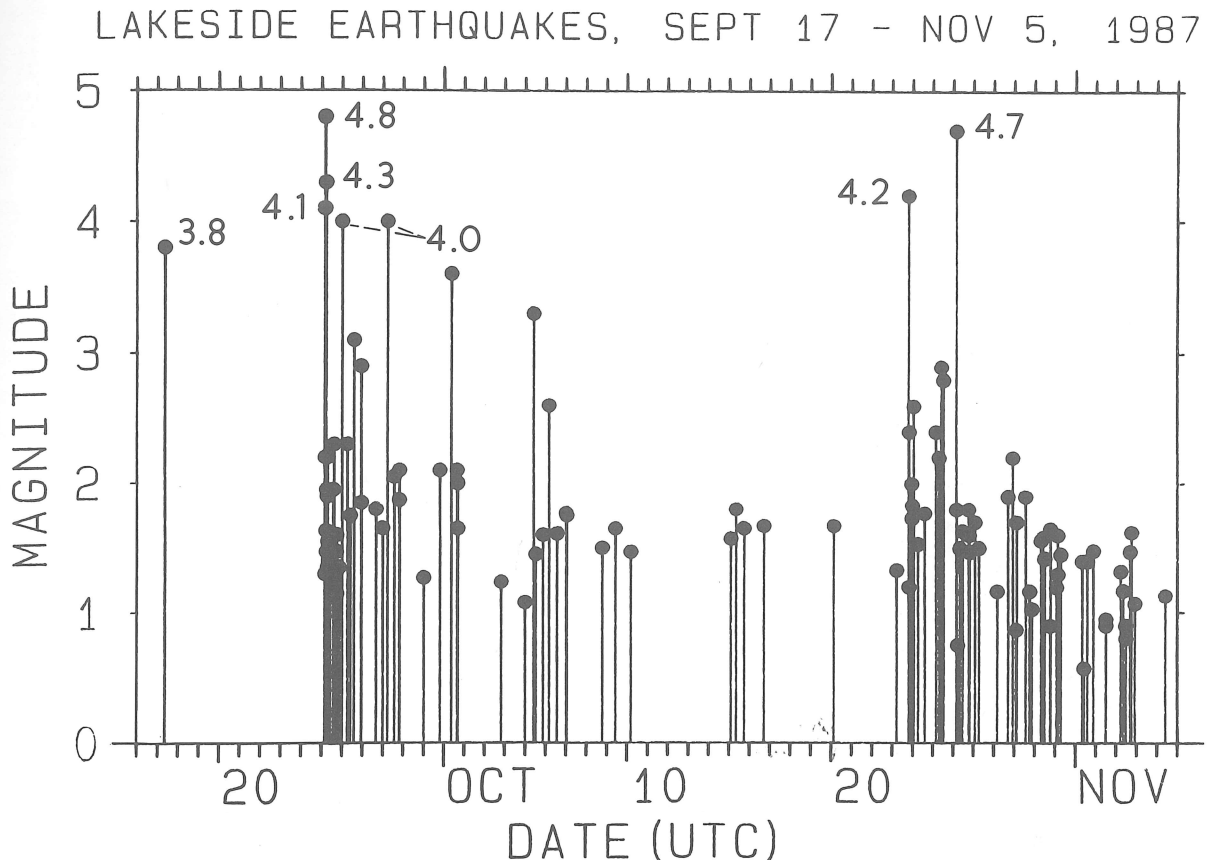LAKESIDE EARTHQUAKES, SEPT 17 - NOV 5, 1987

Fig. 2. Plot of magnitude versus time for the Lakeside earthquake sequence from September 17 through November 5, 1987 (UTC). Magnitudes of the eight $M_L \geq 3.8$ events are labeled. The plot includes all earthquakes in the University of Utah catalog within 15 km of the center of the activity (41° 12' N, 113° 10.5' W). The sample is believed to be complete for $M_L \geq 1.5$. See Nava et al. (1990) and Table 1 for information on the methods used to determine the magnitudes.

September 17, 1987. The first was an M_c (coda magnitude) 2.4 event in 1964 and the second was an M_c 1.3 event on October 18, 1986. We relocated the second earthquake according to the procedure described below. Our relocated epicenter is 8 km NE of the center of the 1987-1988 activity.

CHRONOLOGY OF THE SEQUENCE

Figure 2 is a plot of magnitude versus time for the Lakeside sequence from September 17 through November 5, 1987. All eight earthquakes of $M_L \geq 3.8$ occurred in September and October of 1987. The sequence began with an M_L 3.8 foreshock on September 17. No other events were detected by the University of Utah regional seismic network (Figure 1) until September 25, when three moderate earthquakes occurred within 70 minutes of each other: an M_L 4.1 foreshock, the M_L 4.8 mainshock at 04:27 UTC (10:27 PM. MDT, September 24), and an M_L 4.3 aftershock. An M_L 4.7 event followed on October 26. Following the

M_L 4.7 earthquake, frequent small aftershocks of $M_L \leq 3.1$ continued through March 1988, after which the rate of aftershock activity declined substantially. The University of Utah Seismograph Stations located a total of 237 earthquakes in the Lakeside area from September 1987 through March 1988, including 23 of $M \geq 2.5$ (Table 1) and 110 of $M \geq 1.5$, the magnitude range for which the data set appears to be complete. In contrast, only six small earthquakes of $M \leq 2.4$ were located in this area from April through December of 1988. Our estimated completeness threshold of M 1.5 is based on the frequency-magnitude distribution of the sequence prior to October 7, when some additional telemetered seismic stations were temporarily installed near the Lakeside activity.

Local magnitudes determined from maximum peak-to-peak amplitudes recorded on Wood-Anderson seismographs operated by the University of Utah at Dugway and Salt Lake City, Utah, are almost the same for the two largest earthquakes in the sequence, 4.8 and 4.7 (Table 1).

Table 1
Relocated Hypocenters of All Lakeside Earthquakes of $M_L \geq 2.5$

Date	Origin Time (UTC)	Latitude N (deg min)	Longitude W (deg min)	Depth (km)	M_L	No	Gap (deg)	Dmin (km)	Rms (sec)
9/17/87	08:31:26.00	41 12.23	113 10.49	12.0#	3.8	13	223	66	0.13
9/25/87	04:09:53.97	41 12.89	113 10.03	12.0#	4.1	13	222	66	0.11
9/25/87	04:27:57.52	41 12.24	113 10.88	12.0#	4.8	13	223	67	0.12
9/25/87	05:18:14.90	41 11.97	113 05.72	12.0#	4.3	12	247	60	0.21
9/26/87	00:28:01.98	41 11.94	113 08.73	12.0#	4.0	12	220	6	0.17
9/26/87	14:47:49.23	41 12.02	113 10.58	12.1	3.1c	15	87	14	0.11
9/26/87	23:14:39.37	41 12.81	113 10.88	10.2	2.9	15	86	13	0.11
9/28/87	06:06:52.05	41 13.46	113 10.65	11.9	4.0	16	93	8	0.09
10/01/87	09:16:31.07	41 12.41	113 10.77	10.4	3.6	17	87	9	0.19
10/05/87	10:31:02.93	41 11.98	113 10.34	10.3	3.3	17	87	8	0.12
10/06/87	04:44:25.59	41 12.14	113 11.27	9.6	2.6	16	92	9	0.16
10/23/87	19:44:50.32	41 11.98	113 10.05	10.7	4.2	13	121	8	0.10
10/24/87	01:51:36.90	41 11.55	113 10.48	11.1	2.6	14	119	9	0.09
10/25/87	10:43:02.60	41 11.33	113 10.52	10.8	2.9	14	116	9	0.11
10/25/87	13:17:44.35	41 11.74	113 10.77	11.4	2.8	14	120	9	0.11
10/26/87	04:16:00.85	41 10.90	113 10.49	10.2	4.7	14	113	9	0.31
11/07/87	17:52:34.04	41 13.25	113 11.94	10.2	2.7	12	137	4	0.12
11/17/87	16:20:45.04	41 11.05	113 10.57	10.0	2.8	15	114	3	0.11
1/29/88	00:58:33.59	41 12.22	113 10.73	11.4	2.8c	15	124	4	0.10
1/30/88	05:37:13.04	41 12.22	113 10.86	11.3	3.1	15	125	3	0.12
1/30/88	09:02:38.66	41 12.17	113 10.73	11.2	2.9	15	124	3	0.14
2/05/88	16:14:03.30	41 12.53	113 11.98	11.3	2.9c	11	131	3	0.16
3/02/88	02:03:20.75	41 12.06	113 10.11	11.2	2.8	16	122	4	0.07

\#   indicates fixed focal depth

M_L =   local magnitude. All but three of the magnitudes listed are mean values determined from maximum peak-to-peak amplitudes recorded on Wood-Anderson seismographs at Dugway (distance~115 km, azimuth~165°) and Salt Lake City (distance~120 km, azimuth~113°), Utah, using the distance corrections of Richter (1958). The other three magnitudes, labeled "c", were calculated from signal durations and are more correctly termed coda magnitude, M_c.

No =   number of P-wave arrival times used in the location

Gap =   largest azimuthal separation between stations used in the location

Dmin =   epicentral distance to the closest station used in the location

Rms =   weighted root-mean-square of the travel-time residuals

However, the body-wave magnitudes determined by the U.S. Geological Survey (1987) are 4.7 for the September 25 event and 4.3 for the October 26 event. Examination of the Wood-Anderson seismograms shows that the signal durations and the average amplitudes for the September 25 event are noticeably larger than those for the October 26 event (Figure 3). Application of a method developed by Bolt and Herraiz (1983) to estimate seismic moment from Wood-Anderson seismograms yields moments of 3.8×10^{23} dyne-cm and 1.3×10^{23} dyne-cm for the September 25 and October 26 shocks, respectively. The corresponding moment magnitudes, M_W (see Hanks and Kanamori, 1979) are 5.0 and 4.7. Comparing moment estimates from each Wood-Anderson station separately, the measurements from the Dugway records indicate a factor of 4.7 higher moment for the first event compared to the second, whereas the measurements from the Salt Lake City records indicate a factor of 2.4 difference. Thus, despite the similar local magnitudes, it appears that the September 25 earthquake was clearly the larger of the two, and that the October 26 earthquake can be considered an aftershock. Seismic moments estimated for the other six $M_L \geq 3.8$ events with the Bolt and Herraiz technique are all more than a factor of eight smaller than that of the mainshock. The cumulative seismic moment release of the eight largest shocks is estimated to be 6.6×10^{23} dyne-cm, equivalent to a single earthquake of $M_W = 5.2$.

EARTHQUAKE LOCATIONS

Deployment of Portable Instruments

When the Lakeside sequence began, the closest seismograph station was a permanent station of the University of Utah seismograph network located 60 km to the southeast (Figure 1). Access to the epicentral area was difficult because of the lack of roads and because the earthquakes occurred beneath a broad water-saturated mud flat at the northern end of the Hill Air Force Range, a restricted area used for training and munitions testing (Figure 4). Nevertheless, University of Utah personnel were able to supplement the stations of the permanent network with a reasonable distribution of temporary local stations beginning on September 26, the day after the M_L 4.8 earthquake (Table 2). Initially these consisted of four portable seismographs with smoked-paper recorders (open inverted triangles, Figure 1). Subsequently, these were replaced by four portable telemetry stations (solid inverted triangles, Figure 1), including one located at an epicentral distance of 2 to 6 km from the activity and that was installed by helicopter on October 29 following the M_L 4.7 earthquake. The portable telemetry stations were operated until August 16, 1988, although there were intermittent station failures after late March 1988. The seismometers at all of the temporary stations were high-gain, short-period, vertical-component velocity sensors.
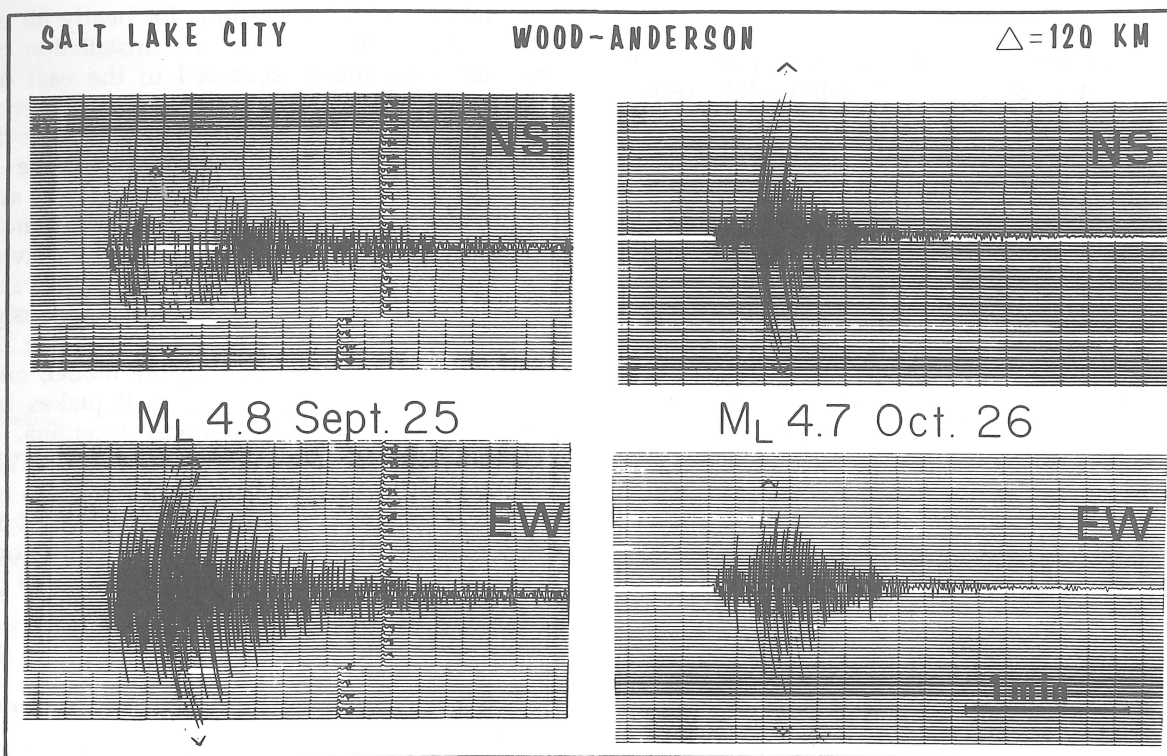
Fig. 3. Seismograms of the two largest Lakeside earthquakes recorded by an electronically-simulated Wood-Anderson instrument on the University of Utah campus in Salt Lake City. The epicentral distance is approximately 120 km. The V's mark the peak amplitudes used to compute the local magnitudes.

Table 2
Stations Used for Relocations of the Lakeside Earthquake Sequence

Station Name	Type†	Latitude N (deg min)	Longitude W (deg min)	Elevation (m)	Station Correction (sec)	First Event Recorded (UTC)* Date	First Event Recorded (UTC)* Time	Last Event Recorded (UTC)* Date	Last Event Recorded (UTC)* Time
ERUT	P	41 10.89	113 12.51	1309	−.11	10/29	03:42	3/26	20:34
HRUT	P	41 13.63	113 04.85	1408	−.09	10/07	00:50	3/26	20:34
HOGS	M	41 13.76	113 04.83	1414	.00	9/26	00:28	10/07	01:39
NFUT	P	41 11.26	113 19.93	1378	−.02	10/07	00:50	3/26	20:34
NNFU	M	41 16.42	113 19.04	1289	−.18	9/26	06:55	10/07	01:39
SJRU	M	41 01.84	113 20.84	1292	−.05	9/26	06:55	10/07	01:39
GVUT	P	41 00.23	113 04.48	1530	+.04	10/07	00:50	3/26	20:34
GRMU	M	40 59.63	113 02.69	1493	+.08	9/28	00:28	10/07	01:39
SNUT	R	40 53.14	112 30.54	1652	+.19	9/17	08:31	3/26	20:34
EPU	R	41 23.49	112 24.53	1436	+.11	9/17	08:31	3/26	01:00
HVU	R	41 46.78	112 46.50	1609	+.17	9/17	08:31	3/26	20:34
ANU	R	41 02.38	112 13.90	1353	−.06	9/17	08:31	3/02	02:29
CPU	R	40 40.34	112 11.78	2377	−.04	9/17	08:31	3/21	07:24
GZU	R	41 25.53	111 58.50	2646	−.12	9/17	08:31	3/26	01:00
PTU	R	41 55.76	112 19.48	2192	−.04	9/17	08:31	3/21	07:24
MOUT	R	41 11.94	111 52.73	2743	−.07	9/17	08:31	3/21	07:24
WVUT	R	41 36.61	111 57.55	1828	+.05	9/17	08:31	3/21	07:24
FPU	R	41 01.58	111 50.21	2816	−.19	9/17	08:31	3/02	02:03
DUG	R	40 11.70	112 48.80	1477	+.19	9/17	08:31	3/02	02:03
NPI	R	42 08.84	112 31.10	1640	+.01	9/17	08:31	3/02	02:03
CWU	R	40 26.75	112 06.13	1945	−.04	9/17	08:31	3/21	07:24

†R= UUSS regional network, M= microearthquake recorder, P= portable telemetry
*From September 17, 1987, through March 31, 1988

Location Procedure

We relocated the Lakeside earthquakes with the computer program HYPOINVERSE (Klein, 1978) and P-wave arrival times from the eight temporary stations (generally four at any one time) plus 13 selected permanent stations located at epicentral distances of less than 125 km (Table 2). The velocity model used for the locations (the Wasatch Front model in Table 3) is a modified version of model B of Keller *et al.* (1975), taken from Bjarnason and Pechmann (1989). Because some of the most distant stations were important for azimuthal control (including some located outside of the area shown in Figure 1), we chose not to apply any distance weighting to the data. We did not use any S-wave arrival times for our relocations because there were no horizontal-component records from nearby stations to provide reliable S-wave data.

Initial epicentral locations for nearly all of the events that occurred before the installation of the portable instruments scattered to the east of the epicenters for the later events. This observation suggested that the earlier events were being systematically mislocated because of the poor azimuthal distribution of stations (Figure 1) and an inadequate velocity model. In an attempt to alleviate this problem, we used an inversion program written by Walter C. Nagy at the University of Utah to solve simultaneously for station delays for the 21 stations in Table 2, the velocity of the second layer of the model, and for hypocenters of 170 Lakeside earthquakes which had reasonably good preliminary locations. Both this program and the version of HYPOINVERSE that we used took the elevation differences of the stations into account in calculating the travel times. Velocity inversion was attempted only for the second layer of the model because this layer
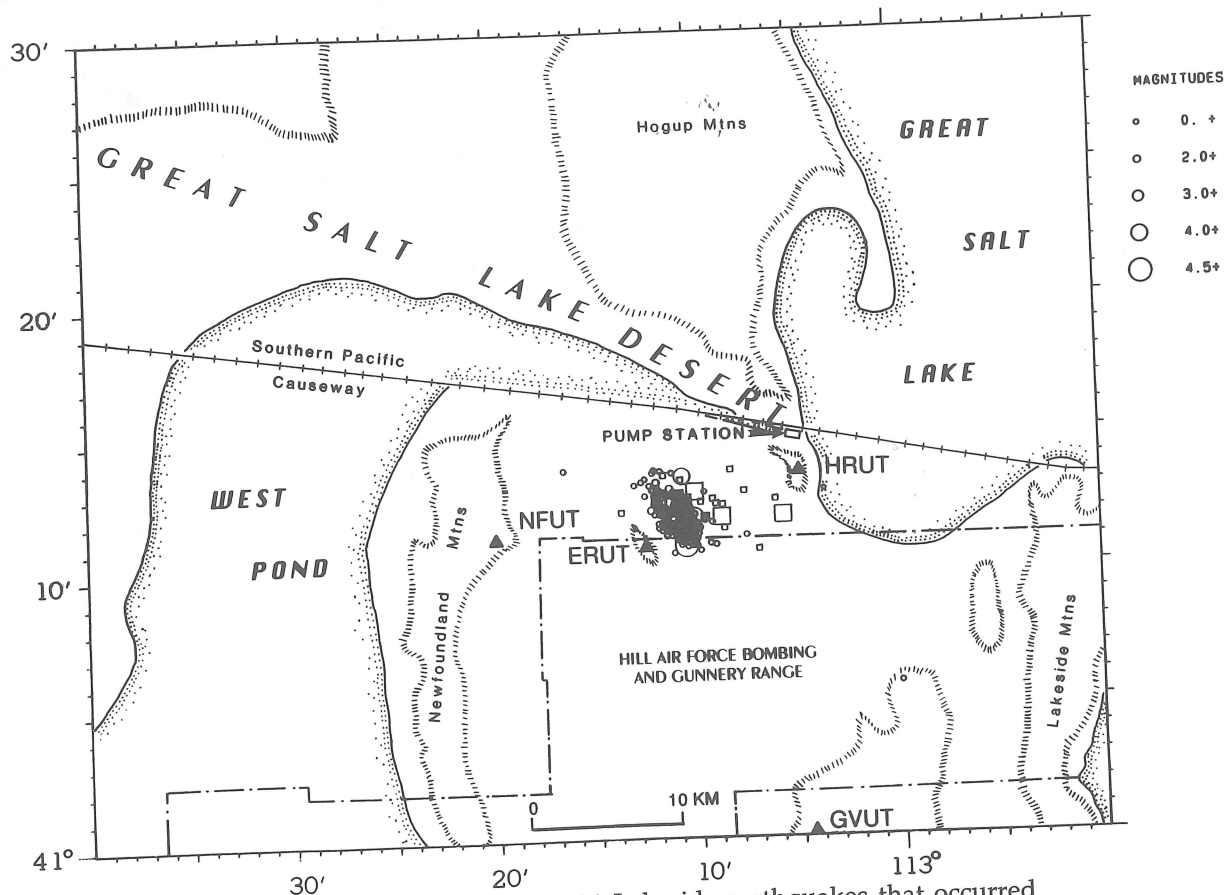
Fig. 4. Relocated epicenters for 221 Lakeside earthquakes that occurred from September 1987 through March 1988. Circles indicate earthquakes that occurred after the first portable stations were installed on September 26, and squares indicate earlier events for which we fixed the focal depths. Symbol sizes are scaled by magnitude as shown. The triangles show the locations of the four portable telemetry stations that were installed in October (Table 2). The shoreline of the Great Salt Lake is shown at its approximate location in late 1984.

<div align="center">

Table 3
Lakeside Velocity Models

Region	P-Wave Velocity (km/sec)	Depth to Top of Layer (km)*
Wasatch Front	3.4	0.0
	5.9	1.5
	6.4	17.1
	7.5	28.0
	7.9	42.0
Colorado Plateau	3.4	0.0
	5.9	1.5
	6.2	17.1
	6.8	27.5
	7.9	42.0
Southeast Idaho	3.4	0.0
	5.9	1.5
	6.8	17.1
	7.9	42.0

</div>

*Datum is 1500 m above sea level

contains all of the hypocenters for the events used in the inversion, and the direct ray paths from these hypocenters to the 21 stations lie primarily within this layer. Our starting velocity model (the Wasatch Front model in Table 3) predicts that these direct rays are the first arrivals out to epicentral distances of 96 to 126 km for sources in the depth range of 6 to 12 km, where most of the Lakeside earthquakes occurred.

The velocity obtained for the second layer from two inversions with different parameters remained within 0.06 km/sec of the starting value of 5.9 km/sec. Because the velocity did not change very much, and because it is questionable whether or not the data are of sufficiently good quality for a velocity inversion, we decided to hold the velocity model fixed and solve only for station delays and hypocenters. Tests showed that the station delays computed by the program were not very sensitive to the parameters of the inversion.

After determining the station delays (Table 2), we used them with the program HYPOINVERSE to relocate all of the Lakeside earthquakes, starting from a trial hypocenter at 9 km depth at the center of the activity. Even when using the station delays, we found it advantageous to fix the focal depths of the 26 earthquakes that were recorded before the portable instruments were installed. Otherwise, the locations for these events suffered from an unconstrained tradeoff between focal depth and epicentral location. The focal depths of the first 26 earthquakes were fixed to 12 km if the magnitude was 3.8 or greater and to 9 km if the magnitude was smaller. The deeper fixed focal depths for the $M_L \geq 3.8$ events were motivated by the observation that all of the focal depths which could be determined for earthquakes in this size range are between 10 and 12 km (Table 1). Use of the station delays reduced the median root-mean-square of the weighted travel time residuals from

0.13 sec to 0.11 sec for the 221 earthquakes in 1987 and 1988 that we relocated.

Hypocentral Distribution

Figure 4 shows epicenters of 221 Lakeside earthquakes that occurred from September 1987 through March 1988 (see Table 1 for a listing of the $M_L \geq 2.5$ events, and Pechmann et al., 1992, for a complete listing). The sample includes all but 16 of the 237 earthquakes that occurred during this time period in the area shown and were large enough to trigger the centralized digital recording system used for the regional seismic network and the portable telemetry stations. The other 16 earthquakes (all of $M \leq 1.3$) are not included because they have less than five measured P-wave arrival times or azimuthal gaps between stations of more than 300°.

Most of the earthquakes in Figure 4 concentrate within a SSE-trending zone that is 6 km long. About half of the epicenters of the early events with fixed focal depths (squares) scatter to the east of this zone, but the scatter is less than when no station delays are used. The epicentral pattern is similar but better-defined on Figure 5, which shows 154 of the best-located earthquakes from Figure 4. The selection criteria were: (1) distance to the nearest station equal to 15 km or less, (2) maximum azimuthal gap between stations of 180°, (3) minimum of six arrival times used for the location, and (4) maximum horizontal and vertical standard errors of 1.5 km. These criteria unfortunately exclude all events that occurred before the first portable station installed west of the activity (NNFU) became operational on September 26 at 01:15 UTC, 21 hours after the mainshock.

Cross sections along line A-A' on Figure 5 show that our hypocenters for this sample of aftershocks concentrate between 6 and 12 km depth (Figure 6). The foci of all three well-located earthquakes of $M_L \geq 4$ lie in the bottom third of this depth range. The aftershock zone appears to have a dip greater than 65°, and perhaps near vertical, but the direction of dip cannot be determined with confidence from the cross sections in Figure 6. The apparent ENE dip of the aftershock zone is due to the fact that the shallowest hypocenters are confined to the WSW half of the 3-km-wide zone. However this pattern, if real, could be interpreted as an upward thinning of the aftershock zone instead of as evidence for an ENE dip.

The apparent dimensions of the aftershock zone inferred from Figures 5 and 6 are 6 by 6 by 3 km. The actual dimensions of the aftershock zone are probably smaller, because the estimated errors in the hypocentral locations are not negligible

WELL-LOCATED LAKESIDE EARTHQUAKES
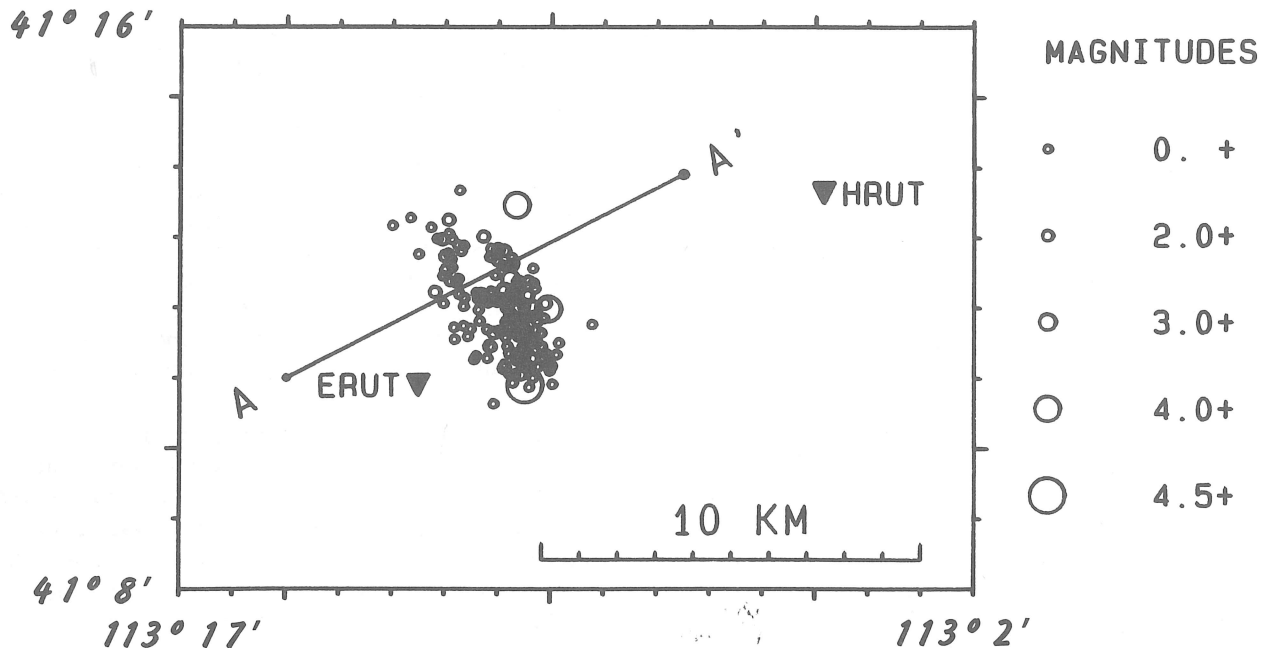## SEPTEMBER 1987 – MARCH 1988

Fig. 5. Map view of 154 well-located Lakeside aftershocks that occurred from September 26, 1987, through March 21, 1988. See text for selection criteria. The two closest portable telemetry stations are shown as inverted triangles. The line A-A' shows the direction of the cross sections in Figure 6, and is taken perpendicular to the preferred nodal plane of the mainshock focal mechanism (Figure 8).

compared to the apparent size of the zone. As expected, tightening the quality selection criteria causes the apparent size of the aftershock zone to decrease. For example, requiring the nearest recording station to be within 6 km and reducing the cutoff values for the horizontal and vertical standard errors to 0.5 km leaves a data set of 17 hypocenters. These hypocenters form a zone having NNW, vertical, and ENE dimensions of 4, 2.5, and 2 km, respectively. This particular sample may be too small to adequately represent the overall size of the aftershock zone, and includes only aftershocks recorded by station ERUT, which was not installed until October 29 (see Figure 5 and Table 2). Nevertheless, it shows that the true dimensions of the aftershock zone might be a factor of two or more smaller than the dimensions that we have inferred from Figures 5 and 6.

A space-time plot of all of the earthquakes located in this study shows the epicenters of the mainshock and its two recorded foreshocks to be near the center of the aftershock zone (Figure 7). This observation weakly suggests bilateral rupture, but is not definitive because of the poor quality of the locations of the earliest events. The epicenter of the largest aftershock is at the southeastern end

of the aftershock zone. Most of the other aftershocks in late October are within 2 km NNW of this M_L 4.7 event. There are no resolvable changes in focal depths with time.

FOCAL MECHANISMS

We attempted to determine focal mechanisms from P-wave first motions for all eight earthquakes in the Lakeside sequence of $M_L \geq 3.8$. Because these earthquakes occurred on the western edge of the University of Utah seismic network, we augmented the data from this network, when possible, with data from seismograph stations in Nevada, Idaho, and Washington. Takeoff angles for the first-arriving P waves were calculated using the relocated hypocenters and three different one-dimensional velocity models for stations located in different regions (Table 3). These velocity models and the accuracy of the takeoff angles computed from them are discussed in Bjarnason and Pechmann (1989), along with further details of the methodology which we used.

Only the focal mechanism for the M_L 4.8 mainshock is well constrained by the available data (Figure 8). The mainshock focal mechanism indicates right-lateral strike-slip motion on a SSE-
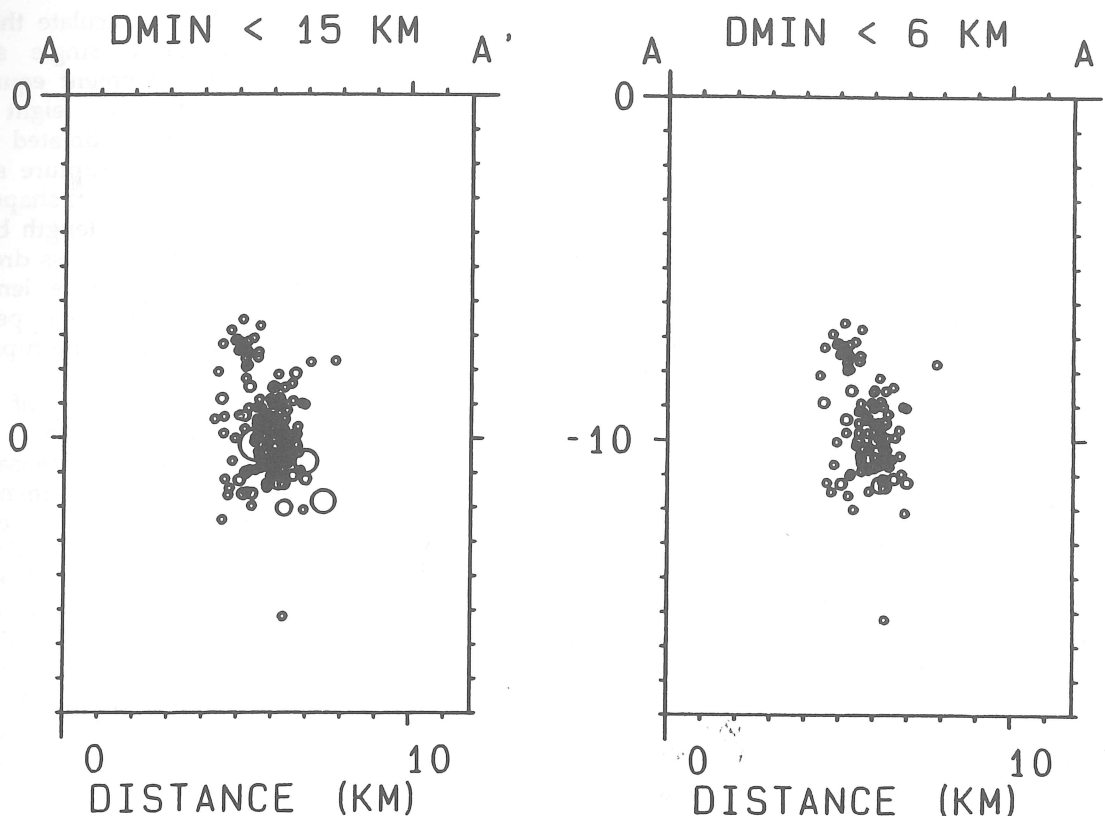
Fig. 6. Hypocentral cross sections with no vertical exaggeration along line A-A' in Figure 5. Circle sizes are scaled by magnitude as in Figure 5. The cross section on the left includes all of the earthquakes from Figure 5. The cross section on the right includes only those earthquakes from Figure 5 for which the distance to the nearest station used in the location, DMIN, is less than 6 km. The median standard horizontal and vertical errors for the hypocenters on both cross sections are 0.5 and 1.0 km, respectively. Note that the hypocentral distribution is similar on both cross sections.

striking fault that dips steeply to the SW or, alternatively, left-lateral strike-slip motion on a nearly vertical fault that strikes ENE. This focal mechanism is fortunately not very sensitive to focal depth which, as explained above, is poorly controlled due to the lack of nearby stations and was fixed at 12 km. The SSE trend of the aftershock zone is parallel to the right-lateral nodal plane of the focal mechanism, suggesting that this nodal plane is the fault plane. The strike, dip, and rake of this nodal plane are 153° ± 4°, 78° ± 10°, and -174° ± 8°, respectively (following the sign convention for rake angle of Aki and Richards, 1980, p. 106).

The first motion data for the largest aftershock (Figure 8, lower right) are compatible with two different possible focal mechanisms: a strike-slip solution similar to that of the mainshock (solid nodal planes) or else normal slip on a fault plane that dips moderately to either the W or to the ESE (dashed nodal planes). The focal mechanisms for

the other six $M_L \geq 3.8$ earthquakes are less well constrained. The first motion data for these events show some variability from one event to another, but in all cases can be fit by solutions showing right-lateral strike-slip faulting on a SE- to SSE-striking plane, or normal or oblique-normal faulting on SE- to SW-striking planes (Figure 8). The tension (T) axes of the focal mechanisms for the mainshock and the largest aftershock have shallow plunges and trend ESE-WNW. The T axes for the rest of the focal mechanisms are constrained by the data to have moderate to shallow plunges and trends between NE-SW and SE-NW.

DISCUSSION

Tectonic Implications

Taken together, the focal mechanism for the mainshock and the distribution of its aftershocks imply that the M_L 4.8 Lakeside earthquake involved right-lateral strike-slip motion on a fault

233

striking SSE and dipping steeply (>65°) WSW. The earthquake occurred beneath a saline mud flat between the Newfoundland and Lakeside mountains (Figure 4), where no strike-slip faults have been mapped. However, the area in question has been covered by Lake Bonneville and the Great Salt Lake several times during the last 30,000 years and at least twice during the last 3,000 years (Currey et al., 1984), so it is possible that evidence of late Quaternary faulting could have been obliterated by fluctuations in the level of the lake.

From the size of the aftershock zone (Figures 5 and 6), we infer that slip during the Lakeside sequence occurred between 6 and 12 km depth on a section of fault with dimensions no larger than 6 by 6 km. All of this inferred rupture zone did not necessarily slip during the mainshock. The southeasternmost third of this zone may have broken during the largest aftershock, some of it, perhaps, for the first time. This admittedly speculative interpretation is suggested by the space-time plot in Figure 7 and the roughly factor-of-three difference in seismic moments between the mainshock and the largest aftershock.

As a check on our estimate of the maximum size of the fault segment which broke during the Lakeside earthquakes, we use equations given by

Boore and Dunbar (1977) to calculate the size of the rupture expected for a single strike-slip earthquake with a seismic moment equal to the cumulative moment of the eight largest earthquakes of the sequence, estimated above to be 6.6×10^{23} dyne-cm. If the rupture surface is assumed to have a 90° dip, a square shape, and an upper edge at least one rupture length below the earth's surface, then for typical stress drops of 10 to 100 bars the calculated rupture lengths are between 5.2 and 2.4 km. Thus, our upper limit of 6 by 6 km for the size of the Lakeside rupture zone is reasonable.

The ESE-WNW-trending T axes of the focal mechanisms for the two largest Lakeside earthquakes (Figure 8) are typical of Wasatch Front earthquakes (Bjarnason and Pechmann, 1989; Patton and Zandt, 1991). Most focal mechanisms for earthquakes in this region show predominantly normal faulting. However, some strike-slip and oblique-slip focal mechanisms are also observed, particularly in the southern Wasatch Front area (Arabasz and Julander, 1986; Jones, 1987; Doser, 1989; Bjarnason and Pechmann, 1989). These observations suggest that, at least locally, the present-day tectonics of the Wasatch Front region involves a complex interplay between normal and strike-slip faulting, as in the southern Great Basin (see Rogers et al., 1991).
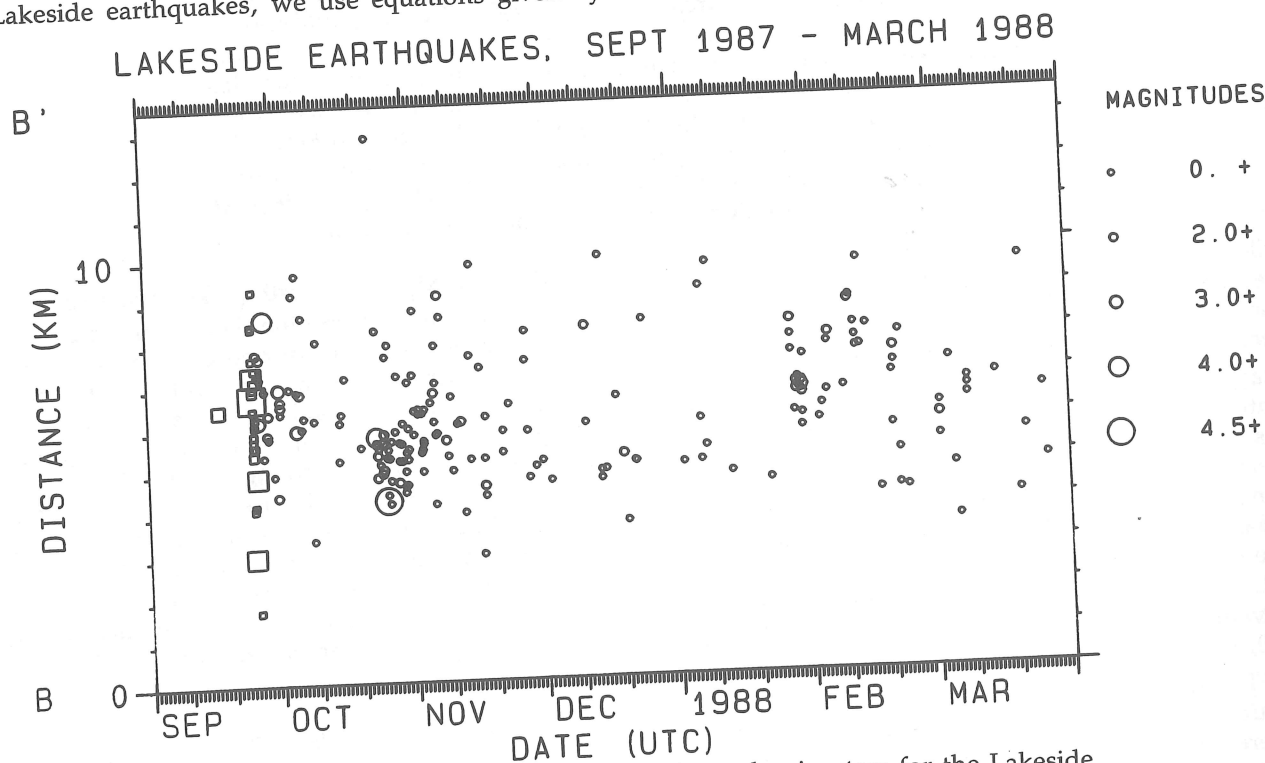
Fig. 7. Space-time plot of the 221 relocated epicenters for the Lakeside earthquakes shown on Figure 4. The space coordinate is the distance NNW along the strike of the inferred fault plane, i.e., along a line perpendicular to line A-A' on Figure 5. Squares and circles as in Figure 4.
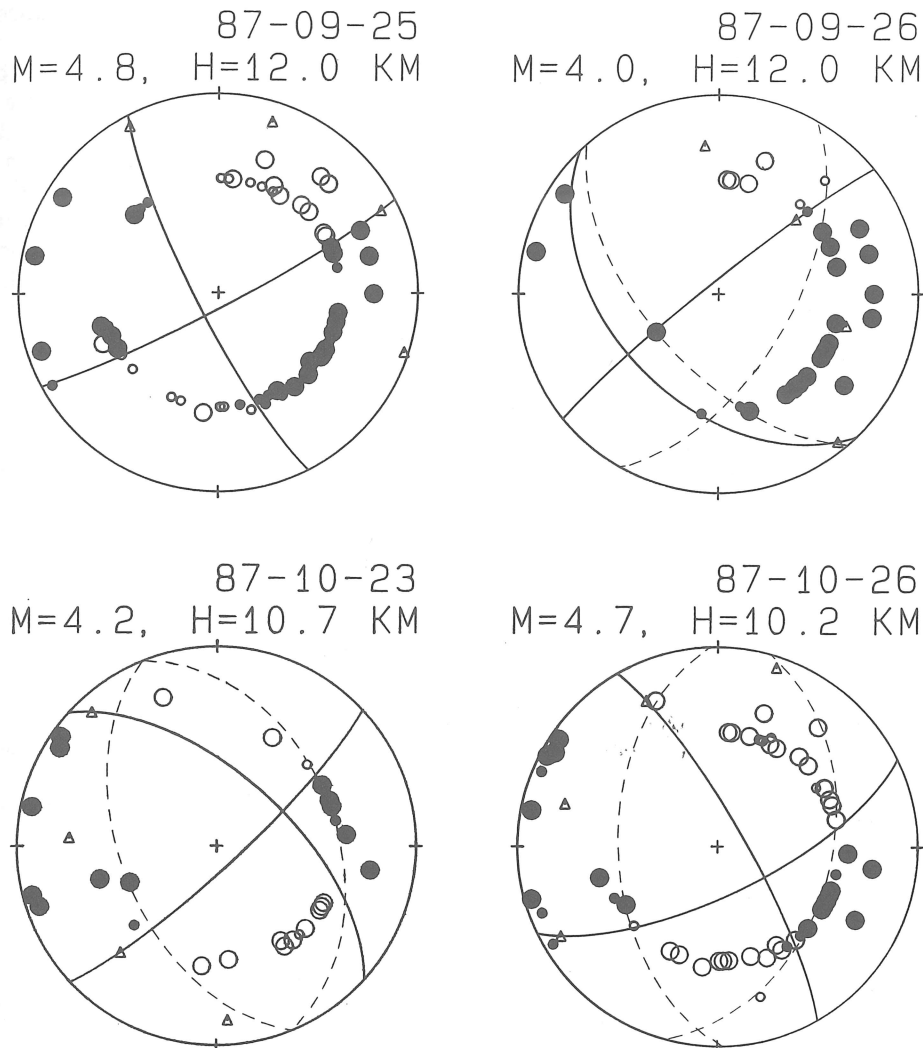
Fig. 8. The four best-constrained focal mechanisms for earthquakes in the Lakeside sequence, including the mainshock (upper left) and largest aftershock (lower right). The date, magnitude (M), and depth (H) are given for each earthquake. P-wave first motions are plotted on a lower-hemisphere projection, with compressions shown as solid circles and dilatations as open circles. Smaller circles indicate readings of lower confidence. The triangles show slip vectors and P and T axes for the solutions shown by the solid nodal planes. The dashed nodal planes show representative alternative solutions. Based on the aftershock distribution (Figures 4 to 6), the SSE-striking nodal plane of the mainshock focal mechanism is the probable fault plane.

In 1934 an earthquake of M_s 6.6 occurred in ...sel Valley, just north of the Great Salt Lake ... 60 km NNE of the 1987-1988 Lakeside ...quakes. The 1934 shock is the largest ...rical (post-1850) earthquake in the Utah ...on, and the only one with documented surface ...ing. The surface faulting consisted primarily ...rtical displacements, up to a maximum of 50 ...on four N-trending fractures which formed a ...m-long zone (Shenon, 1934, 1936). However, ...surface rupture may have been secondary in

view of the pure strike-slip focal mechanism for the mainshock obtained by Doser (1989) from waveform modeling, which shows right-lateral faulting on a SE-striking plane or left-lateral faulting on a NE-striking plane. The focal mechanisms for the 1934 Hansel Valley mainshock and the 1987 Lakeside mainshock indicate that strike-slip movement is not limited to small earthquakes in the Wasatch Front region, and may therefore be contributing significantly to the deformation of this area.

Were the Lakeside Earthquakes Induced?

It is well known that engineering activities that affect elastic and/or fluid stresses in the Earth, such as impoundment of deep reservoirs, occasionally trigger local earthquakes (e.g., Simpson, 1986). The occurrence of the Lakeside earthquakes so close to the West Desert Pumping Station, and only five months after the pumps began operating, raises the question of whether or not the earthquakes might have been induced by the pumping. Possible mechanisms include (1) changes in elastic stresses and/or pore pressure caused by changes in the surface water load and (2) an increase in pore pressure at depth due to diffusion of water from the surface (see Bell and Nur, 1978, and Simpson, 1986). Although we cannot rule out the possibility that the Lakeside earthquakes were induced, we consider it unlikely based on the following reasoning.

In cases where the ambient tectonic stress favors normal or strike-slip faulting, any zones of weakening caused by surface water loading (or unloading) would be expected to be centered under the water load, whether the weakening results from changes in elastic stresses or pore pressure coupled to the elastic stresses (Bell and Nur, 1978). Seismicity in such cases tends to spread out over an active volume rather than cluster along well-defined fault zones (Simpson *et al.*, 1988). The 1987-1988 Lakeside earthquakes occurred on what appears to be a single fault zone between West Pond and the Great Salt Lake in an area that was not flooded by either during the 1980's (Figure 4; Ben Everitt, Utah Division of Water Resources, personal communication, 1992). These observations, and the lack of earthquakes shallower than 6 km depth (Figure 6), all argue against triggering by surface loading. In terms of the surface loading itself, the average depth of West Pond when full was only 0.76 m and the maximum depth was only 2.1 m (Ben Everitt, written communication, 1987). In comparison, the level of the Great Salt Lake rose 6.25 m from 1963 to 1986, with 3.72 m of this increase occurring between 1982 and 1986 (Stephens and Arnow, 1987). The elevation of the lake peaked at 1283.77 m in June 1986 and in April 1987 (Stephens and Arnow, 1987; Mabey, 1987). The lake level declined after April 1987, in part due to the pumping but primarily because of decreased precipitation (Mabey, 1987). Thus, overall the changes in surface loads caused by the rapid rise of the Great Salt Lake between 1982 and 1986 were much larger than those caused by the subsequent pumping project.

Regarding the possibility of pore-pressure changes at hypocentral depths due to fluid diffusion from the surface, a time lag of five months and a hypocentral distance of ~10-15 km from the new West Pond to the foci of the earliest Lakeside earthquakes are not out of the question, especially if a highly permeable fault zone is hypothesized (e.g., Talwani and Acree, 1985, Figure 5). But one still is left with the problem of explaining a hydraulic head large enough to both drive the diffusion and significantly alter fluid stresses at depth. Given that hydrostatic pressure at the surface changes by only 0.1 bar for every meter of water depth, we judge that pore-pressure changes relating to the creation of West Pond (≤ 0.2 bars) were too small to induce seismicity. Again, relative changes in hydrology from the rapid rise of the Great Salt Lake during the years preceding the Lakeside earthquakes would be expected to have been much greater than those caused by the pumping.

Finally, any convincing argument for induced seismicity must demonstrate a clear disparity between prior natural seismicity and the earthquakes in question (e.g., Nicholson and Wesson, 1990; Davis and Frohlich, 1993). In light of (1) scattered background seismicity in widespread parts of the Great Salt Lake Desert (Figure 1) and (2) previous episodic earthquake activity of $M_L \leq 4.0$ within 30 km of the 1987-1988 Lakeside earthquakes (see section on Seismological Setting), the latter earthquakes, although of larger magnitude, cannot be considered unusual.

CONCLUSIONS

1. The 1987 M_L 4.8 Lakeside earthquake involved right-lateral strike-slip motion on a buried fault dipping steeply to the WSW beneath a lacustrine basin west of the Great Salt Lake.

2. From the aftershock distribution, we infer that the 1987-1988 Lakeside earthquakes broke a segment of the fault having dimensions of 6 by 6 km or smaller, and lying within the depth range of 6 to 12 km.

3. Foreshocks of M_L 3.8 and 4.1 occurred eight days and 18 minutes, respectively, before the Lakeside mainshock. Prior to these foreshocks, there had been very little instrumentally-recorded seismicity in the immediate epicentral area.

4. There is no compelling evidence that the 1987-1988 Lakeside earthquakes were related to the West Desert Pumping project.

REFERENCES

Aki, K. and P. G. Richards (1980). *Quantitative Seismology: Theory and Methods*, W. H. Freeman, San Francisco, California, 932 pp.

Arabasz, W.J. and D.R. Julander (1986). Geometry of seismically active faults and crustal deformation within the Basin and Range-Colorado Plateau transition, in *Cenozoic Tectonics of the Basin and Range Province: A Perspective on Processes and Kinematics of an Extensional Origin*, L. Mayer (Editor), *Geol. Soc. Am. Special Paper 208*, 43-74.

Arabasz, W.J., J.C. Pechmann, and E.D. Brown (1987). Evaluation of seismicity relevant to the proposed siting of a Superconducting Supercollider (SSC) in Tooele County, Utah, *Utah Geological and Mineral Survey, Misc. Publ. 89-1*, 107 pp.

Arabasz, W.J., J.C. Pechmann, and E.D. Brown (1992). Observational seismology and the evaluation of earthquake hazards and risk in the Wasatch Front area, Utah, in *Assessment of Regional Earthquake Hazards and Risk Along the Wasatch Front, Utah*, P.L. Gori and W.W. Hays (Editors), *U.S. Geol. Surv. Profess. Paper 1500-A-J*, D1-D36.

Bell, M. L. and A. Nur (1978). Strength changes due to reservoir-induced pore pressure and stresses and application to Lake Oroville, *J. Geophys. Res.* **83**, 4469-4483.

Bjarnason, I.T. and J.C. Pechmann (1989). Contemporary tectonics of the Wasatch Front region, Utah, from earthquake focal mechanisms, *Bull. Seism. Soc. Am.* **79**, 731-755.

Bolt, B.A. and M. Herraiz (1983). Simplified estimation of seismic moment from seismograms, *Bull. Seism. Soc. Am.* **73**, 735-748.

Boore, D. M. and W. S. Dunbar (1977). Effect of the free surface on calculated stress drops, *Bull. Seism. Soc. Am.* **67**, 1661-1664.

Currey, D.R., G. Atwood, and D.R. Mabey (1984). Major levels of Great Salt Lake and Lake Bonneville, *Utah Geological and Mineral Survey Map 73*, scale 1:750,000.

Davis, S.D. and C. Frohlich (1993). Did (or will) fluid injection cause earthquakes?—Criteria for a rational assessment, *Seism. Res. Lett.*, in press.

Doser, D. I. (1989). Extensional tectonics in northern Utah-southern Idaho, U. S. A., and the 1934 Hansel Valley sequence, *Phys. Earth Planet. Interiors* **54**, 120-134.

Hanks, T.C. and H. Kanamori (1979). A moment magnitude scale, *J. Geophys. Res.* **84**, 2348-2350.

Jones, C. H. (1987). A geophysical and geological investigation of extensional structures, Great Basin, western United States, *Ph.D. Thesis*, Massachusetts Institute of Technology, Cambridge, Massachusetts, 226 pp.

Keller, G.R., R.B. Smith, and L.W. Braile (1975). Crustal structure along the Great Basin-Colorado Plateau transition from seismic refraction studies, *J. Geophys. Res.* **80**, 1093-1098.

Klein, F. W. (1978). Hypocenter location program HYPOINVERSE, *U.S. Geol. Surv., Open-File Rept. 78-694*, 113 pp.

Mabey, D. R. (1987). The end of the wet cycle, *Survey Notes (Utah Geological and Mineral Survey)* **21**, no. 2-3, 8-9.

Nava, S. J., J. C. Pechmann, W. J. Arabasz, E. D. Brown, L. L. Hall, P. J. Oehmich, E. McPherson, and J. K. Whipp (1990). *Earthquake Catalog for the Utah Region, January 1, 1986 to December 31, 1988*, Special Publication, University of Utah Seismograph Stations, Salt Lake City, Utah, 96 pp.

Nicholson, C. and R. L. Wesson (1990). Earthquake hazard associated with deep well injection—a report to the U. S. Environmental Protection Agency, *U. S. Geol. Surv., Bull. 1951*, 74 pp.

Patton, H. J. and G. Zandt (1991). Seismic moment tensors of western U.S. earthquakes and implications for the tectonic stress field, *J. Geophys. Res.* **96**, 18,245-18,259.

Pechmann, J.C., S.J. Nava, and W.J. Arabasz (1992). Seismological analysis of four recent moderate (M_L 4.8 to 5.4) earthquakes in Utah, *Utah Geological Survey, Contract Rept. 92-1*, 107 pp.

Richter, C.F. (1958). *Elementary Seismology*, W.H. Freeman and Co., San Francisco, Calif., 768 pp.

Rogers, A. M., S. C. Harmsen, E. J. Corbett, K. Priestley, and D. dePolo (1991). The seismicity of Nevada and some adjacent parts of the Great Basin, in *Neotectonics of North America*, D. B. Slemmons, E. R. Engdahl, M. D. Zoback, M. L. Zoback, and D. D. Blackwell (Editors), *Geol. Soc. Am., Decade Map Vol. 1*, 153-184.

Shenon, P. J. (1934). Hansel Valley earthquake, March 12, 1934, unpublished report, U. S. Geological Survey.

Shenon, P. J. (1936). The Utah earthquake of March 12, 1934 (excerpts from unpublished report), in *United States Earthquakes, 1934*, F. Neumann, *U. S. Coast and Geodetic Survey Serial 593*, 43-48.

Simpson, D.W. (1986). Triggered earthquakes, *Ann. Rev. Earth Planet. Sci.* **14**, 21-42.

Simpson, D. W., W. S. Leith, and C. H. Scholz (1988). Two types of reservoir-induced seismicity, *Bull Seism. Soc. Am.* **78**, 2025-2040.

Smith, R. B. and W. J. Arabasz (1991). Seismicity of the Intermountain Seismic Belt, in *Neotectonics of North America*, D. B. Slemmons, E. R. Engdahl, M. D. Zoback, M. L. Zoback, and D. D. Blackwell (Editors), *Geol. Soc. Am., Decade Map Vol. 1,,* 185-228.

Stephens, D. and T. Arnow (1987). Fluctuations of water level, water quality, and biota of Great Salt Lake, Utah, 1847-1986, in *Cenozoic Geology of Western Utah—Sites for Precious Metal and Hydrocarbon Accumulations*, R.S. Kopp and R.E. Cohenour (Editors), *Utah Geol. Assoc. Publ. 16,* 181-194.

Talwani, P. and S. Acree (1985). Pore pressure diffusion and the mechanism of reservoir-induced seismicity, *Pure Appl. Geophys.* **122**, 947-965.

United States Geological Survey (1987). Preliminary determination of epicenters: monthly listings, U. S. Government Printing Office, Washington, D. C.

ATTENUATION OF MULTIPHASE SURFACE WAVES
IN THE BASIN AND RANGE PROVINCE
Part II: THE FUNDAMENTAL MODE

Brian J. Mitchell, Jai-kang Xie and Wen-jack Lin

Department of Earth and Atmospheric Sciences
Saint Louis University
3507 Laclede Avenue
St. Louis, MO 63103

ABSTRACT

In order to investigate the large errors which sometimes characterize fundamental-mode attenuation coefficient determinations, we have made many such determinations in the Basin and Range province and have plotted particle motion for the observed three-component seismograms. Rayleigh wave attenuation coefficient values determined for four two-station paths across the Basin and Range province fluctuate between about -2.0×10^{-3} km^{-1} and $+3.0 \times 10^{-3}$ km^{-1} at periods between 6 and 33 s. Particle motion plots indicate that many of those determinations are contaminated by arrivals from non-great circle paths and from waves generated at heterogeneities along the path, factors which lead to systematic errors in the measured attenuation coefficient values. Attenuation coefficient determinations for the path MNV to ELK, which is within 20° of being normal to the structural trends of the Sierra Nevada and Great Valley, are, however, relatively free from such contamination. Mean values for that path decrease rapidly with period from about 3.0×10^{-3} to about 0.7×10^{-3} km^{-1} between 6 and 10 s and then decrease slowly to about 0.3×10^{-3} km^{-1} at 33 s. Standard deviations range between 0.2×10^{-3} and 0.3×10^{-3} km^{-1} for most of the period range, but increase to about 0.4×10^{-3} at periods between 6 and 8 s. These results indicate that careful screening, based upon criteria such as three-dimensional particle motion, are necessary to obtain surface wave attenuation data of sufficient quality to use for inverting for crustal anelasticity in complex regions.

INTRODUCTION

This is the second part of a study of the attenuation of surface waves in the Basin and Range province of the western United States. Part I (Xie and Mitchell, 1990) concentrated on the Lg phase and its coda at frequencies between about 0.1 and 10.0 Hz and investigated the effects of ambient noise, station site response, and focussing on Q values measured for those waves. The present paper looks at fundamental-mode surface waves at frequencies between about 0.03 and 0.30 Hz (or periods between about 3 and 30 s). We will assess the usefulness of those waves for studying crustal structure in a region containing major lateral structural complexities.

Studies of regional surface wave attenuation became possible over three and a half decades ago with the development of a method to measure the spectral decay of surface wave amplitudes between two points on the Earth's surface (Sato, 1955). Ten years later, Anderson *et al.* (1965) developed a relationship by which attenuation of surface wave amplitudes could be related to anelastic properties

of the crust and mantle as a function of depth if the elastic properties are known. A process for formally inverting attenuation data, using those relationships and observed attenuation data, was developed using stochastic inversion theory (Mitchell, 1973). Since then, surface wave attenuation values have been measured, and internal friction models have been obtained, for several continental regions (e.g. Lee and Solomon, 1978; Mitchell, 1975, 1980, 1981; Patton and Taylor, 1984; Hwang and Mitchell, 1987; Cong and Mitchell, 1988; Al-Khatib and Mitchell, 1991). The attenuation coefficient values in these studies typically exhibit very large scatter which has been attributed to arrivals from non-great circle path directions between the source and one or both of the stations. The purpose of this paper is to investigate the severity of those effects on attenuation coefficient determinations over relatively short paths in the western United States. We will investigate the extent to which attenuation coefficient values obtained in that region are adversely affected by lateral changes in structure and attempt to separate

those data which can be reliably used to invert for Q structure from those which are too contaminated to be useful.

REGION OF STUDY

We ultimately want to be able to use surface-wave attenuation data obtained over two-station paths in the Basin and Range province to invert for crustal shear-wave internal friction (Q_μ^{-1}) in that region. Those inversion results will be presented in part III of this series of three papers. In principle, these measurements should be straightforward, requiring only that the waves travel from the source along the same approximate great circle azimuth to both stations. The majority of the paths in this study, however, cross a complex series of tectonic features before reaching the first seismic stations (Figure 1). Features in California alone include the Coast Ranges, the Great Valley and the Sierra Nevada. In addition, some events are situated on or outside the coastline of California or Mexico and surface waves from those events may be complicated by the transition between oceanic and continental structure. At best, these features simply contribute a random degree of uncertainty to determinations of attenuation coefficients of surface waves which traverse them. Greater difficulties may, however, arise from focussing, defocussing, or multipathing which may

Table 1
Station Codes and Locations

Station	Location	Latitude (°N)	Longitude (°W)
ELK	Elko, NV	40.7448	115.2388
KNB	Kanab, UT	37.0166	112.8224
LAC	Landers, CA	34.3898	116.4115
MNV	Mina, NV	38.4322	118.1544

cause systematic errors in the attenuation coefficient determinations.

It has long been known that departures from great circle paths between epicenters and stations can occur for surface waves which cross from oceanic to continental structure in California (Evernden, 1954). More recently, Tanimoto (1990) showed how surface waves could be deflected by laterally varying structure within California. He successfully modelled dispersion from a source in southern California to six stations in northern California for which great circle paths were parallel or subparallel to structural trends in the region. Ray paths through the western Sierra Nevada at periods of 20 s were deflected by as much as 60° westward from the expected great circle path.
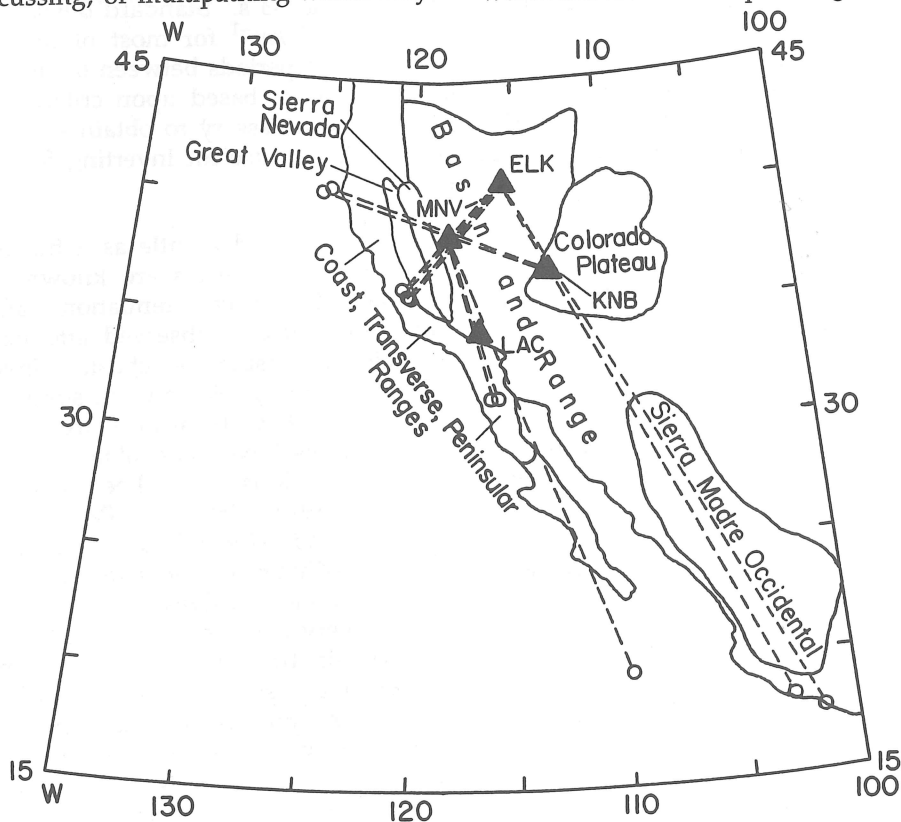

Fig. 1. Map showing source locations, seismic stations, and great circle paths between them. Heavy lines denote approximate boundaries of tectonic provinces traversed by the surface waves.

240

In addition to effects produced by lateral changes in velocity modelled by Tanimoto (1990), it is possible that topography and variations in sediment thickness could distort wave forms and amplitudes. Sedimentary basins, such as the Great Valley, are known to have a strong effect on both surface wave velocities (Oliver and Ewing, 1958) and amplitudes (Kijko and Mitchell, 1983). Sediments are known to be as thick as 5 km in portions of the Great Valley (Meltzer et al., 1987).

ATTENUATION COEFFICIENTS

Seismograms used in this study were written by broadband instruments of the Nevada Test Site Regional Seismic Network operated by Lawrence Livermore National Laboratory. Table 1 gives locations for the four stations of the network and Figure 1 shows their locations relative to source locations and tectonic features. Spectral amplitudes for the vertical component of fundamental-mode Rayleigh waves were obtained for each seismogram using the multiple-filter method (Dziewonski, et al., 1969). We determined Rayleigh wave attenuation coefficients, γ_R, for four two-station paths (MNV-ELK, MNV-KNB, KNB-ELK, and LAC-MNV) at periods between 6 and 33 s. We used the equation

$$\gamma_R(\omega) = -\frac{\ln\left[\frac{A_2(\omega, r_2)}{A_1(\omega, r_1)}\left(\frac{\sin\Delta_2}{\sin\Delta_1}\right)^{1/2}\right]}{r_2 - r_1} \quad (1)$$

where r is epicentral distance in km, Δ is epicentral distance in degrees, A is spectral amplitude, ω is angular frequency, and the subscripts 1 and 2 indicate respectively the nearer and farther stations. γ_R is related to Q_R, the quality factor for Rayleigh waves, by the relation

$$Q_R = \omega/2U_R\gamma_R$$

where U_R is Rayleigh wave group velocity. The factor $\sqrt{\sin\Delta_2/\sin\Delta_1}$ is a correction for geometrical spreading; $e^{-\gamma_R(\omega)r}$ then describes the amplitude decay of Rayleigh waves above that caused by spreading. In the absence of scattering, focusing, multipathing, or other factors produced by complex structure, knowledge of the attenuation coefficient values over a range of frequencies should provide a means to determine intrinsic damping effects as a function of depth in the crust and upper mantle. Interstation phase and group velocities for these paths and crustal velocity models obtained from the inversion of that data are given in Lin (1989).

Attenuation coefficient values obtained for the path MNV-ELK are listed in Table 2 and are plotted in Figure 2. Those values are relatively consistent from event to event. Mean values decrease rapidly from about 3.5×10^{-3} km^{-1} to about 0.7×10^{-3} km^{-1} at periods between 6 and 10 s and decrease slowly to about 0.3×10^{-3} at 33 s. Data for the three other paths (Figure 3), however, exhibit larger scatter, being especially severe for the paths LAC-MNV and KNB-ELK. The large scatter in the plotted values of the Rayleigh wave attenuation coefficients indicates that lateral complexities in the region of study have caused severe distortion to the surface wave amplitudes and that it would be fruitless to try to invert all of the data for
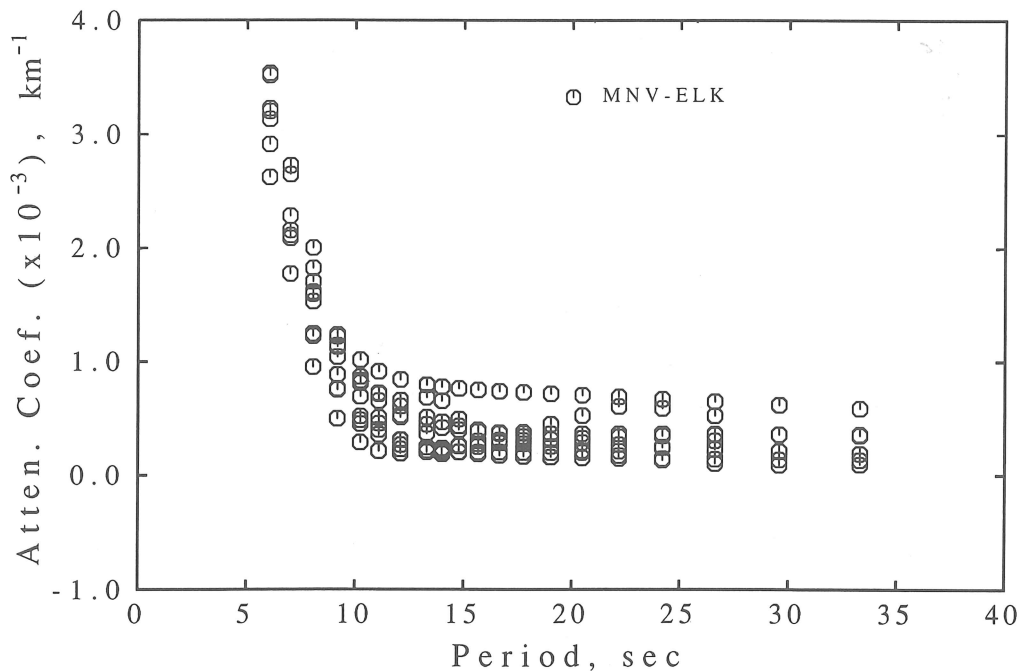

Fig. 2. Fundamental-mode Rayleigh wave attenuation coefficient values for the path MNV to ELK.

anelastic structure. It might also be possible that the consistency of the MNV-ELK data is illusory, and that the data are all adversely affected by lateral complexities in the same systematic manner.

We propose to attempt to explain the large scatter in the data apparent in Figure 3 and to investigate the suitability of the MNV-ELK data for inverting for models of crustal anelasticity.

Table 2
Earthquake Location Parameters (from PDE Monthly Listings)

Date	Origin Time h m s	Latitude (°N)	Longitude (°W)	Depth (km)	m_b	Two-station Path
24 Sep 80	08 08 38.9	36.27	120.17	9	4.8	MNV-ELK
09 May 83	20 09 15.4	19.98	109.45	10	5.5	LAC-MNV
22 May 83	08 39 21.4	36.14	120.22	10	4.2	MNV-ELK
29 May 83	06 55 33.1	40.46	125.44	10	5.1	MNV-KNB
07 Jun 83	05 18 37.4	36.14	120.24	10	4.2	MNV-ELK
09 Jul 83	07 40 50.9	36.24	120.41	10	5.3	MNV-ELK
22 Jul 83	02 39 53.7	36.23	120.42	9	6.0	MNV-ELK
22 Jul 83	03 43 00.6	36.21	120.41	10	5.3	MNV-ELK
25 Jul 83	22 31 39.2	36.22	120.41	10	5.6	MNV-ELK
09 Sep 83	09 16 14.9	36.23	120.26	5	5.3	MNV-ELK
11 Sep 83	11 48 08.0	36.23	120.39	8	5.0	MNV-ELK
04 Aug 84	21 45 52.9	40.25	124.61	5	4.7	MNV-KNB
08 May 85	23 40 18.2	31.74	115.81	6	5.1	LAC-MNV
10 May 85	05 39 36.3	31.71	115.77	6	4.6	LAC-MNV
12 May 85	13 55 08.2	40.38	125.18	10	4.6	MNV-KNB
21 Sep 85	01 37 13.4	17.80	101.65	31	6.3	KNB-ELK
25 Sep 85	07 43 57.0	18.21	102.74	30	5.3	KNB-ELK
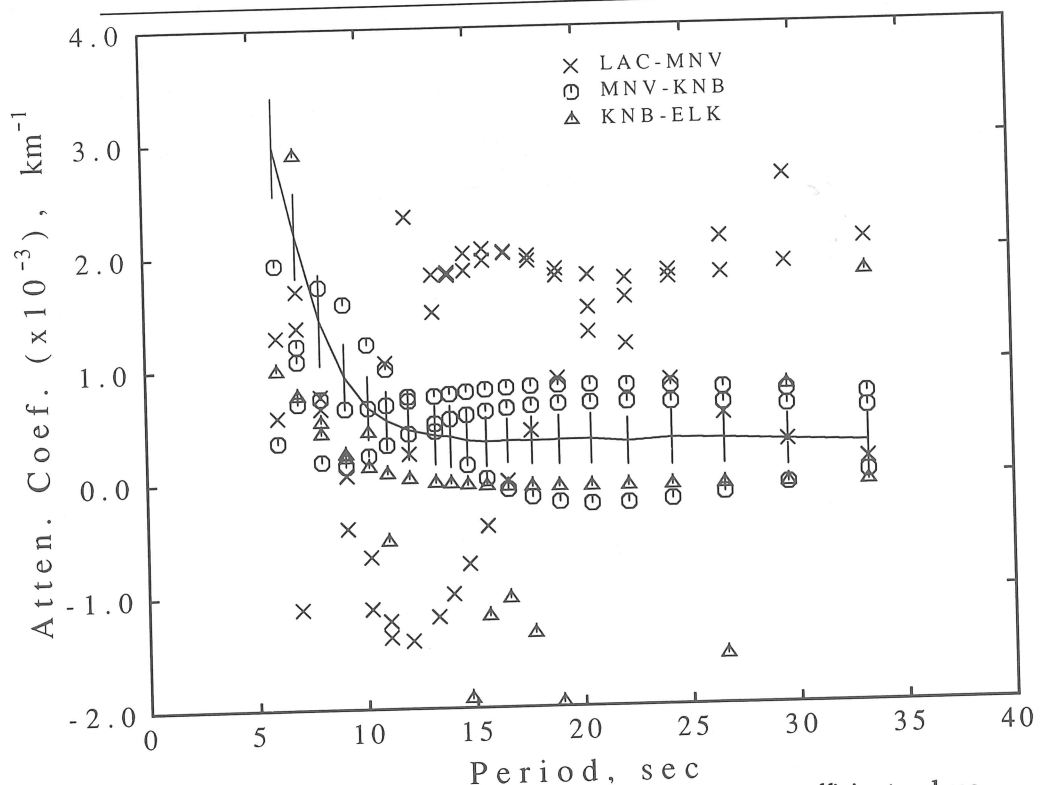
Fig. 3. Fundamental-mode Rayleigh wave attenuation coefficient values for the paths LAC-MNV, MNV-KNB, and KNB-ELK. The solid line indicates average values for the path MNV-ELK and vertical bars denote standard deviations.
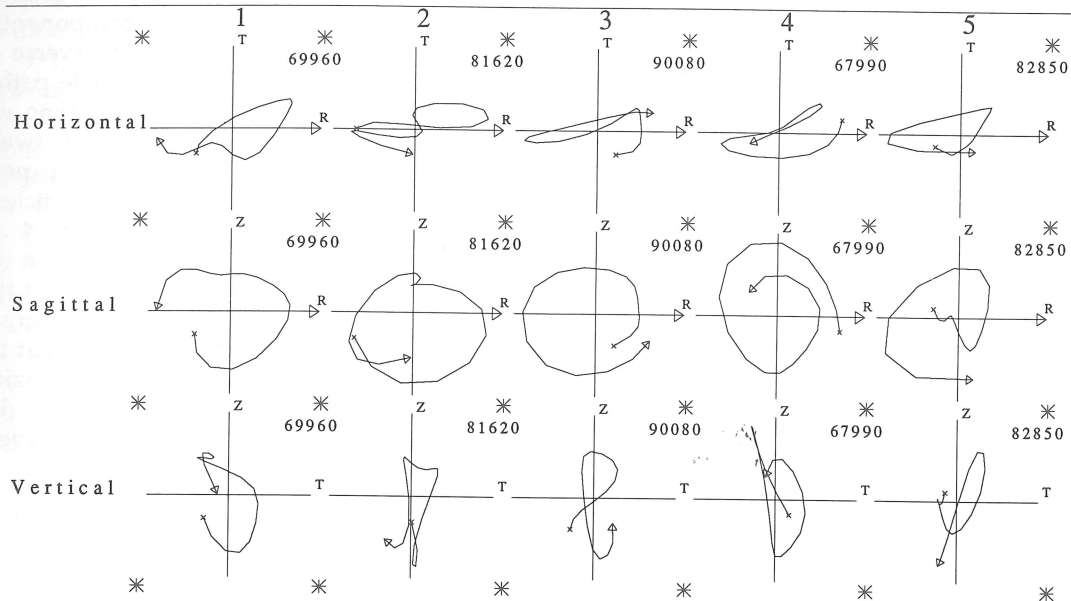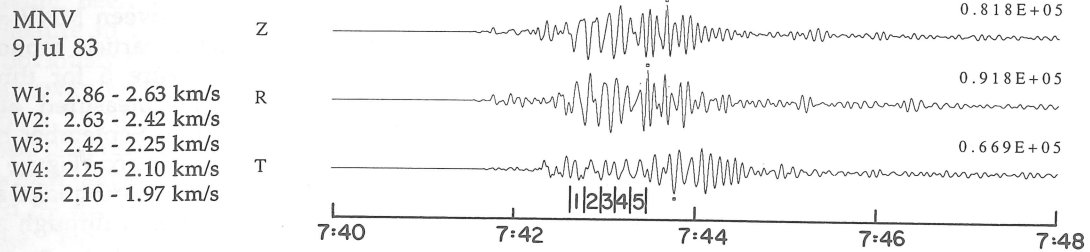
Fig. 4. Seismograms for the earthquake of 9 July 1983 in central California recorded at station MNV. The seismograms are band-pass filtered between 3 and 30 s using a 5-pole Butterworth filter and particle motion is plotted over the velocity interval between 2.86 and 1.97 km/s. The vertical lines below the seismograms indicate time windows for each of the particle motion plots. Window numbers appear above the particle motion plots in the horizontal, sagittal, and vertical (in the direction of propagation) planes and the corresponding velocity windows are given to the left of the seismograms. The number by each diagram gives the maximum relative motion for the corresponding window. The arrows on the axes of the horizontal and sagittal plots denote the expected direction for great circle propagation.

SURFACE WAVE PARTICLE MOTION

The determination of surface wave attenuation coefficients using two-station methods and equation (1) assumes that the waves arrive at both stations along approximately the same great circle azimuth from the source. Significant departures from great circle path propagation will mean that amplitude measurements will not reflect true radial (for Rayleigh waves) or true transverse (for Love waves) motion in the horizontal plane. A more serious problem is that arrivals at two stations from two different non-great circle paths will have left the earthquake focal region at different azimuths. If the source radiation pattern varies rapidly with azimuth, the amplitude differences recorded at two stations will be affected by differences in azimuthally-variable source amplitudes more strongly than by attenuation along the path.

We have estimated the angles of departure from great circle paths for all of the three-component data available to us by calculating three-dimensional particle motion for the surface waves for various velocity windows. In this paper we attribute all deviations of particle motion from expected patterns to be due to non-great circle energy. Other factors which might contribute to those deviations are non-horizontal layering at recording sites and anisotropy of elastic properties. Deviations of particle motion due to those effects are, however, likely to be, at most, only a few degrees (Vig and Mitchell, 1990).

Figure 4 displays seismograms recorded by

station MNV at a distance of 315 km from an earthquake in central California which occurred on 9 July 1983. Particle motion is plotted for five velocity windows between 2.86 and 1.97 km/s. All windows indicate Rayleigh motion, being predominantly radial in the horizontal plane and retrograde elliptical in the sagittal plane. The departures from the radial direction are small and can be explained as being caused by a component of Love wave motion which overlaps the Rayleigh arrivals and produces net ground motion which deviates from the great circle path direction.

Seismograms and particle motion plots of ground motion generated by the same earthquake and recorded at station ELK appear in Figure 5. Since this station is farther from the earthquake (674 km), amplitudes are smaller, but particle motion indicates Rayleigh motion for windows 2 through 4. Departures from the radial direction are larger than those at MNV and are explained by the relatively large Love waves recorded at ELK. Because of differences in group velocities between Love and Rayleigh waves, the departures are in the opposite sense from that observed at ELK.

Paths other than that between MNV and ELK often exhibit less predictable particle motion plots. An example appears in Figure 6 for three components of ground motion measured at station ELK for the earthquake of 25 September 85 which occurred near the coast of Mexico (Figure 1). The great circle path between the earthquake and ELK is 2769 km in length and passes through and near part of the western boundary of the Sierra Madre Occidental. The horizontal components were rotated to obtain radial and transverse ground motion with respect to the great circle path. Particle motion was determined for five time windows corresponding to group velocities between 3.46 and 3.08 km/s, velocities which are expected for Love waves in this region. The particle motion diagrams for windows 2 through 4 indicate predominantly horizontal motion. These windows therefore have recorded Love waves, but the angle of approach deviates greatly from a great circle path. Windows 2 through 4 indicate that the Love waves arrive at station ELK from an azimuth of 45° of more west of the great circle direction. These angles suggest that the waves have arrived
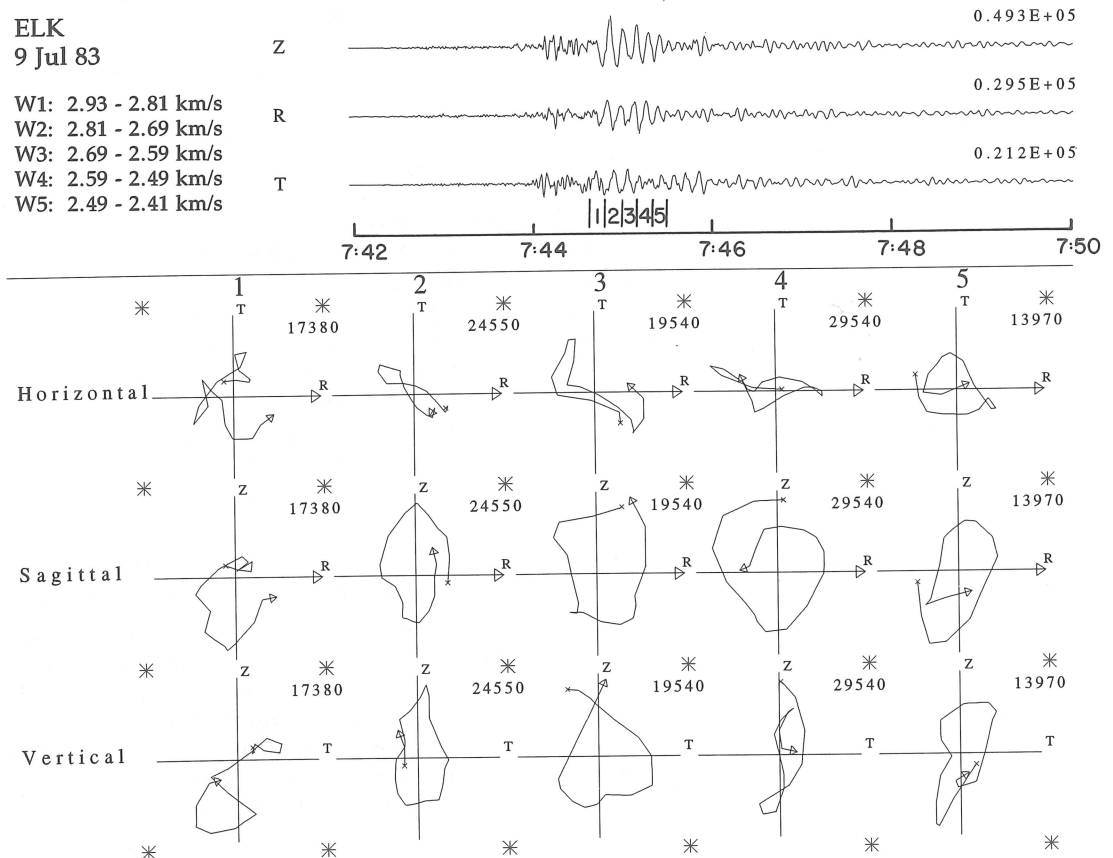

Fig. 5. Seismograms for the earthquake of 9 July 1983 in central California recorded at station ELK. The seismograms are band-pass filtered between 3 and 30 s using a 5-pole Butterworth filter and particle motion is plotted over the velocity interval between 2.93 and 2.41 km/s. See the caption of Figure 4 for an explanation of the details of the plot.

after having been laterally refracted or reflected from a feature to the west. Since the travel times are not obviously larger than expected, that feature is not far away and is probably the Sierra Nevada rather than anything further to the west. This hypothesis is consistent with the plots of Tanimoto (1990) which show that large deflections can be produced by the Sierra Nevada to stations west of that range. Figure 7 shows the same seismograms and particle motion diagrams for the Rayleigh wave window between 3.01 and 2.71 km/s. This motion is less ordered than that for the earlier Love waves, but windows 2 through 4 indicate Rayleigh motion which deviates greatly from a great circle path direction. Window 2 displays the only ground motion for which an azimuthal estimate can be made; motion in the horizontal plane suggests even larger deviations from the great circle path than that for Love waves. Similarly large deflections have been inferred for Lg waves in southern California (Kennett *et al.*, 1990). The direction of approach and the observed velocities in the present study for Rayleigh waves again suggest that these waves have been strongly deflected eastward by the Sierra Nevada.

Seismograms from the Baja California earthquake of 8 May 1985 recorded at station MNV, 772 km from the source, appear in Figure 8. Particle motion is plotted for five velocity windows between 3.30 and 2.72 km/s. Windows 1 and 2 are dominated by Love wave motion arriving at azimuths which deviate between 40 and 45° westward from the great circle azimuth from the source. As for the event of 25 September 1985, these appear to have been deflected by the Sierra Nevada. Rayleigh motion dominates window 3 and arrives from an approximate great circle path in this small interval. These seismograms indicate that Love waves and Rayleigh waves are affected differently for this path. Later arriving energy (windows 4 and 5) retain a suggestion of Rayleigh motion, but are too contaminated by incoherent arrivals to be useful for studying crustal anelasticity.

Some seismograms display predicted Rayleigh and Love motion early in the surface wave trains but deviate from that behavior later in the train. Figure 9 shows the same seismograms as Figure 4, but the particle motion is plotted for velocities between 1.85 and 1.43 km/s. The polarization
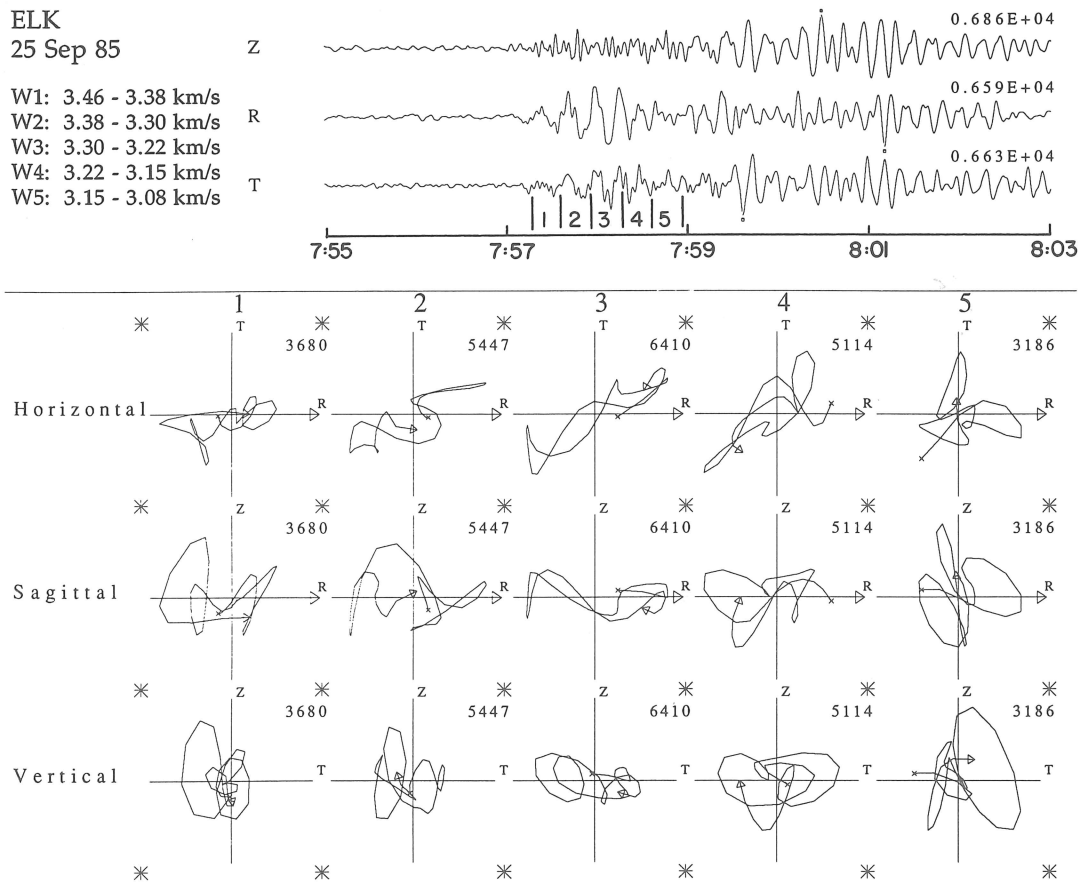

Fig. 6. Seismograms for the earthquake of 25 September 1985 near the coast of Mexico recorded at station ELK with particle motion plotted over the Love wave velocity interval between 3.46 and 3.08 km/s. See the caption for Figure 4 for an explanation of details of the plot.

245

plots for windows 1 and 2 show erratic Rayleigh motion and windows 3 through 5 indicate Love wave motion from an azimuth which is close to the great circle direction from the source. The measured velocities for those Love waves (1.66 to 1.43 km/s) are much lower than velocities which we would expect for this source location. Love waves of that velocity cannot be identified at station ELK which is about 360 km further from the source than MNV. This suggests that the Love waves were generated in a localized region near MNV and that amplitudes died off very rapidly due to geometrical spreading as waves travelled away from that region. If we assume an $r^{1/2}$ falloff from a point source near MNV then amplitudes at ELK will be smaller than those at MNV by a factor of about 19.

Some sets of seismograms in this study exhibit late-arriving Love wave motion which appears to be generated along the path of travel. One such example appears in the upper portion of Figure 10 where large transverse motion arrives between about 2.5 and 4 minutes after the origin time for the central California event of 9 July 83. That

motion is absent, however, on seismograms recorded at the same station for the event of 9 September 1983, even though that earthquake occurred at a point only 8 km closer to station MNV and differed in great circle azimuth by only 2°. This difference in the level of Love wave energy occurs even though the Rayleigh waves on the vertical and radial components are not greatly different and the reported magnitudes of the two events are identical. It suggests that the presence or absence of late-arriving Love waves will be very sensitive to the azimuth at which Rayleigh waves traverse the Sierra Nevada. An alternative explanation might be that the difference in the level of Love wave energy at those late times is due to the different depths for the two events. The depth of 9 July 83 event was reported as being 10 km whereas that of 9 September 83 was given as 5 km. If the difference in level of the late Love wave energy is due to a difference in source depth we would expect that the shallower event would generate the greater amount of that energy since it would be channelled to a greater extent in slow near-surface material. The greater late-arriving
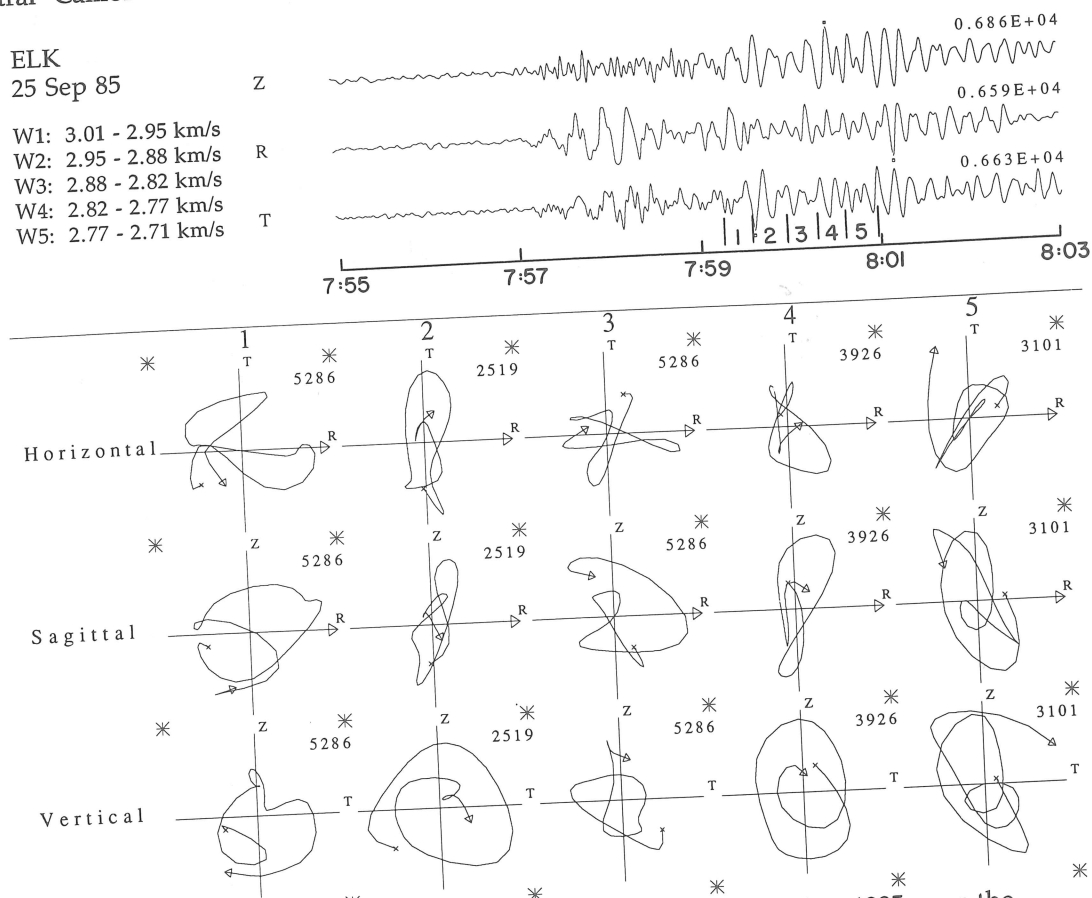

Fig. 7. Seismograms for the earthquake of 25 September 1985 near the coast of Mexico recorded at station ELK with particle motion plotted over the Rayleigh wave velocity interval between 3.01 and 2.71 km/s. See the caption for Figure 4 for an explanation of details of the plot.

Love wave energy is, however, associated with the deeper event and so does not appear to be a source depth effect. Differences in radiation pattern for the two events could, of course, also play a role in the generation of the late Love waves. The similarity of the wave forms for the Rayleigh waves, however, argues against the likelihood of radiation pattern effects being a major contributor to the differences in wave forms of the two events.

DISCUSSION

The particle motion plots in Figures 6, 7, and 8 indicate that some surface wave motion is affected by arrivals from paths which deviate from a great circle, sometimes by a large amount. This is especially true for paths which are sub-parallel to the major structural trends in our region of study. The deviations probably occur because of lateral refraction or reflection from major structural features in the region such as the Sierra Nevada. Data obtained from those paths are likely to produce biased attenuation coefficient values and should not be used to infer models of internal friction. In addition, some seismograms for paths

which are at near normal incidence to the Sierra Nevada include path-generated waves. In the present study, however, they are late in the wave trains and do not adversely affect the portions of the seismograms used for attenuation coefficient determinations.

The path MNV-ELK provides a consistent set of attenuation coefficient values. This path, being nearly normal to the structural trends of the Sierra Nevada and Great Valley, yields particle motion diagrams which indicate pure Rayleigh motion in the radial direction over at least the early part of the Rayleigh wave train. The data for the path MNV-ELK will be used in part III to invert for crustal anelasticity in the Basin and Range province.

CONCLUSIONS

Particle motion diagrams for surface waves in the western United States often reveal complex motion which is produced by lateral complexities in structure. The most severe distortions from expected Love or Rayleigh wave motion occur for long paths which pass through the Sierra Nevada in a direction subparallel to its trend. The Sierra
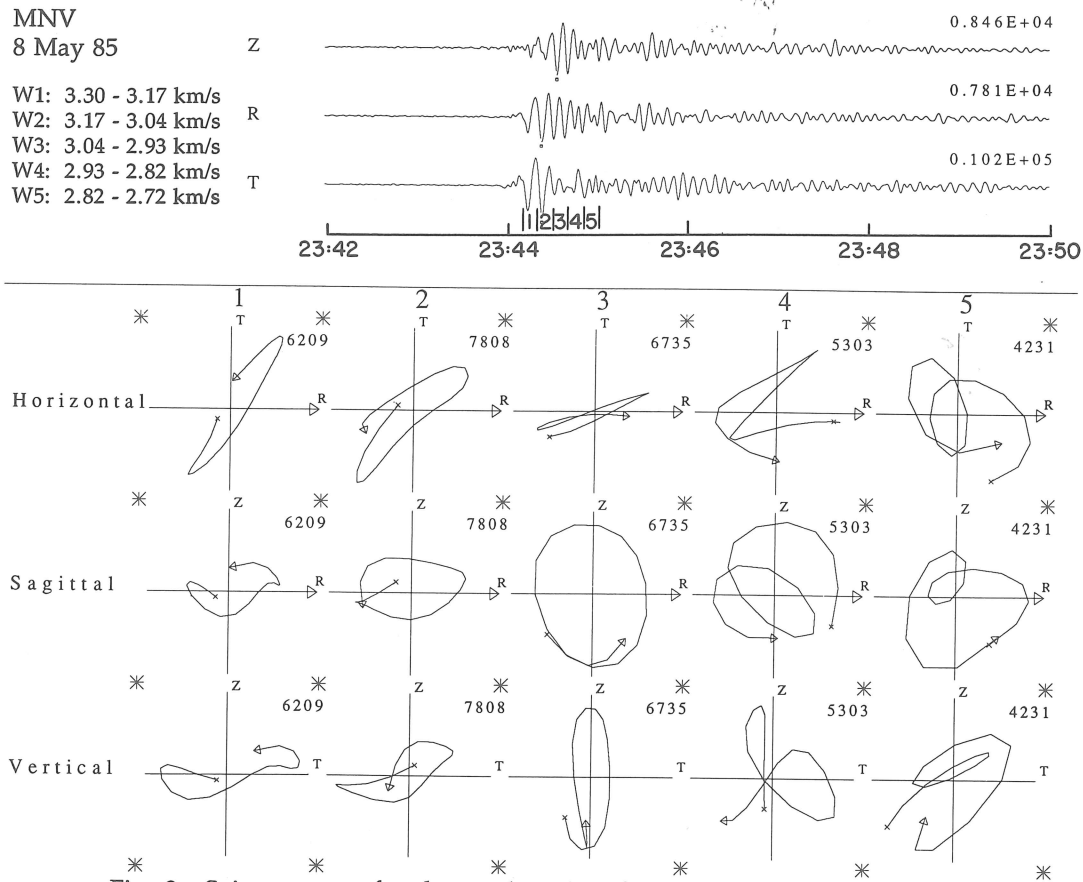

Fig. 8. Seismograms for the earthquake of 8 May 1985 in northern Baja California recorded at station MNV. The seismograms are band-pass filtered between 3 and 30 s using a 5-pole Butterworth filter and particle motion is plotted over the velocity interval between 3.30 and 2.72 km/s. See the caption for Figure 4 for an explanation of the details of the plot.
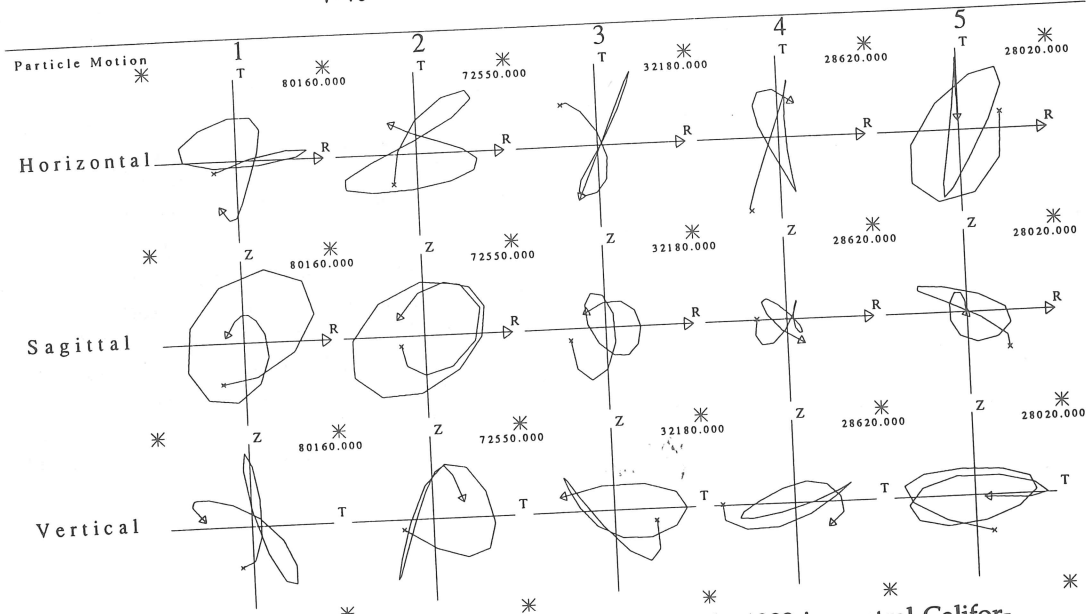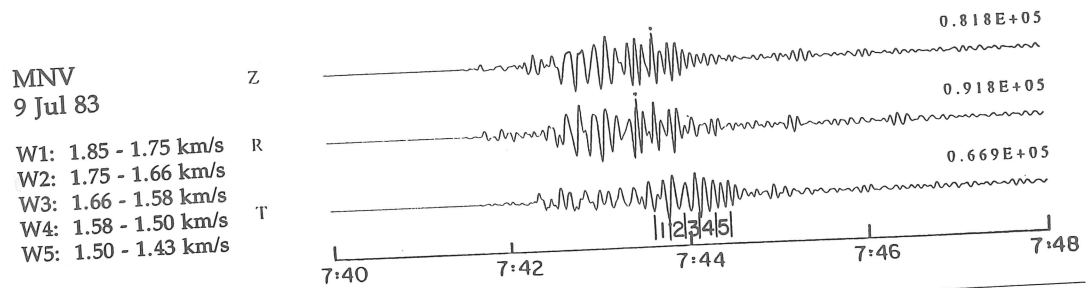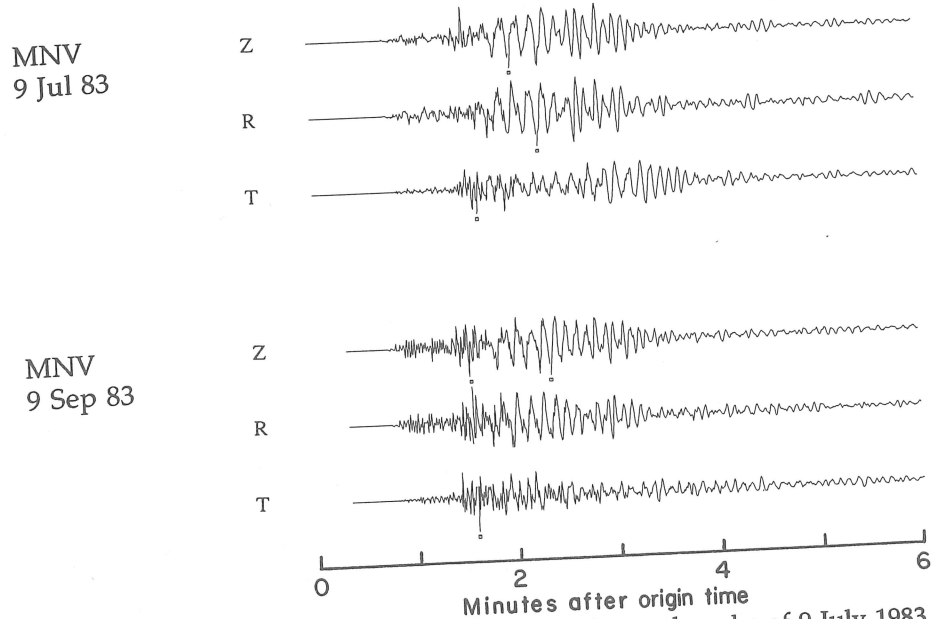
247

Fig. 9. Seismograms for the earthquake of 9 July 1983 in central California recorded at station MNV. The seismograms are band-pass filtered between 3 and 30 s using a 5-pole Butterworth filter and particle motion is plotted over the velocity interval between 1.85 and 1.43 km/s. See the caption for Figure 4 for an explanation of the details of the plot.

Fig. 10. Comparison of seismograms from the earthquake of 9 July 1983 in central California with the earthquake of 9 September 1983 in the same region recorded at station MNV.

Nevada deflects some surface waves from the great circle path in the present study by several tens of degrees and can deflect Love waves and Rayleigh waves by different amounts. Rayleigh motion is converted to Love motion near the eastern margin of the Sierra Nevada for some events but not others, even though the events are not far from one another, suggesting that mode conversion is very sensitive to the angle at which the waves arrive at that margin. If surface waves are to be utilized to invert for anelastic structure, they should be scrutinized carefully to make sure that their particle motion corresponds to Rayleigh or Love wave motion on a great circle path between the event and recording stations. Such screening has produced a consistent data set, with relatively small standard deviations, for a path across the Basin and Range province.

ACKNOWLEDGMENTS

REFERENCES

Al-Khatib, H.H. and B.J. Mitchell (1991). Upper mantle anelasticity and tectonic evolution of the western United States from surface wave attenuation, *J. Geophys. Res.* **96**, 18,129-18,146.

Anderson D.L., A. Ben-Menahem, and C.B. Archambeau (1965). Attenuation of seismic energy in the upper mantle, *J. Geophys. Res.* **70**, 1441-1448.

Cong L., and B.J. Mitchell (1988). Frequency dependence of crustal Q_β in stable and tectonically active regions, *PAGEOPH* **127**, 581-605.

Dziewonski, A.M., S. Bloch, and M. Landisman (1969). A technique for the analysis of transient seismic signals, *Bull. Seism. Soc. Am.* **59**, 427-444.

Evernden, J.F. (1953). Direction of approach of Rayleigh waves and related problems (part I), *Bull. Seism. Soc. Am.* **43**, 335-353.

Evernden, J.F. (1954). Direction of approach of Rayleigh waves and related problems (part II), *Bull. Seism. Soc. Am.* **44**, 159-184.

Franklin, J.N. (1970). Well-posed stochastic extensions of ill-posed linear problems, *J. Math. Analysis Applic.* **31**, 682-716.

Hwang, H.J., and B.J. Mitchell (1987). Shear velocities, Q_β, and the frequency dependence of Q_β in stable and tectonically active regions from surface wave observations, *Geophys. J.R. Ast. Soc.* **90**, 575-613.

Kennett B.L.N., M.G. Bostock, and J.K. Xie (1990). Guided-wave tracking in 3-D: A tool for interpreting complex regional seismograms, *Bull. Seism. Soc. Am.* **80**, 633-642.

Kijko, A., and B.J. Mitchell (1983). Multimode Rayleigh wave attenuation and Q_β in the crust of the Barents shelf, *J. Geophys. Res.* **88**, 3315-3328.

Lee, W.B., and S.C. Solomon (1978). Simultaneous inversion of surface wave phase velocity and attenuation: Love waves in western North America, *J. Geophys. Res.* **83**, 3389-3400, 1978.

Lin, W.J. (1989). Rayleigh wave attenuation in the Basin and Range province, *M.S. Thesis*, Saint Louis University, 55 pp.

Meltzer, A.S., A.R. Levander, and W.D. Mooney (1987). Upper crustal structure, Livermore Valley and vicinity, California coast ranges, *Bull. Seism. Soc. Am.* **77**, 1655-1673.

Mitchell, B.J. (1973). Surface wave attenuation and crustal anelasticity in central North America, *Bull. Seism. Soc. Am.* **63**, 1057-1071.

Mitchell, B.J. (1975). Regional Rayleigh wave attenuation in North America, *J. Geophys. Res.* **80**, 4904-4916.

Mitchell, B.J. (1980). Frequency dependence of shear wave internal friction in the crust of eastern North America, *J. Geophys. Res.* **85**, 5212-5218.

Mitchell, B.J. (1981). Regional variation and frequency dependence of Q in the crust of the United States, *Bull. Seism. Soc. Am.* **71**, 1531-1538.

Oliver, J., and M. Ewing (1958). The effect of surficial sedimentary layers on continental surface waves, *Bull. Seism. Soc. Am.* **48**, 339-354.

Patton, H.J., and S.R. Taylor (1984). Q structure of the Basin and Range from surface waves, *J. Geophys. Res.*, **89**, 6929-6940, 1984.

Sato, Y. (1955). Analysis of dispersed surface waves by means of Fourier transform I, *Bull. Earthquake Res. Inst.* **33**, 33-48.

Tanimoto, T. (1990). Modelling curved surface wave paths: membrane surface wave synthetics, *Geophys. J. Int.* **102**, 89-100.

Vig, P.K., and B.J. Mitchell (1990). Anisotropy beneath Hawaii from surface wave particle motion observations, *Pure and Applied Geophysics* **133**, 1-22.

Xie, J., and B.J. Mitchell (1990). Attenuation of multiphase surface waves in the Basin and Range province, part I: Lg and Lg coda, *Geophys. J. Int.* **102**, 121-137.

ESSSA '93

65th Annual Meeting, Eastern Section, Seismological Society of America

Session Schedule

Wednesday, October 13 (Morning)

9:00 AM - 10:00   Registration

                                  Set up Posters
                                  Posters will remain on display until Friday.

Posters

10:00 - 10:30 (Presiding: A.L. Kafka)

(10:00) FOLIO OF SEISMOTECTONIC MAPS OF THE NEW MADRID AREA, SOUTHEASTERN MISSOURI AND ADJACENT STATES

      S. Rhea and R.L. Wheeler

(10:05) EARTHQUAKES IN THE LAKE ONTARIO REGION

      A.E. Stevens

(10:10) SOURCE DECONVOLUTION AND STACKING OF LONG PERIOD SEISMOGRAMS AT 100 DEGREES TO RESOLVE DISCONTINUITIES IN THE UPPER MANTLE

      T.S. Anderson and V.F. Cormier

(10:15) DO ALL SEISMIC DATA HAVE THE SAME INFORMATION CONTENT?

      R.D. Noubary

(10:20) AMPLITUDE VARIATIONS ON SEISMOGRAMS RECORDED IN THE AREA SURROUNDING WESTON OBSERVATORY: DISTINGUISHING SITE EFFECTS FROM INSTRUMENTAL EFFECTS AND LOCALIZED NOISE

      A.L. Kafka, R.P. Comer and J.V. White

(10:25) DEMONSTRATION OF QUERYING A DATABASE OF SEISMIC PHASES REPORTED BY STATIONS IN THE FORMER SOVIET UNION

      A.L. Kafka and J.C. Battis

(10:30) TOMOGRAPHIC INVERSION OF Rg WAVE GROUP TRAVEL TIMES IN SOUTHERN NEW ENGLAND: INVESTIGATION OF LATERAL VARIATION IN THE SHALLOW CRUST

      A.K. Bowers and A.L. Kafka

Break 10:35 - 10:50

Earth Structure, Attenuation and Analysis of Waveforms
Wednesday, October 13 (Morning, Session I)

10:50 - 12:10 (Presiding: R.P. Comer)

(10:50) SPECTRAL STRUCTURE OF RANDOM INHOMOGENEITIES BENEATH THE JAPAN ISLAND ARC ESTIMATED FROM THE BROADENING OF THE S WAVE ENVELOPE

> K. Obara and H. Sato

(11:10) Q AND CRUSTAL EVOLUTION IN STABLE CONTINENTAL REGIONS

> B.J. Mitchell, Y. Pan, D. Chen, and J. Xie

(11:30) THE ADIRONDACK TELESEISMIC ARRAY: FIRST RESULTS

> S. Mangino and J.J. Cipar

(11:50) ANALYSIS OF P-WAVE TRAVEL TIME RESIDUALS AND POLARIZATION VALUES FOR THE WAKE ISLAND SEISMIC ARRAY

> S.P.S. Gulick and C.A. Powell

Regional Seismic Networks
Wednesday, October 13 (Afternoon, Session II)

1:10 - 2:50 (Presiding: J.E. Ebel)

(1:10) THE COOPERATIVE NEW-MADRID SEISMIC NETWORK: PROGRESS REPORT

> J.M. Chiu, S. Brewer, R. Smalley, G. Steiner, A.C. Johnston, R. B. Herrmann
> and E.J. Haug

(1:30) OPERATION OF THE WASHINGTON REGIONAL SEISMOGRAPH NETWORK

> R.S. Ludwin, S.D. Malone, A.I. Qamar, and R.S. Crosson

(1:50) ENHANCED SEISMIC MONITORING IN NORTHERN ONTARIO: 1978 - 1990

> R.J. Wetmiller, M.G. Cajka, and G.S. Lohda

(2:10) VELOCITY ANOMALIES UNDER THE SOUTHERN APPALACHIAN REGIONAL SEISMIC NETWORK

> G. Vlahovic and C.A. Powell

(2:30) SCATTERING AND ATTENUATION IN NEW ENGLAND DERIVED FROM SHORT-PERIOD SEISMOGRAMS

> R.D. Cicerone, C.G. Doll, Jr. and M.N. Toksoz

Break 2:50 - 3:10

Sources
Wednesday, October 13 (Afternoon, Session III)

3:10 - 5:00 (Presiding: N. Barstow)

(3:10) SOURCE CHARACTERISTICS OF M=1.6-4.4 EARTHQUAKES IN THE CHARLEVOIX SEISMIC ZONE: RELATIVE SOURCE PARAMETER ESTIMATION WITH THREE-COMPONENT DATA

Y. Li, C. Doll, Jr. and M.N. Toksoz

(3:30) AVERAGE STABLE CONTINENTAL EARTHQUAKE SOURCE PARAMETERS BASED ON CONSTANT STRESS DROP SCALING

A.C. Johnson

(3:50) DETERMINATION OF RUPTURE DURATION AND STRESS DROP FOR EARTHQUAKES IN NEW ENGLAND

Q. Feng and J.E. Ebel

(4:10) AN EXTENDED SOURCE RUPTURE MODEL FOR SEISMIC RISK ESTIMATION FROM SUBDUCTION ZONE EARTHQUAKES NEAR PUGET SOUND

L.D. Porter, T. Tabataaie, M. Tatatabaie and J.P. Singh

(4:30) EARTHQUAKE MONITORING BY THE WEO SEISMOGRAPH STATION 1982 TO 1993

J.A. Drysdale

(4:50) THE 1993 SOUTHERN INDIAN EARTHQUAKE: PRELIMINARY THOUGHTS

P. Talwani

Thursday, October 14 (Morning)

8:00 a.m. - 8:30   *ESSSA Business Meeting*

Seismicity and Tectonics I
Thursday, October 14 (Morning, Session IV)

8:30 - 10:30 (Presiding: P. Talwani)

(8:30) SEISMOTECTONICS STUDIES OF THE NEW MADRID SEISMIC ZONE FROM PANDA DATA

J. M. Chiu, Y.T. Yang, K.C. Chen, Z.S. Liaw, S.C. Chiu, and A.C. Johnston

(8:50) THE NORRIS LAKE EARTHQUAKE SWARM OF SUMMER, 1993: PRELIMINARY FINDINGS

L.T. Long, A.Kocaoglu, R. Hawman and P. Gore

(9:10) AUGUST 08, 1993, AIKEN, SOUTH CAROLINA EARTHQUAKE

P. Talwani and D.A. Stevenson

(Seismicity and Tectonics I, continued)

(9:30) METEOROLOGICAL WATER AND SEISMICITY IN EASTERN TENNESSEE

R. A. Webb

(9:50) THE 1993 EARTHQUAKE SEQUENCE IN COLUMBIA MARYLAND

N. Barstow, J. Armbruster, S. Horton, L. Seeber, R. Such, E. Cleaves and J. Reger

(10:10) RELATIONSHIP OF SEISMICITY TO GEOLOGIC STRUCTURE IN BERKS COUNTY, PENNSYLVANIA

C.K. Scharnberger

Break 10:30 - 10:50

Seismicity and Tectonics II
Thursday, October 14 (Morning, Session V)

10:50 - 12:10 (Presiding: L.T. Long)

(10:50) SPATIAL VARIATIONS IN SHEAR-WAVE SPLITTING IN THE CHARLEVOIX SEISMIC ZONE OF QUEBEC

C. Doll, Jr., Y. Li and M.N. Toksoz

(11:10) CORRELATION OF FOCAL-PLANE SOLUTIONS AND FAULTING IN THE EASTERN UNITED STATES

P.J. Barosh

(11:30) COMPARISON OF SINGLE-STATION BACKAZIMUTH ESTIMATES WITH REGIONAL EVENT LOCATIONS IN THE CENTRAL APPALACHIANS

M.C. Chapman, S. Huang and J.A. Snoke

(11:50) MULTIFRACTAL PHASE TRANSITIONS: THE ORIGIN OF SELF-ORGANIZED CRITICALITY IN EARTHQUAKES

C. Hooge, S. Lovejoy, D. Schertzer, S. Pecknold, F. Schmitt, J.F. Malouin

Earthquake Hazards & Prediction
Thursday, October 14 (Afternoon, Session VI)

1:30 - 4:50 (Presiding: C. Doll and R. Wetmiller)

(1:30) PROBABILISTIC SEISMIC HAZARD MAPS AND ASSOCIATED GROUND MOTION TIME HISTORIES FOR VIRGINIA

     M.C. Chapman

(1:50) EFFECTS OF THREE-DIMENSIONAL AND ANISOTROPIC CRUSTAL STRUCTURE ON EARTHQUAKE STRONG GROUND MOTIONS

     V.F. Cormier and W. Su

(2:10) A ONE-DIMENSIONAL FINITE ELEMENT MICROCOMPUTER PROGRAM TO DETERMINE NON-LINEAR SOIL RESPONSE

     C. Zhu and A. Urzua

(2:30) GEODYNAMIC EVOLUTION AND SEISMIC HAZARD ZONING OF THE PANNONIAN BASIN

     A. F. Grachev

(2:50) A SEISMIC HAZARD STUDY FOR THE STATE OF VERMONT

     J.E. Ebel and R. Bedell

Break 3:10 - 3:30

(3:30) METHODOLOGY AND RESULTS OF HISTORICAL NEW ENGLAND EARTHQUAKE RESEARCH

     K. Langone

(3:50) EVALUATION OF WEDGE-TYPE PSEUDOLIQUEFACTION FEATURES IN CENTRAL CONNECTICUT

     H.M.A. Kemppinen, R.L. Gelinas and D.C. Amick

(4:10) EVALUATION OF LIQUEFACTION-SUSCEPTIBLE MATERIALS NEAR MODERATE MAGNITUDE HISTORICAL EARTHQUAKES

     R.L. Gelinas, H.M.A. Kemppinen and D.C. Amick

(4:30) HOW EARTHQUAKES OCCUR WITHOUT WARNING

     Y. El Bekraoui

(4:50) REFRACTION SURVEYS TO INVESTIGATE DEPTH TO BEDROCK BENEATH TWO SITES OF THE WESTON OBSERVATORY SEISMIC ARRAY

     S.H. Koester and A.L. Kafka

Precursors, Migration and Strong Ground Motion
Friday, October 15 (Morning, Session VII)

8:30 - 9:30 (Presiding: R. Wheeler)

(8:30) THREE-DIMENSIONAL KIRCHOFF MIGRATION ANALYSIS OF VSP DATA FROM AN ITALIAN GEOTHERMAL FIELD

R.L. Gibson, Jr. and M.N. Toksoz

(8:50) SEISMIC PRECURSORS IN THE RADIATION BELTS: AN EVALUATION

J.C. Battis

(9:10) CHARACTERISTIC FEATURES OF GROUND MOTIONS SIMULATED DUE TO LARGE EARTHQUAKES IN CENTRAL UNITED STATES, INCLUDING EFFECTS OF IRREGULAR STRUCTURE

C.K. Saikia

Break 9:30 - 9:50

Special Session: Aftershock Surveys in The Eastern United States
Friday, October 15 (Morning, Session VIII)

9:50 - 11:50 (Presiding: D. Johnson)

(9:50 - 10:10) AFTERSHOCK SURVEYS IN THE EASTERN US: WHY AND HOW?

L. Seeber, J.G. Armbruster, N. Barstow, D. Johnson and S. Horton.

(10:10 - 10:30) IRIS/PASSCAL (J. Fowler)

(10:30 - 10:50) NCEER (K. Jacob)

(10:50 - 11:50) Discussion

SOURCE DECONVOLUTION AND STACKING OF LONG PERIOD SEISMOGRAMS AT 100 DEGREES TO RESOLVE DISCONTINUITIES IN THE UPPER MANTLE

Thomas S. ANDERSON and Vernon F. CORMIER, Department of Geology and Geophysics, University of Connecticut, Storrs, CT 06269-2045

A search is made to improve the resolution of the stacking of long period seismograms by the method of source deconvolution. The method of deconvolution consists of spectral division of the time windowed empirical source function. The range of study is 100 to 100.5 degrees. An emphasis was placed on resolving a P660sPP arrival due to an upper mantle discontinuity. The results show an improvement of the resolution of the major phases as well as the phase that may be due to an upper mantle discontinuity, the P660sPP.

CORRELATION OF FOCAL-PLAN SOLUTIONS AND FAULTING IN THE EASTERN UNITED STATES

Patrick J. BAROSH, P.J. Barosh and Associates, Concord, MA 01742

Focal-plane solution promised to be the key in revealing present day fault movement in the eastern U.S. where very few Holocene fault breaks are known. Early attempts to use them to locate faults in the field, however, proved disappointing, but this conceivably was due to epicentral or other error. The gradual increase in both numbers of fault-plane solutions and information on the most recent fault movements in the region now shows there is very little correlation between them. The hypothesis that fault-plan solutions reflect relative direction of actual fault movement must be reexamined.

The fault motions and orientations indicated by focal-plan solutions in New England, for example, are nearly random. This is geologically implausible. Faults are not random, in trend or movement, but generally occur in sets, which may be remarkably uniform over wide areas of a geologic province. Thee random solutions are certainly not reflective of principal active faults in the region. The post-Triassic fault pattern is well known in places, yet the focal-plane solutions do not reflect it and may describe faults that are not known to exist.

The apparent lack of relevancy of focal plan data may have several causes. It may be due to the method used or that the earthquakes studied are too small to send a clear signal. Perhaps the initial movements depicted occur alaong some locking block and not along the main fault zone. But perhaps solutions simply do not work in the crust of the eastern U.S.

The hypothesis of focal-plan solutions needs to be thoroughly tested in the eastern U.S. before applying them to interpretations of earthquakes.

THE 1993 EARTHQUAKE SEQUENCE IN COLUMBIA MARYLAND

N. BARSTOW, J. ARMBRUSTER, S. HORTON, L. SEEBER, R. SUCH, Lamont-Doherty Earth Observatory of Columbia University, Palisades, NY 10964: E. CLEAVES, J. REGER, Maryland Geologic Survey, Baltimore, MD.

A sequence of small earthquakes beginning in March, 1993 were centered in Columbia MD; the largest ones, Mc=2.5-2.8, were felt by many people as far as Baltimore and Washington DC. Events as small as M=0 began to be felt locally on March 5th, but a M=2.5 event on March 10 was the first reported from instrumental data (the closest station is 120 km from Columbia). Epicenters from the felt reports are demonstrably more reliable than epicenters from the regional stations. Nine earthquakes $0 \leq M \leq 1.5$ (five $1 \leq M \leq 2$, four $0 < M \leq 1$, and no M<0) were recorded locally by chart and/or digital recorders between March 15 and April 9; eight of them were also felt. The $-1.5 \leq M < 0$ range which is above the instrumental detection threshold and below the felt level was devoid of seismicity. Clearly, the sequence did not exhibit a typical magnitude distribution. Seven hypocenters are well constrained: they define a 1/2 km long northwest trend centered at 39 11.53N, 76 51.94W and at a depth of 1/2 km. A composite focal mechanism yields best fit nodal planes 002/45°W and 321/52°NE. The northwest-striking, northeast-dipping, reverse and left-lateral plane is consistent with the hypocenter distribution. The northeast-trending P axis conforms with regional stress directions and supports the notion that stress direction at typical seismogenic depths can be inferred from measurements at shallower depths sampled by wells. The combination of a source zone a few tenths of a km across and a small moment release (Mmax=2.8) suggests a low stress drop and is consistent with the relatively low corner frequency ($\approx$30 hz) and estimated stress drop (1-96 bars) for the largest locally recorded event (M=1.5). Although Maryland has not experienced $M \geq 4$ earthquakes in historic time, sequences such as the one in 1993 are relatively common, about 5/century according to catalogs. This rate could actually be substantially higher since archival material reveals several felt earthquakes which are not in the catalogs. The 1993 Columbia source is $\approx$2km from the Rockhill Jurassic Diabase dike which is mapped across the Piedmont into southeastern Pennsylvania. This dike was also spatially associated with the Mblg=4.2 1984 Marticville PA earthquake, the Randallstown MD earthquakes of 1990 and 1991 and a sequence in Sinking Springs PA that started in May 1993. A possible role of this dike and related brittle fault system in recent seismogenesis is being investigated.

SEISMIC PRECURSORS IN THE RADIATION BELTS: AN EVALUATION

James C. BATTIS, Earth Sciences Division, Geophysics Directorate, Phillips Laboratory, 29 Randolph Road, Hanscom AFB, MA 01731-3010

Over the past six years scientists from the former Soviet Union have reported a possible time association between the detection of anomalous particle flux.events in the inner radiation belts and earthquake activity. The first observations of this phenomenon were three flux anomalies detected during a Soyuz-7 mission in 1985. These events persisted between one and six minutes, were observed near the South Atlantic geomagnetic anomaly between L-shells 1.2 and 2.0, and were between two and 100 times normal flux levels. The initial study suggested that these events could not be explained by any commonly accepted mechanism. It was hypothesized that they might be related to seismic activity. Subsequently, an 33 additional anomalous flux events were identified from low-altitude satellite missions that traversed the South Atlantic geomagnetic anomaly. Global seismicity around the times of these events was analyzed and it was noted that seismicity increased in the 24 hours centered onthe flux anomalies. Further, a higher than expected number of earthquakes, of magnitude four or greater, were found to occur between 2.5 and 3 hours following the anomalous flux events.

This paper will review the Russian analysis using the data provided in the literature. Beyond reproducing the Russian statistical study I have carried out further tests on the relationship between flux anomalies and seismicity. Preliminary results maintain the general increase in global seismicity in the 24-hour window surrounding the flux events. The results do not, however, sustain the concept of a 2.5 to 3 hour precursory signal as previously suggested. Limitations of the statistical analysis and plans for further studyof this problem using proton flux data from the 1990-1991 CRRES satellite mission will also be discussed.

HOW EARTHQUAKES OCCUR WITHOUT WARNING

Yazid El BEKRAOUI, 6200 Gulfton #2105, Houston, TX 77081

Earthquakes are due to complex motions, the earth undergoes, which result an outcoming force that modify the structure of the crust. Some picutres illustrate the impact of that force.

TOMOGRAPHIC INVERSION OF Rg WAVE GROUP TRAVEL TIMES IN SOUTHERN NEW ENGLAND: INVESTIGATION OF LATERAL VARIATION IN THE SHALLOW CRUST

Allyn K. BOWERS, Hager-Richter Geoscience, Inc., Salem, NH 03079; Alan L. KAFKA, Weston Observatory, Dept. of Geology and Geophysics, Boston College, Weston, MA 02193.

Tomographic inversion of Rg wave group travel-times was used to investigate lateral variation in the seismic velocity structure of the shallow crust underlying southern New England (SNE). Group velocity dispersion curves for Rg waves with periods between 0.5 and 2.0 sec have been published in a number of previous studies of Rg dispersion in SNE. Dispersion curves from these previous studies and from our own analyses were converted to group travel-time data. Two dimensional tomography was then used to estimate group velocities for blocks into which two study areas in SNE were divided. Lateral variation in group velocity across SNE was estimated from these results. A combination of the maximum likelihood inverse and forward modeling was used to determine the vertical velocity structure beneath some of these blocks as well as beneath other subregions of SNE. The results suggest that three dimensional variation exists within the shallow crust underlying SNE, both within areas where the crystalline basement is at or near the surface and within the Hartford Rift basin, which is covered by layers of sediments and sedimentary rocks.

PROBABILISTIC SEISMIC HAZARD MAPS AND ASSOCIATED GROUND MOTION TIME HISTORIES FOR VIRGINIA

Martin C. CHAPMAN, Department of Geological Sciences, Virginia Polytechnic Institute and State University, Blacksburg, Virginia, 24061-0420

Seismic hazard in Virginia is being examined on a county-by-county basis. The objective of the study is to provide a consistent representation of the hazard, organized along jurisdictional boundaries useful to regulators and planners in

the state and local governments. The chief products are maps and tables depicting the 1 Hz and 3.3 Hz pseudo-relative acceleration response (5% damping) with 10% probability of exceedance in 50 years, analogous to the preliminary spectral response maps of the 1991 edition of the NEHRP recommended provisions for the development of seismic regulations for new buildings. Additionally, information necessary for the construction of simulated ground motion time series compatible with the chosen hazard level at various localities within Virginia are derived.

Hazard functions are calculated for the largest population center in each Virginia county. Seismic source zones and earthquake frequency-magnitude recurrence relationships are defined on the basis of the historical record, the results of 15 years of network monitoring and several recent geological and geophysical investigations. Ground motions are computed using the Boore and Joyner (1991) models for deep soil sites in the eastern United States. This hazard model is used to directly identify the magnitude-distance combination(s) compatible with the mapped oscillator response values and their associated probabilities of exceedance. This is accomplished by evaluating the magnitude-distance probability density functions for the 1 Hz and 3.3 Hz oscillator responses at the 475 year return period hazard level. The "most likely" events (in terms of magnitude and distance) contributing to hazard are defined by the maxima of the density function. Methods developed by Boore (1983) and Boore and Atkinson (1987) are used to generate simulated ground motion time series corresponding to these events. By providing information on duration and character of ground motion, these simulations greatly expand the utility of the hazard analysis.

COMPARISON OF SINGLE-STATION BACKAZIMUTH ESTIMATES WITH REGIONAL EVENT LOCATIONS IN THE CENTRAL APPALACHIANS

Martin C. CHAPMAN, Shaosong HUANG and J. Arthur SNOKE, Department of Geological Sciences, Virginia Polytechnic Institute and State University, Blacksburg, Virginia 24061-0420

The study examines the accuracy of single-station backazimuth measurements from polarization analysis of near regional P and Rg wave arrivals. The data set consists of 37 signals from mining explosions in the distance range 100 to 300 km, recorded at station BLA, Blacksburg, Virginia. The station-source backazimuth estimates derived from the three-component station are compared with results derived from independent information, primarily from regional network epicenter locations. For P wave signal/noise ratios in excess of 2.0, the mean backazimuth error of the single-station estimate is 6 degrees (for sources in the northwest quadrant) and the standard deviation is 21 degrees. Generally, only the initial (1 second or less) portion of the P wave arrival is polarized in the source-station azimuth. Off-azimuth arrivals consisting of converted and scattered energy appear early in the P coda. Emergent P wave arrivals from the delay-fired explosions, combined with steep apparent angles of incidence (averaging 22 degrees) complicate the single-station, three-component location problem.

Several of the explosion signals exhibit strong Rg phases. By making use of the 90 degree phase difference between vertical and radial components of the Rayleigh wave, it is possible to derive backazimuth estimates with accuracy comparable to those obtained from the P wave arrival. Together, the two measurements can increase the reliability of the single-station backazimuth estimate.

THE COOPERATIVE NEW MADRID SEISMIC NETWORK: PROGRESS REPORT

J.M. CHIU, S. BREWER, R. SMALLEY, G. STEINER, and A.C. JOHNSTON Center for Earthquake Research and Information, Memphis State University, Memphis, TN 38152; R.B. Herrmann and E.J. Haug, Department of Earth and Atmospheric Sciences, Saint Louis University, 3507 Laclede Ave., St. Louis, MO 63103.

Additional 32 broadband seismic stations and up to 50 short-period three-component seismic stations will be deployed in the central U.S. to provide modern seismic monitoring for the New Madrid seismic zone and its surrounding regions. Tentatively, CMG-3 and CMG-40T sensors will be used for the broadband stations. On-site trigger and/or continuous recordings at 20 samples/sec or higher rate with remote dial-in capability will be used for the CMG-3 stations. Either digital telemetry or front-end gain-ranging using analog telemetry will be applied to the CMG-40T stations. With two existing broadband stations, one at Memphis with a borehole CMG-3 and the other at Cathedral Caves with STS-1, and one broadband station to be installed by USGS soon at the old WWSSN OXF station, the central U.S. will be covered by 35 broaband stations. Short period stations will mainly be distributed around the most active areas in the NMSZ to provide better spatial coverage of the micro earthquakes. Seismic signals from a few selected stations will be transmitted in real-time via three VSAT stations to Memphis and St. Louis for trigger detection and data archiving. Each VSAT site will be equipped with a PC-based seismic data acquisition system for trigger detection, on-site recording, satellite communication, and remote retrieval of all data. Portions of short-period and broadband signals will also be transmitted via microwave network to Memphis for real-time digital data acquisition.

SEISMOTECTONICS STUDIES OF THE NEW MADRID SEISMIC ZONE FROM PANDA DATA

J.M. CHIU, Y.T. YANG, K.C. CHEN, Z.S. LIAW, S.C. CHIU, and A.C. JOHNSTON, Center for Earthquake Research and Information, Memphis State University, Memphis, TN 38152

The active faults of the central New Madrid seismic zone were imaged by the well-located hypocenters determined from the PANDA (Portable Array for Numerical Data Acquisition) data recorded between October 1989 and August 1992. Our results corroborate the vertical faulting of the southwest (axial), north-northeast, and western arms and the southwest dipping central segment. Single-event focal mechanism solutions for 102 earthquakes along these active fault segments were determined by using first motion data only. Focal mechanisms for earthquakes along the northwest segment show predominantly left-lateral strike-slip fault movement and predominantly right-lateral strike-slip movement along the southwest segment. Both are consistent with many previous studies. Focal mechanisms for earthquakes along the central segment are, however, very complicated. Normal mechanisms are dominant in the northern central segment, north of Ridgely, Tennessee, where a gently southwest-dipping fault (~ 30°) is determined by PANDA data. Reverse mechanisms are dominant in the southern central segment, south of Ridgely, TN, where a steeply southwest-dipping fault (~ 48°) is determined. The complicated patterns of focal mechanisms in the NMSZ cannot be interpreted simply by compressive east-west regional stress alone. Other additional factors, including the interactions between the adjacent segments, or postseismic relaxation by one or more of the 1811-1812 earthquakes, or other nearby tectonic activities such as the right-lateral strike-slip Crittenden County Fault zone, etc., can not be overlooked in trying to interpret regional tectonics in the NMSZ.

SCATTERING AND ATTENUATION IN NEW ENGLAND DERIVED FROM SHORT-PERIOD SEISMOGRAMS

Robert D. CICERONE, Charles G. DOLL, Jr., and M Nafi TOKSÖZ

Earth Resources Laboratory, Department of Earth, Atmospheric, and Planetary Sciences, Massachusetts Institute of Technology, Cambridge, MA 02139

The energy-flux model of seismic coda, developed by Frankel and Wennerberg (1987), is used to derive estimates of scattering (Q_S^{-1}) and intrinsic attenuation (Q_I^{-1}) in New England. The model predicts the amplitude of the coda wave vs. time as a function of frequency, Q_S^{-1}, and Q_I^{-1}. A non-linear inversion scheme is developed which allows for the estimation of Q_S^{-1} and Q_I^{-1} as a function of frequency. The method employs non-linear least squares via the Levenberg-Marquardt algorithm to estimate Q_S^{-1} and Q_I^{-1} by fitting the model to a narrow-bandpassed filtered envelope of the seismic coda at discrete frequency points. The inversion is performed on 49 earthquakes recorded by the MIT Seismic Network between 1989 and 1993. Preliminary results indicate that, at short distances (i.e. less than 20 km.), there is strong scattering and intrinsic attenuation is not important. At larger distances, scattering is not as strong and attenuation becomes more important as the distance of propagation increases. Further study is under way to confirm these results by the addition of more events to the database to provide broader coverage, and also by performing a tomographic reconstruction of scattering and attenuation to determine if the scattering correlates with geologic structures and seismogenic zones.

EFFECTS OF THREE-DIMENSIONAL AND ANISOTROPIC CRUSTAL STRUCTURE ON EARTHQUAKE STRONG GROUND MOTIONS

Vernon F. CORMIER and Wei-Jou SU, Department of Geology and Geophysics, University of Connecticut, Storrs, CT 06269-2045

Earthquake strong ground motions are synthesized for spacially extended sources in crustal structures having three-dimensional variation and anisotropy using a method of narrow Gaussian beams. Experiments with a three-dimensional structure and distributed slip history appropriate for the Loma Prieta earthquake demonstrate that the magnitude of

amplitude variations due to known regional three-dimensional structure can be similar to that incorporated in more local site effects. Experiments with variable rupture area, rupture velocity, and rise time for a distributed source in a cracked, transversely isotropic, medium demonstrate that the first motion of the S wave is the most robust signature of anisotropy, remaining parallel to the strike of vertically aligned cracks as rupture size and history vary.

SPATIAL VARIATIONS IN SHEAR-WAVE SPLITTING IN THE CHARLEVOIX SEISMIC ZONE OF QUEBEC

Charles DOLL, Jr., Yingping LI, and M. Nafi TOKSÖZ, Earth Resources Lab, Massachusetts Institute of Technology, Cambridge, Massachusetts 02142.

Shear-wave splitting has been observed in diverse geographic areas around the world including Hawaii (Munson *et al.*, 1992), Turkey (Tian-Chang *et al.*, 1986) and southeastern Quebec (Buchbinder, 1985 and1986). In particular, Buchbinder (1985 and 1986) observed shear-wave splitting up to 8.7 % along 18 different paths in the Charlevoix Seismic Zone (CSZ) and interpreted it as being associated with vertical cracks striking 30° east of north within the seismic zone. In this study, we have expanded the number of earthquakes and paths to permit observation of spatial changes, if any, in shear-wave splitting in the interior of the CSZ. 32 earthquakes, located along a well-defined seismic lineation trending 30° east of north and extending approximately the entire length of the CSZ, provide extensive coverage to estimate spatial variation in shear-wave splitting. We are applying a waveform cross-correlation method to about 120 S arrivals to measure the amount of SH - SV splitting precisely. This is supplemented by particle motion analysis. Preliminary results for 35 S travel paths, providing full azimuthal coverage around 9 earthquakes distributed over the whole length of the seismic lineation, show splitting amounts generally greater in the NE part and less in the SW part of the CSZ. In most cases the S component travels faster with north-south particle motion and slower with east-west particle motion.

EARTHQUAKE MONITORING BY THE WEO SEISMOGRAPH STATION 1982 TO 1993

JANET A. DRYSDALE, Geological Survey of Canada, Ottawa, Canada, K1A 0Y3.

A digital seismograph station has been operating on the north shore of Lake Ontario, east of Toronto, since April 1982. The station was situated at Welcome (WEO) to improve the regional monitoring capability of the Eastern Canadian Telemetered Network (ECTN). WEO is operated by the Geological Survey of Canada (GSC) and funded by Ontario Hydro, who have an interest in monitoring any earthquake activity near their nuclear power plants in southern Ontario. In 1982, the only other Canadian network station in southwestern Ontario was the analogue regional station located at Effingham, near Niagara Falls.

Since the installation of WEO, scattered low-level activity has been confirmed under Lake Ontario and in the Burlington-Hamilton region. Any event of magnitude 2.5 or greater within 150 km of WEO could be located. Smaller magnitude events could be detected, but generally not located. Twenty-one earthquakes (magnitude 0.9 - 3.4) have been located within 150 km of WEO. Without WEO, these small events (magnitude < 3) would have been less accurately located or not even detected. Locating the Lake Ontario events was also made possible through data exchanges with stations located in northern New York State and University of Western Ontario (UWO) stations located near London, Ontario and since 1991, at the western end of Lake Ontario. To date, no convincing spatial relationship with geophysical features has been identified.

WEO, the only ECTN station not situated on bedrock, is sited on more than 30 metres of unconsolidated overburden. As a result the station amplifies ground noise. On average, noise results in about 12% of unreadable analogue records. Downtime due to technical or telephone line problems has been extremely small, less than 1% of operating time. The station is closing in the fall of 1993. In its place, a broadband, three-component, continuously-recording national network station with near real-time satellite transmission to Ottawa will open at Sadowa, about 100 km to the north, on the Canadian Shield. Additional data will continue to be provided by four digital, three-component, telemetered stations operated by UWO, and funded by Ontario Hydro, which began monitoring the western Lake Ontario region in the fall of 1991. One of these stations is situated very close to the present WEO location. These additional stations, plus the fact that noise tests have shown the new Sadowa site to be much quieter than the WEO site, should improve detection and location of events in the south-central Ontario region.

A SEISMIC HAZARD STUDY FOR THE STATE OF VERMONT

John E. EBEL, Weston Observatory, Department of Geology and Geophysics, Boston College, Weston, MA, 02193; and Richard BEDELL, Homestake Mining Company, Sparks, NV, 89431

A study by Weston Observatory is being carried out for the Vermont Emergency Management Agency to assess the seismic hazard of Vermont, to indicate what types of damage Vermont may experience in realistic earthquake scenarios, and to recommend measures Vermont may undertake to reduce losses in earthquakes. Most of the earthquakes in Vermont occur along the western and eastern borders of the state, and the biggest known earthquake to date in Vermont itself had a magnitude of 4.3. However, Vermont has been shaken at the IMM V or greater level a number of times by earthquakes from outside the state, particularly those in 1732, 1940 and 1983. Probabilistic hazard analysis calculations were carried out for repeat times of 50, 100, and 250 years and were compared to the national maps put out by the U.S.G.S. The analysis in this study agrees with the U.S.G.S. maps in central Vermont, but the hazard found in this study is approximately double the U.S.G.S. values along the western edge of the state. A magnitude 5.5 earthquake in the eastern Adirondacks, a magnitude 6.25 earthquake in the western Quebec seismic zone near Montreal or a magnitude 5.5 earthquake in central New Hampshire would each be damaging earthquakes in parts of Vermont. Thus, the most significant hazard to Vermont comes from seismic zones outside the state boundaries.

Determination of Rupture Duration and Stress Drop for Earthquakes in New England

Qiuchun Feng and John E. Ebel
Department of Geology and Geophysics, Boston College
Chestnut Hill, MA 02167

ABSTRACT

In this study we determine the time function durations, seismic moments and stress drops for earthquakes from New England and vicinity. A simple method in which the source time function is approximated by a simple pulse shape such as triangle, trapezoid and box car is used to determine the duration of the source time function. Theoretical P-wave seismograms are formed by convolving the source time function with instrument response. A relation is thereby established between the source time function duration and the pulse width of the first P-wave onset on seismograms from the New England Seismic Network (NESN). A moment tensor inversion method is applied to determine the source focal mechanism and seismic moment.

Twelve earthquakes with magnitudes from 2.3 to 4.0 recorded by the NESN operated by Weston Observatory of Boston College are analyzed. One of them with an aftershock of magnitude 1.9 is analyzed by decovolving the aftershock from the main shock for its time function, and is in very good agreement with the result from the method described above. Moment tensor inversion results also show quite good agreement with the P-wave first-motion solutions in the orientations of the focal mechanisms.

For the earthquakes, the source time functions increase from 0.035 second to 0.143 second with the magnitudes from 2.3 to 4.0, the seismic moments vary from 7.7 x 10^{19} dyne-cm to 1.7 x 10^{21} dyne-cm, and the stress drops range from 26 bars to 201 bars. Generally, the rupture durations decrease as the magnitudes decrease. The stress drops are not correlated with earthquake magnitude. The stress drops of these earthquakes in New England are not significantly different from those of earthquakes with similar magnitudes in western North America.

EVALUATION OF LIQUEFACTION-SUSCEPTIBLE MATERIALS NEAR MODERATE MAGNITUDE HISTORICAL EARTHQUAKES IN NEW ENGLAND

Robert L. Gelinas, Hannu M.A. Kemppinen, and David C. Amick, Earth Science Group, Ebasco Services Incorporated, 2211 West Meadowview Road, Greensboro, N.C. 27407

Neotectonic field investigations were performed in two areas of New England that have experienced moderate magnitude historical earthquakes. These are coastal Massachusetts (1727 MMI VII Newburyport and 1755 MMI VII-VIII Cape Anne earthquakes) and central Connecticut (1791 MMI VI-VII Moodus-East Haddam earthquake). These earthquakes were near the liquefaction-threshold magnitude 5.5 event, and caused sporadic liquefaction phenomenon in the greater Newburyport area and minor ground fissuring and boulder dislocations near Moodus-East Haddam. The field reconnaissance consisted of identifying and observing sandy soil exposures for evidence of seismically-induced liquefaction that may have been generated during these historical events, or by older (prehistoric) earthquakes. The best outcrops in both study areas lie along rivers and in coastal marshes, dictating that reconnaissance be conducted by boat. Outcrops along rivers in MA/NH/ME are generally limited, with the exposed sediments deposited in a wide variety of glacial/postglacial depositional environments. These materials have great variability in sediment type and liquefaction potential; however, no evidence of liquefaction related phenomenon was observed. Broad expanses of Holocene salt water marsh from Rockport, MA, to Portsmouth, NH, are underlain by fine-grained, loose, saturated sands. While the marsh materials (typically 1-3 m sections of organics/peat, silt and sand) are nonliquefiable, the *underlying* sandy marsh substrates have a moderate to very high liquefaction potential. No evidence of liquefaction flowage was observed in the submarsh sands, or injections/dikes/sills

emplaced into the overlying marsh. Carbon-14 dating of samples taken from the base of these marshes (including dates obtained during the course of this study and those in the published literature) indicate that these marshes are typically 1500-3000 + years old. The fact that these undisturbed (yet liquefiable) sandy substrates are overlain by 1500-3000 year old marshes suggests that large magnitude earthquakes (≥M6.0) have not occurred in the study area during this span of time (i.e., the middle to late Holocene). These observations, and the findings of other workers, indicate that liquefaction associated with historical MA/NH earthquakes was not widespread and occurred at locations where conditions for liquefaction were especially ideal. The southern-central Connecticut study area contains very similar environments in which exposures were investigated, principally fluvial, palludial (swamp), and palustrine (marsh). Exposures containing liquefiable sediments along the Connecticut river are limited. Many suitable materials (from a grain size standpoint) are situated in high bluffs that front the river, and are currently unsaturated and therefore nonliquefiable. The tidal range of coastal Connecticut is appreciably less than that of MA/NH/ME, resulting in low-lying marsh banks during ebb tide and limited exposure of marsh substrate materials. We utilized a 2.4 m fiberglass probe to determine marsh thickness and nature of marsh substrate. Our findings indicate that many marshes in the study area are thicker than 2.4 m. Although glacial outwash sands do form many marsh substrates at depth, the thick sequences of nonliquefiable marsh material act to inhibit the liquefaction process by: (1) acting as a cohesive cap that is virtually impossible to breach by a liquefied sand slurry, and (2) presenting a lithostatic load that prevents the liquefaction process from initiating. No evidence of seismically-induced liquefaction was identified during our reconnaissance in southern-central Connecticut; however, exposures of sediments conducive to liquefaction were more limited than in the MA/NH/ME coastal area.

THREE-DIMENSIONAL KIRCHOFF MIGRATION ANALYSIS OF VSP DATA FROM AN ITALIAN GEOTHERMAL FIELD

Richard L. GIBSON, Jr. and M. Nafi TOKSÖZ, Earth Resources Laboratory, Massachusetts Institute of Technology, Cambridge, MA 02142.

The elastic Kirchoff integral provides a useful tool for the imaging of seismic data collected in 3D earth structures. We apply this integral in a form appropriate for the VSP geometry in order to migrate seismic data collected in such experiments. A rapid implementation of the itegral solution is obtained by using paraxial ray tracing to compute the far-field, high-frequency Green's tensors for both compressional and shear waves in the elastic medium.

This imaging capability is important in the analysis of geothermal reservoirs, where the location of thin, reflective fracture zones is a common goal, and a VSP survey utilizing four source locations and 41 three-component receiver locations was conducted in the Colla 2A well of the Larderello geothermal field in Italy for this prpose. The shallow geological structures of this field, which have been mapped using surface seismic data, have strongly three-dimensional shapes, leading to complicated seismic wave propagation. Reflections originating from weakly reflecting features, ossibly fracture zones, below the depth of the receivers are apparent in the data.

We use a 3D velocity model of this area to investigate the potential of Kirchoff migration for the location of such fracture zones in the subsurface. The resolution of the algorithm is estimated by comparison of migration results for a point s catterer inboth a homogeneous model and in the 3D model of the Larderello field. In both cases, the migration obtains a smeared estimate of the location of the scatterer. The three-dimensionality of the Larderello model alters the shape of the imaged reflector, but the differences are relatively minor. When the migration results from two or more source points are combined, a better estimateof the location can be obtained. Applicaton of the migration to the observed VSP data has difficulty in resolving subsurface features due to noisy data, varying site conditions for the different sources, and uncertainties in receiver locations in the highly deviated borehole. The images can be mproved by considering *weakly* three-dimensional migration, where the imaging is performed in a volume which allows only comparatively small lateral propagation effects.

GEODYNAMIC EVOLUTION AND SEISMIC HAZARD ZONING OF THE PANNONIAN BASIN

A.F.Grachev,
Institute of Physics of the Earth,Russian Academy of Science,Moscow

The present-day structure of the Pannonian basin has been developed during the last 10 m.y. within the Carpathian structural loop as a result of synorogenic rifting. The lithosphere stretching has been caused by uprise and spreading of anomalous mantle material with simultaneous isostatic uplift of of the Carpathians and Eastern Alps folded basement. In contrast to earlier proposed models such model accounts for the extended development of listric faults in the Pannonian and Quaternary sediments, the abrupt change of the calc-alcaline volcanism to alcaline at the end of the Sarmathian age and also the diffuse character of seismicity.

It is very important to underline that the north-eastern part of the Pannonian basin where the calc-alcaline volcanics have been erupted for the last 10 m.y. represents the recent local area of compression.

The tectonic subsidence curves analysis, based on new deep drilling and seismostratigraphy data allows to define the two stages in the subsidence and sedimentation history: fast subsidence during the Early Pannonian and gradual subsidence for the Late Pannonian-Quaternary. The Mako and Bekes troughs situated in the south-eastern part of the Pannonian basin are the certain exception. To the very beginning of the Pannonian age there were deep basins (up to 1 km depth) at that place and the isostatic subsidence under the the load of sediments resulted their subsequent development.

As a result of the geodynamic analysis we have selected the main geological and geophysical parameters for the geodynamic zoning. From these parameters on a grid of 20x20 km (a unit cell equal to average square focal area) we distinguished five geodynamic zones using procedures of factor and cluster analysis.Knowing the geological and geophysical parameters for every elementary cell and Mmax magnitudes of earthquakes for some of the cells it is easy to determine Mmax magnitudes for every given place.

ANALYSIS OF P-WAVE TRAVEL TIME RESIDUALS AND POLARIZATION VALUES FOR THE WAKE ISLAND SEISMIC ARRAY

Sean P. S. GULICK and Christine A. POWELL, Department of Geology, UNC Chapel Hill, Chapel Hill, NC 27599-3315

Travel time residuals for 78 teleseismic events recorded by the Wake Island Seismic Array (WIA) were analyzed. The six station seismic array (only five operable at time of recordings) has a 45 km aperture and is set on the ocean floor at a depth of approximately 5 km, off the shore of Wake Island in the northwest Pacific Ocean.

Residuals versus azimuth of approach and versus epicentral distance were plotted and analyzed. Residuals versus azimuth showed a scattering about zero and no consistent pattern. In addition, the analysis provided no evidence for either varying velocity structure beneath individual stations or regional velocity structure extending across the array.

Trends were observed in P-wave polarization values (azimuth of approach and ray parameter) that are consistent for individual source regions. This observation suggests that lateral heterogeneity has been sampled in the vicinity of the source region. Broader trends in azimuth and ray parameter anomalies suggest the presence of heterogeneity in the lower mantle.

Multifractal Phase Transitions: The Origin Of Self-Organized Criticality In Earthquakes

C. Hooge*, S. Lovejoy*, D. Schertzer**, S. Pecknold*, F. Schmitt**, J.-F. Malouin*

*Department of Physics, McGill University 3600 University St., Montreal, Quebec, H3A 2T8 CANADA

**Laboratoire de Meteorologie Dynamique Universite, Pierre et Marie Curie, 4 Place Jussieu, F-75252 Paris Cedex 05 France

Two basic empirical laws about earthquakes are known: the space-time scaling of their distribution (the hypocenters form a fractal set), and the divergence of statistical moments (the Gutenberg-Richter law). Until now, these laws have not simultaneously coexisted in a coherent theoretical framework. Even deterministic models exhibiting self-organized criticality fail to provide a general connection between the two. Largely as a consequence of this, no empirical analysis has been able to simultaneously deal with the spatial distribution of the earthquakes and with their intensities. We arguethat the fundamental seismic processes are scaling space-time tensor (e.g. stress-strain) processes involving (tensor) space-time multifractal fields resulting from Lie cascades. Although the observed earthquake displacements (and the associated seismic fields) are nontrivially (and nonlinearly) related to these fields, we will nevertheless expect multifractals to provide the appropriate theoretical framework and analysis methods. This motivates the study of the (normalized) powers of seismic fields from the USGS earthquake catalogue by summing various powers of ground motion displacements onto grids. Every hitherto existing scaling analysis has been on a single (eta=0) special case; the only case with no intensity information. By applying multifractal analysis technique (trace moments) on all the members, we show that the seismic fields are indeed multifractals. Finally, using multifractal theory, we show that multiscaling of the seismic fields leads via multifractal phase transitions to (generalized) Gutenberg-Richter exponents. These exponents are shown to obey a simple theoretical formula which arises due to a well understood dressing of the fundamental seismic fields. Contrary to the usual deterministic framework which situates the origin of the self-organized critical behavior of earthquakes in deterministic toy-models, we demonstrated the possibility of an alternative: self-organized criticality of earthquakes can originate from stochastic space-time tensorial multifractal processes.

AVERAGE STABLE CONTINENTAL EARTHQUAKE SOURCE PARAMETERS BASED ON CONSTANT STRESS DROP SCALING

Arch C. Johnston, CERI, Memphis State Universty, Memphis, TN 38152

Sufficient good-quality data are now available from $4.0 < M_w < 6.8$ intraplate earthquakes [intraplate in the most restrictive sense, i.e., stable continental regions (SCR) that average source properties can be specified without using intraplate events from active continental or oceanic regions. I consider constant stress drop scaling most appropriate for this, based on the work of Somerville [EPRI Tech. Rpt. NP-4789, 1986] and Johnston [EPRI Tech. Rpt. TR-102261, 1993]. The appropriate average SCR (Brune) stress drop $(\Delta\sigma)$ is very sensitive to the proper relation between corner frequency f_0 (or period T_0) and duration of the source time function τ_d. For example, Somerville (above ref.) takes $\tau_d = f_0^{-1}$, yielding $\Delta\sigma = 82$ bars; Herrmann and Goetz [BSSA 71, 1981] derive $\tau_d = (2/\pi)f_0^{-1}$ yielding $\Delta\sigma = 22$ bars. For the average SCR earthquake, I take the average of this range, $\Delta\sigma = 52$ bars, which yields a strain drop $\Delta\varepsilon = d/W = 1.58\times10^{-4}$ (for rigidity $\mu = 3.3\times10^{11}$ dyn/cm^2), a high but not unreasonable value (cf. Kanamori and Anderson [BSSA 65, 1975]).

The source scaling below is based on the relation $\log(\tau_d) = -7.88 + 0.333\log(M_0)$, M_0 in dyn-cm, derived from $\log(M_0)$–$\log(\tau_d)$ pairs of 40 SCR earthquakes in Johnston (above ref.). The average isoseismal radii for *felt* and *MMI VI* areas are from the same reference.

$\log M_O$	M_w	length L	width W	slip d	τ_d	f_0|T_0	*felt* radius	I_{VI} radius
16.00	0.0	5.8 m	5.8 m	1 mm	0.0028 s	303 Hz	—	—
17.50	1.0	18 m	18 m	3 mm	0.0089 s	95 Hz	—	—
19.00	2.0	58 m	58 m	9 mm	0.028 s	30 Hz	—	—
20.50	3.0	183 m	183 m	2.9 cm	0.088s	9.6 Hz	25 km	—
21.25	3.5	325 m	325 m	5.1 cm	0.16 s	5.3 Hz	55 km	—
22.00	4.0	577 m	577 m	9.1 cm	0.28 s	3.0 Hz	100 km	—
22.75	4.5	1.0 km	1.0 km	16 cm	0.50 s	1.7 Hz	220 km	10 km
23.50	5.0	1.8 km	1.8 km	29 cm	0.88 s	1.0 s	350 km	22 km
24.25	5.5	3.3 km	3.3 km	51 cm	1.6 s	1.9 s	500 km	42 km
25.00	6.0	8.0 km	4.1 km	91 cm	2.8 s	3.3 s	650 km	75 km
25.75	6.5	15 km	7.0 km	1.6 m	5.0 s	5.9 s	820 km	130 km
26.50	7.0	30 km	11 km	2.9 m	8.8 s	10.4 s	1000 km	210 km
27.25	7.5	70 km	15 km	5.1 m	16 s	19 s	1200 km	340 km
28.00	8.0	150 km	22 km	9.1 m	28 s	33 s	1450 km	520 km
28.45	8.3	200 km	33 km	13 m	39 s	46 s	1600 km	670 km
28.75	8.5	250 km	42 km	16 m	49 s	58 s	1700 km	790 km

There are no SCR stress drop data above M_w 6.7. The double corner that would manifest itself for rectangular rather than square faults is not tabled here, and the aspect ratio *W/L* for the larger events is arbitrary but consistent with the sparse $M_w>6$ data.

EVALUATION OF WEDGE-TYPE PSEUDOLIQUEFACTION FEATURES IN CENTRAL CONNECTICUT

Hannu M.A. Kemppinen, Robert L. Gelinas, and David C. Amick, Earth Science Group, Ebasco Services Incorporated, 2211 West Meadowview Road, Greensboro, N.C., 27407

Over the past decade significant advances in assessing seismic hazard have been made by using paleoliquefaction features to determine spatial and temporal distribution of large prehistoric earthquakes. A search for evidence of paleoliquefaction features in New England identified wedge-like deformation features in late Wisconsinan age glacial outwash deposits. Based on comparisons of their morphology to seismically-induced liquefaction features identified in other areas some investigators have proposed a seismic origin and postulate the occurrence of a large earthquake in central Connecticut about 1300 years ago. As studies of paleoliquefaction features have progressed, the characteristics and internal morphology of true seismically-induced liquefaction features have been refined. Based on this understanding, the wedge-like deformation features in New England that were previously assigned seismic origin were re-examined. Our new study included careful examination of the physical properties of the features and collection of samples for laboratory analyses to better determine if they are truly related to past large earthquakes or a non-seismic phenomena. This investigation consisted of a detailed field mapping and laboratory analyses, which called for grain size distribution and grain surface texture studies, complemented with chemical and mineralogical analyses for defining the make-up of the materials from the features and their host sediments. The results of our investigation suggest that these structures formed at the close of Wisconsinan glaciation during a period of permafrost climatic conditions. The fissure portion of a wedge structure is likely an ice-wedge cast, whereas the overlying sediment plug is probably a periglacial involution feature. No evidence supporting a seismic origin of these structures was identified, and the following observations argue against this mode of genesis: (1) no evidence of any kind was found of liquefaction flowage, including injections, sills, dikes or conduits, (2) sediment plugs in the upper portion of the wedges have low liquefaction susceptibilities, and have physical properties that are similar to the overlying eolian mantle but are different than purported liquefaction source beds, (3) materials that underlie the sediment plug are continuous with, and part of the adjacent fluvial sediments, and are not part of a "washed zone" as previously reported, and (4) no evidence of significant liquefaction at depth has been observed in lacustrine sequence underlying the wedges. The identification of periglacial involution features, recent identification of patterned ground in the study area, and research of structures on fossil Lake Hitchcock suggest that permafrost conditions, however brief, may have existed in early postglacial times.

DEMONSTRATION OF QUERYING A DATABASE OF SEISMIC PHASES REPORTED BY STATIONS IN THE FORMER SOVIET UNION

Alan L. KAFKA, Weston Observatory, Dept. of Geology and Geophysics, Boston College, Weston, MA 02193; James C. BATTIS, Phillips Laboratory, Directorate of Geophysics, Hanscom AFB, MA, 01731.

To evaluate the extent to which a given set of stations can be used to monitor nuclear explosions in a given area, it is important to know what seismic phases can be observed at those stations from events of a given size and type occurring in the area being monitored. A preliminary assessment of what phases could be recorded at a given station can be obtained by analyzing phase information that has actually been reported to the International Seismological Centre (ISC) as part of routine monitoring of earthquakes and explosions. Since there would inevitably be questions regarding the completeness and reliability of phase information provided by station operators in a foreign country, it would be helpful to examine in advance the reporting characteristics of any station that might eventually be used in a treaty verification scenario.

To address these issues, we have developed software to create database relations containing seismic phase data reported by stations in the ISC Bulletins. The ISC data are now available on a CD-ROM, and software has been developed by the United States Geological Survey/National Earthquake Information Center (USGS/NEIC) to extract the data from that CD-ROM. Using the USGS/NEIC programs as a starting point, our programs read data extracted from the ISC computer files and create database relations containing ISC phase data for a given station. The data for these relations are stored in computer files that can be loaded into a database management system. In this presentation, we use stations in the former Soviet Union to demonstrate the type of investigation that can be done once a database has been created for a given set of stations.

AMPLITUDE VARIATIONS ON SEISMOGRAMS RECORDED IN THE AREA SURROUNDING WESTON OBSERVATORY: DISTINGUISHING SITE EFFECTS FROM INSTRUMENTAL EFFECTS AND LOCALIZED NOISE

Alan L. KAFKA, Weston Observatory, Dept. of Geology and Geophysics, Boston College, Weston, MA 02193; Robert P. COMER and James V. WHITE, TASC, Reading, MA, 01867.

To what extent do seismic waves recorded from regional and teleseismic events vary across distances of less than a few hundred meters at typical seismic observatories? We have addressed this question by analyzing seismograms recorded by the Weston Observatory Seismic Array (WESSA). The variation in geology and shallow crustal structure in the area underlying the WESSA is not particularly complex, and the array sites are either on bedrock or buried in only several meters of soil overlying bedrock. Also, the aperture of the WESSA is only about 0.5 km, and many of the stations are less than 100 m from each other. Thus, only minor variations in amplitudes of seismic waves would be expected from one site to the next. In fact, even with strong signal-to-noise ratios and carefully calibrated instruments, we find surprisingly large variations.

We analyzed spectral amplitude variations of regional and teleseismic signals recorded by the WESSA. In the frequency band of 1.0 to 8.0 Hz, spectral amplitude ratios between WESSA channels are often as great as 1.5, in many cases exceed 2.0, and sometimes exceed 3.0. We have investigated the extent to which these differences in amplitude can be attributed to true site effects rather than effects of instruments and/or localized noise sources. We used the following criteria to discern whether observed spectral amplitudes can be attributed to true site effects: (1) Spectral amplitudes of the signal must exceed spectral amplitudes of pre-event noise by at least a factor of 3.0; and (2) Spectral amplitude ratios must also exceed our estimates of the error in calibrating the instruments. Based on these criteria, between 1 and 3 Hz, amplitude variations as great as a factor of 1.2 appear to be attributable to site effects. Between 3 and 8 Hz, amplitude variations as great as a factor of 1.5 appear to be attributable to site effects. Our results imply that considerable care may be needed in interpreting seismic amplitudes measured at single, isolated instruments.

REFRACTION SURVEYS TO INVESTIGATE DEPTH TO BEDROCK BENEATH TWO SITES OF THE WESTON OBSERVATORY SEISMIC ARRAY

Stephan H. KOESTER and Alan L. KAFKA Weston Observatory, Dept. of Geology and Geophysics, Boston College, Weston, MA 02193.

Refraction surveys were conducted at two sites of the Weston Observatory Seismic Array to determine depth to bedrock and subsurface velocity models. A minimum of eight lines of data were analyzed for each site. Each line consisted of twelve 10 Hz geophones spaced at either 10 or 20 foot intervals resulting in lines ranging from 120 to 210 feet in length from the shot point. The geophone lines were arranged in a radial pattern extending from the shot point, which was located at the array site. The data consists of 10 stacked seismograms for each forward and reverse seismic line. The seismograms were analyzed and interpreted using the SeisView analysis program distributed by EG&G Geometrics.

A simple two layer model was used to interpret the data. Preliminary analysis suggests the following results: The depth to bedrock beneath site 1 is about 11 feet. The P-wave velocity of the soil beneath that site is estimated at 1,700 ft/sec, and the underlying bedrock velocity is about 11,200 ft/sec. Beneath site 9, the depth to bedrock is estimated at 20 feet. The P-wave velocity of the soil is about 1,850 ft/sec, and the velocity of the underlying bedrock is about 12,400 ft/sec.

METHODOOGY AND RESULTS OF HISTORICAL NEW ENGLAND EARTHQUAKE RESEARCH

Kathleen Langone. Earthquake Historian, 145 Mammoth Road, Londonderry, New Hampshire, 03053.

When conducting historical research, some understanding is needed of the historical periods to properly interpret the earthquake records. Such things as the attitudes of the people towards these events and architectural construction are important. Some of the key earthquake periods in New England, such as the mid-1700's, were filled with numerous types of life-threatening events (war, pestilence, etc.), resulting in many historical reports never mentioning seismic activity. However, many sermons mention the events, partly due to the ministers interpreting the earthquakes as acts of God. In contrast, military writings of the French-Indian War are usually devoid of useful information. Sermons, personal journals and letters have proved to be the most fruitful for seismic information. A summary has been complied of common trends in the historic records including structural damage, perceived seismic wave direction and liquefaction features from the 1600's through 1940.

SOURCE CHARACTERISTICS OF M=1.6 - 4.4 EARTHQUAKES IN THE CHARLEVOIX SEISMIC ZONE: RELATIVE SOURCE PARAMETER ESTIMATION WITH THREE-COMPONENT DATA

Yingping LI, Charles DOLL, Jr., and M. Nafi TOKSÖZ, Earth Resources Lab, Massachusetts Institute of Technology, Cambridge, Massachusetts, 02142.

The source time function (STF) of an earthquake is an important parameter that characterizes the rupture process of an earthquake. To estimate the STF from observed seismograms requires isolating the source effects from those of the path and site. For earthquake pairs, having similar hypocenters and focal mechanisms, we can treat the waveform of the smaller event as an empirical Green's function (EGF) and deconvolve it from that of the larger event to retrieve the relative STF of the larger earthquake. We applied the EGF method to five earthquakes (M=0.2 - 4.4), occurring in the Charlevoix Seismic Zone between 1989 and 1992, to obtain STFs of the four larger events and to estimate other source parameters, such as fault length and stress drop. We also compared the STFs estimated using three-component waveforms to examine the slight difference between the larger events and the EGF event. Our results demonstrate the power of the EGF method to estimate relative source parameters and reveal the rupture process.

THE NORRIS LAKE EARTHQUAKE SWARM OF SUMMER, 1993; PRELIMINARY FINDINGS

Leland Timothy LONG and Argun KOCAOGLU, School of Earth and Atmospheric Sciences, Georgia Institute of Technology, Atlanta, GA 30332, Robert HAWMAN, Department of Geology, University of Georgia, Athens, GA 30602, and Pamela GORE, DeKalb College,Clarkston, GA 30034.

During the summer of '93, residents of the Norris Lake, GA,vicinity were bothered by an incessant swarm of earthquakes. Although the largest was only a magnitude 2.4, we counted over 2400 events of which approximately 20 percent were felt. The swarm began with a 4-day sequence June 8-12, 1993. The residents, accustom to quarry explosions, suspected the quarries of irregular activities. To resolve the issue, seismic instruments were placed in the epicentral area. Ten to 20 events were detected per day for the next two weeks. The swarm then escalated to a peak of over 100 per day August 16. Activity following the peak has died down as would be expected for an aftershock sequence (through September 1). The larger events were felt with intensity IV within 2 km of their epicenter, and noticed (intensity II) at least to a distance of 15 km. Some incidence of cracked wallboard and foundations have been reported but no significant damage has been documented. Preliminary locations based on data from temporary deployment of digital event recorders, suggest an average depth of 1.0 km. The hypocenters are in the Lithonia gneiss, a massive rock resistant to weathering and used locally as a building stone. The epicenters are one to 4 km southwest of Norris Lake and 1 to 3 km from the Blue Circle Quarry. The cause of the seismicity is not yet known; however, the earthquakes are characteristic of reservoir induced earthquakes in the Georgia and South Carolina Piedmont. Possible sources for fluids to induce seismicity include: Norris Lake, a small shallow recreational lake which has existed since the 1930's, the Quarry which is still active and unusually dry, and ground water associated with local ponds.

OPERATION OF THE WASHINGTON REGIONAL SEISMOGRAPH NETWORK

Ruth S. LUDWIN, Stephen D. MALONE, Anthony I. QAMAR, and Robert S. CROSSON, Geophysics Program, University of Washington, Seattle, WA 98195

Since 1980, the Washington Regional Seismograph Network (WRSN) has recorded earthquake data using a real-time event-triggered digital recording system. While the system examines all incoming data, digitally sampled data are permanently recorded only when seismic signals are detected by a computer algorithm ("event-triggered"). Before 1980, analog seismic signals from all stations were continuously recorded on photographic Develocorders.

Triggering is done by grouping stations into overlapping sub-networks. When signal amplitudes increase at a sufficient number of stations in one or more subnets, all channels in the network are recorded for a time window. Analog time channels are digitized, and recorded with the seismic data so phase arrival times can be accurately determined.

The recorded data are automatically processed by computer routines which compute a preliminary occurrence time, location, and magnitude for each event. Two separate processes are used to make the procedure robust. One process uses individual station trigger times (each accurate

to a precision of about 1.5 seconds), works on the multiplexed data, and is very rapid. The other process starts after the data have been demultiplexed, and uses phase-picking software. In the event of a large local earthquake, the automatic processing sets off an alarm system to alert a seismologist. The alarms include an audible signal, electronic mail, FAXes to emergency agencies, telephone calls, and a radio pager. (The alarm system also provides notification in the event of power or computer failure, lack of disk space, and some types of software failures.)

Final origin time, location, and magnitude for each earthquake are determined within a few days, after the seismic data have been reviewed by an analyst. The analyst determines the the times of seismic wave arrivals to a precision of .01-.1 s., durations of the seismic signals (for magnitude determination), and identifies P-wave polarities for routine determination of a focal mechanism.

THE ADIRONDACK TELESEISMIC ARRAY: FIRST RESULTS

Stephen MANGINO, University of Cambridge, Cambridge, UK
John J. CIPAR, Earth Sciences Division, Phillips Laboratory, Hanscom AFB, MA 01731

The Adirondack Mountains of northern New York State consist primarily of >1.1 b.y. Grenville age rocks that form a roughly 200-km circular exposure located just west of the Appalachian fold and thrust belt on the North American craton. Characterized as a 'breached dome' of Cenozoic age, the Adirondack High Peaks region have significant elevation of ~1.2 km relative to the surrounding terrain. We have operated a cross-shaped array of 5 broadband seismic stations just south of the High Peaks region centered at 44º N, 74º W between July and November, 1992. Each station consists of a RefTek 72A-02 data logger with Omega timing and a Guralp CMG-3T (0.01-50 Hz) triaxial seismometer that records data in 16-bit continuous mode at 10 samples per second. The long axis of the array is coincident with both the 1988 NYNEX refraction profiles and the 1984 COCORP reflection profile. Broadband station RSNY is located ~75 km NNW of the array. The array aperture is 15x20 km.

Using the array, we will estimate the wave number and apparent slowness of body wave phases that propagate across the array. Beam forming will be used to enhance body and surface wave signals for low-magnitude teleseismic events with respect to ambient seismic noise. We plan to stack the beamformed three-component traces in order to obtain a response polarized in the vertical radial plane. With such data, we can estimate the shear wave structure of the crust using the receiver function method and compare our results to earth structures determined independently from seismic refraction and reflection data, and to the RSNY receiver structure. Measurement of the variation in arrival time and amplitude as a function of predicted amplitude compared to array azimuth will enable us to study prominent lateral velocity heterogeneities beneath the array.

Q AND CRUSTAL EVOLUTION IN STABLE CONTINENTAL REGIONS

Brian J. MITCHELL, Yu PAN, Dibo CHEN, and Jia-kang XIE, Dept. of Earth and Atmospheric Sciences, Saint Louis University, St. Louis, MO 63103

Values of Lg coda Q (Q_c) and its frequency dependence (η) at frequencies near 1 Hz are now available in sufficient quantity to allow synoptic comparisons of those values for different continents and various regions within continents. Tomographically derived values have been obtained for all of Africa, all of Australia, and most of Eurasia and numerous path-averaged values are available for North America, South America, the Arabian Penninsula, and India. As previously reported, there are large differences (by a factor of 5 or more) in Q_c between stable and tectonically active regions. We further find that even within stable regions there are significant variations in Q_c which can be related to the times of coalescence of the continents. The oldest continent, North America, is characterized by the highest Q_c values whereas continents which coalesced later, such as Eurasia have a lower range of Q_c values.

Frequency dependence values for Q_c usually decrease with increasing values of Q_c in stable regions. Assuming that Q_c values are primarily determined by intrinsic Q in the crust, we performed combined inversions of intermediate-period surface-wave attenuation and observed values of Q_c and its frequency dependence. In order for such inversions to explain the observed relation between frequency dependence and Q for Lg coda, models require a low-Q layer at mid-crustal depths. One exception to the usual situation in which η decreases with increasing Q_c occurs in eastern Europe where both Q_c and η are high. We find that the high η values in that region can be explained by a rapid increase in intrinsic shear wave Q from very low values produced by Cenozoic and Mesozoic sediments to high values at greater depths.

DO ALL SEISMIC DATA HAVE THE SAME INFORMATION CONTENT

Reza D. NOUBARY, Department of Mathematics and Computer Science, Bloomsburg University, Bloomsburg, PA 17815.

Seismic hazard assessment and earthquake prediction requires detailed analysis of the available information. The raw material of such investigations are the past data which are often incomplete and insufficient. In this respect one important question relates to quantification of the information contained in the available data. For example, occurrence of a large earthquake in a region with low seismicity may be expected to be more informative than a similar event in an active region. The purpose of this article is to present some basic concepts of the information theory and discuss its relevance to the seismic data analysis.

SPECTRAL STRUCTURE OF RANDOM INHOMOGENEITIES BENEATH THE JAPAN ISLAND ARC ESTIMATED FROM THE BROADENING OF THE S WAVE ENVELOPE

Kazushige OBARA (Earth Resources Laboratory, MIT, Cambridge, MA, 02142-1324; on leave from National Research Institute for Earth Science and Disaster Prevention, Tsukuba, Ibaraki, 305, JAPAN). Haruo SATO (Geophysical Institute, Faculty of Science, Tohoku University, Aoba, Sendai, Miyagi, 980, JAPAN)

Broadening of seismogram envelopes around direct S waves of deep earthquakes was analyzed to reveal the spectral structure of random inhomogeneities of the upper mantle and the crust in relation with the volcanic front in the Kanto-Tokai area, the central part of Japan. 58 earthquakes that occurred in the Pacific subducting slab ranging from 80 to 500 km in depth were observed at 73 stations and used in this analysis. The time width of the envelope around S arrival is narrow at stations located along the Pacific coast line and little depends on frequency and hypocentral distance. The dependence becomes gradually strong as the station moves from east to west. In particular, the envelope broadening is quite large on the west of the volcanic front. Such an envelope broadening is explained by the effect of the diffraction and multiple forward scattering on the seismic wave propagation through the random inhomogeneities with wavelengths longer than the seismic wavelength. Adopting the parabolic approximation, the numerical simulation indicates that the spectral structure of the random inhomogeneity much affects the frequency dependence of the envelope broadening. The frequency dependence of the observed result was compared with the numerical simulation in order to estimate quantitatively the random inhomogeneity. We found that the autocorrelation function of the randomness is represented by the Gaussian type on the east of the volcanic front, whereas, it is close to the exponential type on the west of the volcanic front. That is, the short wavelength inhomogeneities are relatively stronger on the back arc side of the volcanic front than that on the fore arc side. The difference in the random inhomogeneities might be related with the volcanic activity. We can conclude that the volcanic front, which was originally defined as a clear boundary of the distribution of volcanos, can be interpreted as a boundary discriminating the characteristics of the random inhomogeneities in the subduction zone.

AN EXTENDED SOURCE RUPTURE MODEL FOR SEISMIC RISK ESTIMATION FROM SUBDUCTION ZONE EARTHQUAKES NEAR PUGET SOUND

Lawrence D. PORTER, Amir TABATABAIE, Mansour TABATABAIE, and J. P. SINGH, Geospectra, Inc., Richmond, CA 94806

This study presents an extended source rupture model for evaluating seismic risk from subduction zone earthquakes. Estimates of engineering seismic hazard are particularly important for critical structures such as bridges and power plants.

The components of the subduction zone model are arbitrary plates positioned to match the actual subduction zone and the seismic risk elements are micro zones within each plate. In previous models the contributions from the risk elements are determined by the distance from the site to the center of each micro zone.

In this model the center of each micro zone is the starting point of an earthquake source rupture, where the rupture area is an exponential power of the magnitude (Hanks & Kanamori (1979), Wyss (1979)). The rupture is confined to the component surface, and if component boundaries are encountered the rupture perimeter is extended in the remaining free directions until the entire rupture area is mapped on the component surface. The distance for determining seismic attenuation is the distance of closest approach to the site, which is usually less than that in previous models. Such a model yields an increase in seismic risk estimates over those obtained without the extended source.

As a case example this model is applied to the Tacoma Narrows Bridge near Puget Sound. The subduction zone under Puget Sound is modeled with the aid of four rectangular components: an interface zone running north-south and dipping slightly to the east, a second interface zone to the north rotated 12 degrees to the northwest, an interplate zone to the east running north-south and descending to the east, and a horizontal square centered on the site. Estimates are given for the acceleration and response spectra at the site.

FOLIO OF SEISMOTECTONIC MAPS OF THE NEW MADRID AREA, SOUTHEASTERN MISSOURI AND ADJACENT STATES

Susan RHEA and Russell L. WHEELER, U.S. Geological Survey, P.O. Box 25046, M.S. 966, Denver Federal Center, Denver, CO 80225.

The folio contains five 1:250,000-scale maps because the amount of seismotectonic data could not fit legibly on a single map. The map area (lat 35-37° N., long 89-91° W.) includes the alignments of the most abundant network epicenters between Memphis, Tenn., and Cairo, Ill., the meizoseismal areas of the great 1811-1812 earthquakes, and the locations of five damaging shocks since then. Map A focuses on seismicity, showing epicenters, single-earthquake focal mechanisms, stress orientations, seismograph and accelerograph locations, and sand blow concentrations. Network epicenters are also part of the halftone base for maps B-E. Map B focuses on crustal structure, showing large features inferred from gravity, aeromagnetic, seismic reflection and refraction, and magnetotelluric surveys. Map C shows lines of geophysical surveys and models. Map D emphasizes bedrock geology, showing geologic and subcrop contacts, structure contours on a locally important unconformity between bedrock and poorly lithified to unlithified strata, selected wells and faults, and structure of the Mississippi Valley graben. Map E focuses on surficial and hydrologic features, repeating sand blow concentrations from map A and showing sites of logged trenches, earthquake-induced landslides, courses of the Mississippi River since 1765, fluvial and hydrologic anomalies, selected topographic features, geodetic monuments, and elements of the Bootheel lineament as interpreted from aerial photographs and Landsat images.

CHARACTERISTIC FEATURES OF GROUND MOTIONS SIMULATED DUE TO LARGE EARTHQUAKES IN CENTRAL UNITED STATES, INCLUDING THE EFFECTS OF IRREGULAR STRUCTURE

CHANDAN K. SAIKIA, Woodward-Clyde Consultants, 566 El Dorado Street, Pasadena, CA 91101

In this study, we made deterministic assessment of peak ground accelerations (PGA) and duration versus R (where R is the closest distance to a receiver from a seismogenic zone) and developed improved relations for PGA attenuation for three hypothetical New Madrid earthquakes with M_w of 6.5, 7.0, and 7.5, respectively. Each event is represented by an extended fault. The high-frequency ground motion is simulated using a semi-empirical method which includes the effects of varying crustal structure and asperity on the fault surface. The variation in the attenuation curves is developed using simulated PGA for both increasing and constant stress-drop models in the chosen magnitude range, and is found to be small. The curve decays more slowly with increasing earthquake magnitude, resulting in fall-off rates for each magnitude which exhibit a near-fault flattening. By investigating the influence of multi-bounce rays, we find that the lower crustal structure affects the attenuation curve significantly, even at a distance of 40 km away from the seismogenic zone. We also find that the envelopes of the ground motion time histories are affected by the contributions of these rays. In particular, the duration extends over a longer time window if these rays are present. We extended this study to include the effects of irregular crustal models, especially the effect of micro-basins which suggests that this can be a physical mechanism for prolonged ground motions if a receiver is located at the edge of an irregular structure. The asperity models are also employed to simulate low-frequency ground motions at several sites in Saint Louis which used a deterministic simulation method where the path effect between each fault element and a receiver is computed using a frequency-wavenumber algorithm. The crustal model used in this study was obtained by modeling both the peak amplitude and travel times of weak motions recorded on the Saint Louis University network from several small-magnitude earthquakes.

RELATIONSHIP OF SEISMICITY TO GEOLOGIC STRUCTURE IN BERKS COUNTY, PENNSYLVANIA

Charles K. SCHARNBERGER, Millersville University, Millersville, PA 17551.

A magnitude 2.8 (MbLg) earthquake on 10 May, 1993, was the latest event in an earthquake history of Berks County that extends back to at least 1906. Epicenters have been located just north of the Gettysburg-Newark Mesozoic Basin, with the possible exception of the 1906 event which was felt most strongly on the southern margin of the basin.

The maximum intensity zone (MMI V) for the 10 May event was located in Spring Township, about 5 km. WSW of the City of Reading. The overall pattern of isoseismals is elongated in the direction N50°E, roughly parallel to the regional Paleozoic structural trend. The maximum intensity zone, however, is elongated approximately north-south.

Epicenter locations for earthquakes in 1954, 1972 and 1993 define a NE trend parallel to the Paleozoic structure, which includes several thrust faults. Conjecture reported in newspaper stories at the time of the 1972 earthquake series attributed the seismicity to the Paleozoic thrusts. It seems more likely that younger faults cutting across both the Paleozoic structures and the margin of the Triassic Basin are involved. Two such faults are mapped west of the Borough of Sinking Spring, one striking N25°W, the other N20°E. The latter fault coincides closely with the maximum intensity zone (MMI VI) of the 7 January, 1954, earthquake, which caused minor damage in Sinking Spring.

Mesozoic diabase dikes striking generally NE are mapped both north and south of Sinking Spring. What, if any, role these dikes play in Berks County seismicity is unknown at this time.

AFTERSHOCK SURVEYS IN THE EASTERN US: WHY AND HOW

L. Seeber, J.G., Armbruster, N. Barstow, D. Johnson , and S. Horton Lamont-Doherty Earth Observatory, Palisades NY 10964

The deployment of portable instruments in the vicinity of active sequences in the northeastern US has produced unique data about earthquake sources in this intracratonic area. Temporary networks of opportunity are probably going to be even more important in a future with severely diminished regional networks. How do earthquake ruptures relate to pre-existing structure? Is the earthquake process self-similar over the entire magnitude range? Is there a low limit to the size of an earthquakes in a sequence? Do very shallow sources in the transition region between weathered and unweathered rock differ from deeper sources? Are very shallow sources insignificant 'noise', in terms of tectonics and hazard, which confuse the pattern of deeper seismicity? What portion of the total attenuation occurs in the fractured near-surface layer? What are the site-response characteristics of a thick saprolite layer? These are some of the questions raised by the data from the March-April 1993 sequence of very shallow and small earthquakes in Columbia MD (Barstow et al., at this meeting). To address these as well as other fundamental questions raised by many previous aftershock studies in the northeastern US, future temporary networks need to have resolution in the frequency range of corner frequencies typical of very small events (30-100 hz) and need to be capable of locating the source(s) quickly for an early optimal network geometry. Instrumental field deployments during sequences of felt events can also uniquely address questions from an interested and concerned public. The importance of this task in the absence of regional networks was well illustrated by the 1993 MD sequence. The main shock was small (M=2.7), but was centered in a populated area near the Nation's Capital and was felt by tens of thousands of people. Without local instrumentation, some of the earthquakes would have been felt, but not detected instrumentally and most instrumental locations would have had greater uncertainty than macroseismic locations. Aftershock studies offer seismology in the eastern US a unique opportunity for gaining public attention. Aftershock studies in the post regional-network era need a new financial basis. Potentially interested agencies typically need a research plan before making funds available and they cannot cover the cost of work already accomplished. A strategy for solving this classical Catch-22 problem will probably include a pot of moneys allocated for this purpose and a procedure where decisions involving funding of field efforts can be taken immediately by a standing committee.

EARTHQUAKES IN THE LAKE ONTARIO REGION

Anne E. STEVENS, Geological Survey of Canada, Ottawa, Canada K1A 0Y3.

When the geographical distribution of earthquakes over many decades is analyzed for tectonic or hazard applications, the accuracy of the earthquake locations should always be carefully considered. On small-scale maps, the location uncertainties may be similar to the size of the plotted symbols. On larger-scale maps, however, it is especially important to explicitly show the uncertainties, whether by symbol character or error bars. Otherwise, apparent groupings of epicentres may be assigned a significance that is not justified by the basic data.

Earthquakes catalogued in the Lake Ontario region are chosen to illustrate the importance of examining the change in average epicentral accuracy over a period of 150 years. Maps demonstrate clearly that the poor accuracy of pre-instrumental and early-instrumental locations prevents identification of any significant trends. Locations since the early 1970s are much more accurate, but still uncertain on average by 10 km or so. The actual earthquake activity in the Lake Ontario region during the last two decades has been quite scattered, without any trends of tectonic significance. The same analysis method can be readily applied to other regions of eastern North America.

AUGUST 08, 1993 AIKEN, SOUTH CAROLINA EARTHQUAKE:

Pradeep TALWANI, Department of Geological Sciences, University of South Carolina, Columbia, SC 29208; and Donald A. STEVENSON, Westinghouse Savannah River Company, Aiken, SC 29802.

On August 08, 1993 at 09:24 (UTC) a felt earthquake of duration magnitude 3.2 occurred in south central South Carolina. The earthquake was located ~13km east northeast of Aiken using data from stations of the South Carolina and the Savannah River Site Seismic Networks. A small aftershock occurred at 1600 (UTC) on the same day. The earthquake was widely felt (with over 100 felt reports), and awoke several residents. Felt effects included small articles falling from shelves in the epicentral area (estimated maximum MMI V). The most common description was that of an explosion. Felt reports were reported from Windsor, Montmorenci, Aiken, New Ellenton, Clearwater, Eureka and Edgefield county. The focal mechanism shows left lateral strike slip on a steeply dipping northwest striking fault plane. The epicentral location lies on the flanks of a local gravity high with the same strike, suggesting possible causal association. This event is similar in character to small events that occurred in Neeses and Jackson, South Carolina in 1992.

VELOCITY ANOMALIES UNDER THE SOUTHERN APPALACHIAN REGIONAL SEISMIC NETWORK

G. VLAHOVIC and C. A. POWELL, Department of Geology, UNC Chapel Hill, Chapel Hill, NC 27599-3315

Travel time residuals for 106 teleseismic events recorded by the Southern Appalachian Regional Seismic Network and Tennessee Valley Authority Network were analyzed. Lateral velocity structure under the networks was investigated using the Aki inversion method. Results were compared to the upper mantle P-wave velocity inversion for the northern Appalachians (Taylor and Toksoz, 1979), and a three-dimensional velocity model based upon P- and S-wave polarization residuals for eastern Tennessee and western North Carolina (Powell, 1992).

Analysis of travel time residuals showed the existence of a significant velocity gradient across the Ocoee crustal block, located in eastern Tennessee and western North Carolina; negative residuals are located to the west and positive residuals to the east. Analysis of residuals versus azimuth of approach indicates that high velocities in eastern Tennessee terminate in southwest Virginia and in northwest Georgia. Plots of normalized residuals versus ray parameter and azimuth of approach for near-by stations are similar, suggesting that the source of the travel time anomalies is regional and extends to the upper mantle.

The Aki inversion method was applied to 67 well recorded events using different block configurations. Results are stable with a variance improvement of more than 70 % and good agreement between different starting models and generalized and stohastic solutions. The main features found are a high velocity zone between 0 and 120 km depth west of the eastern boundary of the Ocoee block in eastern Tennessee, and low velocities east of the Ocoee block. In the layer between 120 and 200 km depth there is a ridge of low velocity striking northwest - southeast, perpendicular to the strike of the Appalachians. This ridge extends from Kentucky, through eastern Tennessee and western North Carolina to Georgia. Below 200 km the anomaly pattern is irregular.

The velocity structure found is in good agreement with velocity models proposed for the northern Appalachians (Taylor and Toksoz, 1979) and southern Appalachians (Powell, 1992). Both models propose high velocities in the Grenville basement and low velocities associated with accreted terranes (east of the Blue Ridge for the southern Appalachians).

METEOROLOGICAL WATER AND SEISMICITY IN EASTERN TENNESSEE

WEBB, R. A.. Raleigh, NC 27615

Correlations between earthquake frequency, strain release and stream flow or rainfall have been suggested as an explanation of intraplate siesmicity. With a high level of seismicity and excellent long term rainfall records, the Tennessee river valley in Eastern Tennessee is an ideal region in which to test this hypothesis. Earthquake data for the period 1911- 1991 was obtained from the SEUSSN catalog. Monthly rainfall records for the Eastern Region were extracted from the Monthly Climatic Data published by the NOAA. There was a cross-correlation coefficient of 0.60 between the residual of the cumulative earthquake strain and the residual of the cumulative rainfall. The best correlation was obtained when the strain release lagged the rainfall by 5 years. There was also a significant correlation between the residual of cumulative earthquake frequency(mg>=3.0) and rainfall. In the late 1970's there was a period of above average rainfall. This coupled with the full instrumentation of the area in the 1980's affords an opportunity to evaluate the effect of rainfall on earthquake strain release as a function of depth.

ENHANCED SEISMIC MONITORING IN NORTHERN ONTARIO: 1978 - 1990

Robert J. Wetmiller, Geological Survey of Canada, Ottawa, Canada K1A 0Y3; Mary G. Cajka, Atomic Energy of Canada Ltd., Ottawa, Canada K1A 0Y3; and Ganpat S. Lohda, Atomic Energy of Canada Ltd., Whiteshell Research Laboratory, Pinawa, Manitoba R0E 1L0

Since 1978 the Canadian government (Earth Physics Branch before 1986 and the Geological Survey thereafter), in cooperation with Atomic Energy of Canada Ltd., has operated a regional seismograph network in northern Ontario. The network has included at least four seismograph stations (short-period, single component) since 1984, expanding to six stations in 1987, which monitor seismic activity over a 1-million-km^2 region of the Precambrian Shield, between 46 N and 53 N, stretching across northern Ontario from the Quebec to the Manitoba border. Station uptime has averaged 95%. Considerable effort has been devoted to investigating quarry/construction blasting and mining-induced seismic events so that we have some confidence that almost all earthquakes occurring in the region with magnitude 2.5 or greater have been detected. In all, 124 earthquakes have been located, the largest magnitude 4.3 in the Temiskaming region, and 96 suspected earthquakes, mostly magnitude 1.5 or less, have been recorded on single stations. The network has provided valuable baseline seismicity data on low magnitude earthquake activity that are now being used to refine the Canadian National Building Code seismic zoning in the region. Three areas of relatively enhanced seismicity have been identified from these studies: the Temiskaming region along the Quebec-Ontario border, a broad band in the Sudbury-Kapuskasing region, and an small area in the Atikokan region. The magnitude-frequency relationships for the northern Ontario earthquakes are broadly consistent with those determined for other Shield regions, but for assessment of longer-term seismic hazard in stable Shield regions the information derived from relatively short-term seismicity monitoring efforts needs to be supplemented with additional information about possible prehistoric earthquakes. Lake bottom coring, sonar mapping of lake sediments, and studies of postglacial faulting are three techniques that hold much promise for providing such information in Shield regions.

A ONE-DIMENSIONAL FINITE ELEMENT MICROCOMPUTER PROGRAM TO DETERMINE NON-LINEAR SOIL RESPONSE

Chun Zhu, Department of Geology and Geophysics, Boston College, Chestnut Hill, MA02167; Alfredo Urzua, Prototype Engineering,Inc., 57 Westland Ave, Winchester, MA 01890

Observations made after destructive earthquake have shown correlation between damage and local geology. At level ground sites, earthquake effects include:

a.- a modification of the amplitude, frequency content and duration of the ground shaking caused by the soil amplification.

b.- the failure, settlement or liquefaction of the soil near the ground surface.

Several methods for evaluating the effect of local soil conditions are presently available. Most of these are based on the assumption that the main soil response is caused by the propagation of shear waves from the underlying rock formation.

The purpose of this article is to introduce a microcomputer program to analyze the non-linear one-dimensional soil response under earthquake conditions. The soil model is represented by an hyperbolic stress strain relationship (f= G*U/(1+U/Ur)).

Typical soil profiles for the Boston area are analyzed, and the results compared with SHAKE, a program that utilizes the linear equivalent technique and solves the problem in the frequency domain.

AUTHOR INDEX

EASTERN SECTION
SEISMOLOGICAL SOCIETY OF AMERICA
65'TH ANNUAL MEETING

MINUTES

Minutes of the Eastern Section Seismological Society of America Executive Committee meetings. The 65th annual ESSSA meeting was held October 12 - 15, 1993 at the Campion Center, Weston Observatory, Weston, MA 02193. Weston Observatory is affiliated with Boston College, Chestnut Hill, MA 02167-3809.

The first meeting was held on October 12, 1993 and was convened at 8 P.M. Present were Robert Wetmiller, John Ebel, Waverly Person, Arch Johnston and Pradeep Talwani. Christine Powell was absent.

The meeting opened with a discussion of Seismological Research Letters (SRL). Bob Herrmann wrote a letter stating that volume 64, numbers 3 and 4, 1993 will be his last issue. Bob has been doing the typesetting for SRL on a volunteer basis. Bob Wetmiller will write a letter to him thanking him for his time and effort. The possibility of awarding Bob Herrmann a certificate to acknowledge his contribution was discussed. SRL will have to move to a new typesetter. The changes will free Margaret Hopper from editorial duties. The possibility of presenting Margaret with a certificate was discussed as well as an award for Bill Reinhart. Bill did the production before Bob Herrmann. Doug Nielson was suggested as a replacement for Bob. Doug has presented estimates for typesetting costs to Arch Johnston. We will consider Doug for volume 65 (1994). Bob Wetmiller will write to Doug and ask him to confirm his estimate for four issues. A question was raised concerning how much responsibility the ESSSA had for the abstract issue; this had been handled by Margaret Hopper. Bob Wetmiller will clear this up. Waverly presented the treasurers report showing that the expenses for volume 65 will be covered.

A discussion followed that reviewed the choice of an editor for SRL. Lucy Jones wrote a proposal for the new SRL in April that Bob Wetmiller, with consultation of the ESSSA executive committee, agreed to. The new SRL will have a main editor and an eastern section editor. Bob Wetmiller took part in the BSSA publication committee meeting in which the selection for the main editor for SRL was discussed. During this meeting, it was decided that the new SRL will begin in 1995 and John Ebel will be asked to be the editor. The discussion at the ESSSA meeting then involved how to choose the Eastern Section editor. A decision was made to allow the board of directors to make this decision. A letter will be written by Bob Wetmiller to the SRL advisory committee and other appropriate people (e.g. former advisory committee members) asking for suggestions for the Eastern Section editor. A list of candidates will be drawn up and a person selected.

Pradeep Talwani offered to hold the next ESSSA meeting at Columbia, South Carolina and his offer was accepted formally. The tentative dates are October 10 - 12, 1994. Arch Johnston presented that status of papers submitted to SRL; he has enough material to complete volume 64. More papers are needed for 1994.

A brief meeting was held the following morning, October 13. A nominating committee was organized to elect a new member of the board. Russ Wheller, Noel Barstow and Alan Kafka formed the committee.

A third meeting was held during lunch on October 13. Present were Robert Wetmiller, John Ebel, Waverly Person, Chris Powell and Pradeep Talwani.

The discussion opened with possible locations for future ESSSA meetings. A tentative location for 1995 is Lamont Observatory. Chapel Hill, NC is another possibility for either 1995 or 1996.

The discussion then centered on how to incorporate student posters into the student award evaluation. We decided to restrict the student award to oral presentations for the time being.

A nominating committee for the Jesuit Society award was selected. The potential members are Gil Bollinger, Brian Mitchell and Andy Murphy. An announcement will appear in SRL and BSSA asking for nominations. These will be sent to the secretary and passed on to the committee.

The discussion then centered on the need for a separate ESSSA dues. This question arose because the publication costs for SRL will be covered by the main society starting in 1995. A separate, nominal dues was thought to be necessary to help maintain eastern section functions. Several suggestions for use of the dues were made including travel for students to the ESSSA meeting and air fare for award recipients.

John Ebel will serve as editor for the new SRL. A separate editor for the eastern portion of SRL must be selected. A plan for what information SRL will contain should be formulated and the eastern section selected by the SSA meeting in April, 1994.

A final meeting was held on October 13 with the executive committee members and Tom Heaton, Susan Newman, and Arch Johnston.

The first issue discussed was the need for a separate dues for the ESSSA. The national dues will cover SRL costs but a separate dues for the ESSSA will help maintain the identity of the eastern section. The identity will be maintained through the annual meeting, the existence of the executive committee, and allocation of funds for the SRL editorial committee and editorial advisory board. We must have a budget in mind for the eastern section of SRL and a proposal for a separate budget line for ESSSA activities for the April meeting. It would be best to have this for the Fall AGU.

The SSA meeting in April, 1994 will be large and should attract new members. The IRIS meeting will follow. The SSA meeting will be held in Hawaii in 1997. The 1996 location has not been selected.

The discussion was summarized as follows:

- separate funding for the ESSSA will continue and will probably be collected by the SSA. The amount will be nominal.

- publication costs for the eastern section of SRL will be taken from the SSA budget.

- The editor for the eastern section portion of SRL will be chosen with the approval of John Ebel.

- John Ebel will provide an indication of the budget required for SRL.

- the bylaws of the ESSSA will be provided to the SSA board members by the Fall AGU. The board will determine if the proposed changes in SRL are compatible with the bylaws.

- a proposal for what the ESSSA dues will be used for should be given to Susan by August, 1994.

The following announcements were made at the banquet held on October 14 by Bob Wetmiller.

- the student award for best paper was presented to Sean Gulick. Sean is a student at UNC Chapel Hill.

- the new member selected for the board is Jer-Ming Chiu. Jer-Ming is associated with the Center for Earthquake Research and Information, Memphis State University.

Treasurer's Report: September 30, 1992 - September 30, 1993

Assets as of September 30, 1992 $37,745.15

Receipts
    Dues and subscriptions $12,618.00
    Reprints (back issues)   68.00
    Publication fees   6,500.00
    Special issue copies   350.00
    Gift (Wheeler)   300.00

        Total Receipts $19,836.00 $19,836.00 $57,581.15

Disbursements
    Publication of Seismological Research Letters
     Volume 63, No. 4   3,761.08

Other Expenses
    Best student paper $ 100.00
    Shipping & mailing special issues   190.47
    Mailing back issues   37.76
    Paste up material   132.00
    Mailing Vol. 64, No. 1 Ixtapa   35.59
    U.S. Post Office (Bulk Rate)   75.00
    Money Market Certificate (from Jesuit Society) 6,000.00

        Total Dispursements $ 6,570.82 $ 6,570.82 $10,331.90

        Total $47,249.25

Assets as of September 30, 1993

    Available cash $47,249.25
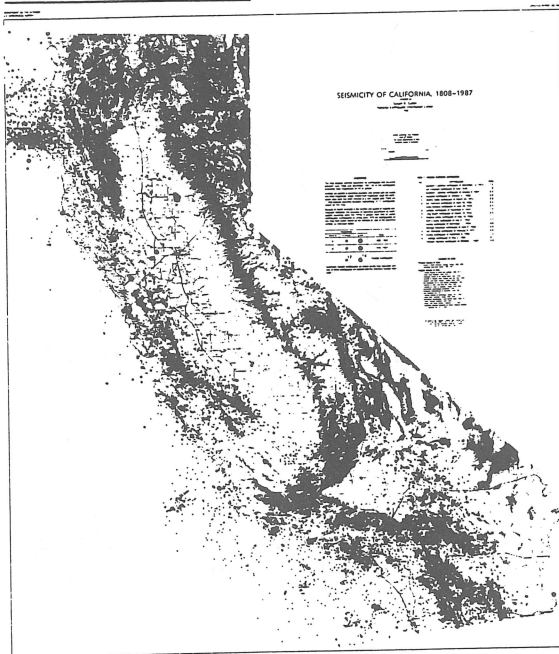   Money Market Certificate   6,000.00

        Total   53,249.25

Respectfully submitted:

Waverly J. Person

Waverly J. Person
Treasurer

National Earthquake Information Center

SEISMICITY MAPS

The U.S. Geological Survey, National Earthquake Information Center now has full-color seismicity maps of Alaska, California, and Hawaii. These maps present earthquakes on very-detailed, elevation-tinted, shaded-relief base maps. The three-dimensional illusion of these maps enable the viewer to obtain a clearer understanding of where earthquakes occur in relation to geographical features such as mountains, valleys, lakes and cities. For further information regarding prices and availability, please write to the address below:

National Earthquake Information Center
U.S. Geological Survey
Box 25046, Denver Federal Center, MS 967
Denver, CO 80225
Attn: Susan Goter

FICHE 1 OF 2

U.S. DEPARTMENT OF THE INTERIOR/GEOLOGICAL SURVEY
NATIONAL EARTHQUAKE INFORMATION CENTER
PRELIMINARY DETERMINATION OF EPICENTERS